Copyright Warning & Restrictions

The copyright law of the United States (Title 17, United States Code) governs the making of photocopies or other reproductions of copyrighted material.

Under certain conditions specified in the law, libraries and archives are authorized to furnish a photocopy or other reproduction. One of these specified conditions is that the photocopy or reproduction is not to be "used for any purpose other than private study, scholarship, or research." If a, user makes a request for, or later uses, a photocopy or reproduction for purposes in excess of "fair use" that user may be liable for copyright infringement,

This institution reserves the right to refuse to accept a copying order if, in its judgment, fulfillment of the order would involve violation of copyright law.

Please Note: The author retains the copyright while the New Jersey Institute of Technology reserves the right to distribute this thesis or dissertation

Printing note: If you do not wish to print this page, then select "Pages from: first page # to: last page #" on the print dialog screen

ABSTRACT

LONG-TERM MANAGEMENT AND CONDITION ASSESSMENT OF CONCRETE CULVERT

by
Zhenting Zou

Infrastructure is the backbone of national security, economic growth, public safety and other aspects of the society. Nationwide, the condition of America's infrastructure was graded as "D+" by the American Society of Civil Engineers (ASCE) in 2013.

Owners and responsible agencies have employed various cost-effective maintenance and repair methods as well as analytical tools to repair and extend the service life of the infrastructure. However, without a long-term plan, maintenance work can be delayed by lack of funds. Maintenance delay may cause significant reduction in condition state leading to premature failure of the infrastructure. Consequently, a long-term rehabilitation plan is needed to find the best time and the amount of investment needed to avoid catastrophic failures.

In this research, three methods are proposed to compute the long-term annual investments for a culvert network. They are modified worst first method, network optimization approach and estimation by the maximum deterioration rate. The performance of a 15-culvert system was evaluated using the above methods. The method based on maximum deterioration rate is very simplistic and can only be used to estimate the lower bound value of the investment. In the modified worst first method, a fixed yearly budget is allocated and the project level corrective actions are suggested for each culvert for each year. Then the budget allocation is changed and the analysis is repeated. One could imagine this procedure as current practice of fixed budget allocation projected

into the future. To do the network optimization approach, the computer program LINGO was used for the budget optimization. Developed constraints and one objective function were used based on financial requirements. Based on the simulation results, the modified worst first method is computationally intensive but provides the optimum budget. The method using maximum deterioration rate provides the lower bound value and should be used as the absolute lowest value that should be allocated. The optimization method uses computer programming and provides an upper bound value for small networks. It is anticipated that for large culvert networks the network optimization approach can be used to provide reasonable long-term annual budgets.

A long-term maintenance plan for culvert networks can be accomplished only if correct condition states of all culverts are known by inspection. However, the culvert material influences the inspection method. Concrete, metal and plastic are the most common culvert materials. In the USA, 78% of culverts are made of concrete because concrete culverts are strong, durable, and economically preferable.

In the research, several common concrete inspection methods were reviewed. By comparing all these methods, ultrasound was found to be the most reliable, fastest, and most widely used NDT method. Ultrasound wave velocity is related to the elastic properties of the material. Thus, a finite element analysis was used to simulate concrete with voids. Concrete blocks with different void sizes and distributions under dry and fully saturated conditions were simulated. Using back-calculated Young's modulus values, ultrasound wave velocity was computed and compared with experimental results from the literature. A good comparison provided a theoretical basis for the relationship between ultrasound velocity and material porosity.

Ultrasound velocity and ultrasound diffusion method to characterize concrete were reviewed in this research. However, these methods are unable to account for the influence of the fluid in voids. Therefore, a new hypothesis of shock wave transmission in voids was studied. When high frequency and high energy ultrasound are applied to concrete, a shock wave will be generated at the edge of the voids and propagate through the voids. An ideal 1-D model was used to simulate shock wave velocity propagation. The high sound pressure of the solid will move like a piston to generate shock wave in voids. First, shock speed was studied by solving the Riemann Problem. After the piston stops, rarefaction will be generated and its speed is much faster than the shock. The interaction of rarefaction waves with shock waves was studied. The results show that when the rarefaction hits the shock, the shock wave velocity is reduced. Furthermore, the energy lost was also studied during the rarefaction interaction with the shock. The total energy is the same but due to the reaction the energy is spread during the propagation. Consequently, bigger voids will allow more of the rarefaction to interact with the shock and the velocity of the shock will decrease. In addition, the energy will spread to a longer volume and the total energy density will decrease, causing a reduction of wave amplitude.

LONG-TERM MANAGEMENT AND CONDITION ASSESSMENT OF CONCRETE CULVERT

by
Zhenting Zou

A Dissertation
Submitted to the Faculty of
New Jersey Institute of Technology
in Partial Fulfilment of the Requirements for the Degree of
Doctor of Philosophy in Civil Engineering

John A. Reif, Jr. Department of Civil and Environmental Engineering

2017 August

APPROVAL PAGE

LONG-TERM MANAGEMENT AND CONDITION ASSESSMENT OF CONCRETE CULVERT

Zhenting Zou

Dr. Jay N. Meegoda, Dissertation Advisor Professor of Civil and Environmental Engineering, NJIT	Date
Dr. Methi Wecharatana, Committee Member Professor of Civil and Environmental Engineering, NJIT	Date
Dr. Bruno M. Goncalves da Silva, Committee Member Professor of Civil and Environmental Engineering, NJIT	Date
Dr. Bruce G. Bukiet, Committee Member Associate Professor of Mathematical Sciences, NJIT	Date
Dr. Thomas Juliano, Committee Member Associate Professor of Engineering Technology, NJIT	Date

BIOGRAPHICAL SKETCH

Author: Zhenting Zou

Degree: Doctor of Philosophy

Date: August 2017

Undergraduate and Graduate Education:

- Ph.D. in Civil Engineering
  New Jersey Institute of Technology, Newark, NJ, 2017

- Master of Science in Civil Engineering
  New Jersey Institute of Technology, Newark, NJ, 2013

- Bachelor of Science in Civil Engineering
  Tongji University, Shanghai, P.R. China, 2010

Major: Civil Engineering

Publications:

Meegoda J., Rudy S., Zou Z. and Agbakpe M., (2017). "Can Fracking be Environmentally Acceptable?" American Society of Civil Engineers (ASCE) Journal of Hazardous, Toxic, and Radioactive Waste, Vol.21, Issue 2.

Meegoda J. and Zou Z., (2015). "Long-Term Maintenance of Culvert Networks", American Society of Civil Engineers (ASCE) Journal of Pipeline Systems Engineering and Practice, Vol. 6, Issue 4.

To my beloved family

For Endless

Love, Support and Encouragement

ACKNOWLEDGEMENT

I would like to extend thanks to the many people who so generously contributed to the work presented in this thesis. Without the guidance of my committee members, help from friends, and support from my family, I would never have been able to finish my dissertation.

Foremost, I would like to express my sincere gratitude to my advisor Professor Jay N. Meegoda for the continuous support of my Ph.D. study and research, for his patience, motivation, enthusiasm, and immense knowledge. His guidance helped me in all the time of research and writing of this thesis. I could not have imagined having a better advisor and mentor for my Ph.D. study. I will forever be thankful to Professor Bruce G. Bukiet for his scientific advice and knowledge and many insightful discussions and suggestions. He is my primary resource for getting my mathematics questions answered and was instrumental in helping me crank out this thesis, all in five months.

Additionally, special thanks are given to my committee members Professor Methi Wecharatana, Professor Thomas Juliano and Professor Bruno M. Goncalves da Silva for their insightful comments and encouragement, but also for the challenging questions which gave me incentive to widen my research from various perspectives. I would also like to thank Professor Jonathan H. Luke, and Professor Ivan Guzman.

Finally, I would like to thank my father Mr. Jianming Zou, my mother Mrs. Ronghua Li and Ms. Yue Xu. They were always supporting me and encouraging me with their best wishes.

TABLE OF CONTENTS

TABLE OF CONTENTS
(Continued)

TABLE OF CONTENTS
(Continued)

LIST OF TABLES

LIST OF FIGURES

CHAPTER 1

INTRODUCTION

1.1 Background Information

Infrastructure is the backbone of national security, economic growth, public safety and other aspects of society. Nationwide, the condition of America's infrastructure was graded as "D+" by the American Society of Civil Engineers (ASCE) in 2013. To improve the condition, an investment of 3.6 trillion dollars is needed. This number was 2.2 trillion dollars in 2009 and 1.6 trillion dollars in 2005. The huge and growing gap between infrastructure needs and available resources is obvious. Citizens across America can easily find evidence of the gap in their quality of daily life, in congested roads, unsafe bridges, failed culverts and poorly maintained tunnels, which are all public assets.

Over three trillion dollars are needed to upgrade the nation's mostly aging infrastructure through various bonds and public funds. Most of that is spent on new construction and replacement of old infrastructure. It can be convincingly argued that it would be cost effective over the long term to spend a good portion of that investment in taking a proactive course in managing the maintenance of the infrastructure rather than waiting and being forced to merely react to disruptive incidences. The importance of a proactive maintenance management policy becomes more pronounced when considering vital civil infrastructure systems such as pipes, pavements and bridges. This importance emanates from the fact that an unexpected failure of a component of these complex systems usually creates disruptions which could have cascading effects leading not only to havoc and its consequences of inconvenience, but also to major economic effects

requiring colossal expenditures to contain the damages incurred from such premature failures.

Various maintenance treatments are employed by civil infrastructure agencies to slow deterioration and restore the condition state of pavements, bridges, pipes, signs and other physical assets. However, budget constraints and other factors have often led to delaying or eliminating the application of such treatments or application of simple repairs to excessively deteriorated systems. A delay or elimination of appropriate maintenance can be expected to adversely influence condition and performance and lead to a reduced level of service, to early deterioration, and eventually to the need for costly rehabilitation or replacement. Analytical tools are currently available to quantify the consequences of delayed application of maintenance treatments for highway pavements, bridges, pipes and other assets. However, processes for using these tools to demonstrate the potential savings and performance enhancement resulting from applying maintenance treatments at the right time and optimum allocation of funds are not readily available. For this reason, research is needed to develop such methodologies. This information will help civil infrastructure agencies to better assess the economic benefits of maintenance actions and their role in enhancing the level of service of civil infrastructure. In addition, incorporating these methodologies into asset management systems would provide a means for optimizing the allocation of resources.

The MAP-21 (Moving Ahead for Progress in the 21st Century, 2012) program for transportation assets defines asset management as a strategic and systematic process of operating, maintaining, and improving physical assets, with a focus on both engineering and economic analysis based upon quality information, to identify a structured sequence

of maintenance, preservation, repair, rehabilitation, and replacement actions that will achieve and sustain a desired state of good repair over the life cycle of the assets at minimum practicable cost. This is also a requirement of Phase II of the Governmental Accounting Standards Board, Statement No. 34 (GASB-34) where public agencies are required to maintain or improve the overall condition state of their infrastructure systems with annual funding/investment, where the minimum yearly amount needed should be provided by a comprehensive asset-management system (McNamee et al., 1999).

1.2 Objective and Approach

Infrastructure in the US is in need of urgent maintenance and rehabilitation. Preservation of culvert networks, a major component of US infrastructure systems, at an acceptable level of serviceability subject to the stringent yearly maintenance and rehabilitation (M&R) budgets is a major challenge for culvert network owners and managers. Decision-makers of the government, industry or private sector are required to develop an optimum financial plan to minimize the total cost of maintenance rehabilitation and various improvements of the culvert network performance during a given planning horizon. This research presents a discussion on budget planning for maintenance and rehabilitation scheduling, and optimization of a culvert network. Any maintenance and rehabilitation (M&R) expenditure should be justified such that the net increase in the asset value is more than the cost of rehabilitation, where the net worth of an asset is based on performance rather than on book value. Phase II of Governmental Accounting Standards Board, Statement No. 34 (GASB-34) requires owners to maintain or improve the overall condition state of their infrastructure systems with substantial annual investment.

Current underground infrastructure asset accounting is based on a linear depreciation and not based on assessment of present state or condition state. To ensure long-term culvert durability and compliance with federal accounting requirements, culvert network owners are exploring ways to implement culvert inspection and management programs. This is a requirement stipulated by the Governmental Accounting Standards Bureau, in the Basic Financial Statements and Management's Discussion and Analysis for State and Local Governments (i.e. GASB-34 Standard, 1999). The GASB-34 requires culvert network owners to declare the present worth of infrastructure assets and to provide information on maintenance costs and future replacement costs. It also requires reporting of infrastructure assets as a depreciated cost, scheduled based on the historical cost or a discounted replacement cost. In the "GASB-34 Modified Approach" reporting the present cost of preserving eligible infrastructure is allowed in lieu of reporting depreciation or replacement costs.

Culvert network owners have found that funds made available to maintain infrastructure are insufficient to meet GASB-34 requirements. Thus, the need exists for adopting an optimal strategy that requires accurate information on the present state of infrastructure to be able to predict future performance. The modified approach lays out the requirements towards an efficient culvert maintenance and management system. It requires culvert network owners to:

- Maintain an up-to-date inventory of eligible infrastructure assets.
- Perform condition assessments of eligible infrastructure assets at least every three years.
- Summarize the results, noting any factors that may influence trends in the information
- Estimate the annual cost of maintenance for infrastructure assets, at or above the established condition level.

- Ensure that the result of the three most recent condition assessments meet or exceed the established desirable overall condition level.
- Compare the estimated maintenance cost of infrastructure assets at or above the established condition level based on amounts spent during each of the past five reporting periods.

Many culvert network owners have yet to implement culvert management plans based on the `Modified GASB Approach.' Collecting and interpreting data in order to assess the present condition state with respect to deterioration requires accessibility to underground infrastructure and the ability to perform a proper condition assessment. Therefore, the above is a justification for implementing a preventive maintenance program, which incorporates user costs associated with culvert failures, which may be due to flooding, roadway collapses causing traffic delays and expensive repairs. In many cases, indirect costs can easily exceed direct costs, and ignoring them can lead to less than optimal decisions. However, meeting the GASB-34 requirements requires sufficient yearly funds to perform timely repair and maintenance of the culverts network. Hence, optimization of the long-term maintenance strategy is needed. To compute the optimum time and optimum allocation of funds to rehabilitate or replace culverts in a network, first those culverts should be inspected and culvert condition states should be determined (Meegoda et al., 2004). As a result, it is vital to know the condition state of the pipe network before a pipeline maintenance and rehabilitation (M&R) plan is developed.

A culvert's material influences the inspection method. Concrete, metal and plastic are the most common culvert materials. The United States has approximately 4,000,000 miles (6,437,376 kilometers) of roadway, making it the largest in the world with millions of culverts hidden underneath (Najafi, et al., 2008). The majority of these culverts are made of concrete; for example, a Minnesota DOT (2012) report shows that 78% of

culverts are made of concrete. Since the 19th century, concrete culverts have been used extensively, because they have a service life that exceeds 100 years, which indicates durability. According to the American Concrete Pipe Association (ACPA, 2008), most important transportation systems are supported by concrete culverts and have proven to be strong, durable, and economically preferable to serve needs of the country and will continue to meet any demand identified in the future. Consequently, this research is focused on condition assessment and long-term management of concrete culverts.

In this thesis, a methodology is developed for optimum time as well as optimum allocation of funds to rehabilitate or replace culverts based on their performance and user costs. Several computations are performed and results are discussed in order to determine the best approach of computing the minimum yearly (M&R) expenditures. The purpose of this thesis is to generate discussion among concerned agencies and asset owners on the topic of the minimum investment needed to maintain culvert networks at the current overall condition state in order to maintain an acceptable level of service for infrastructure systems. This is an attempt to start a dialogue on long-term culvert maintenance and not to solve a problem or develop a standard, specification or regulation. The specific objectives of this research are:

- Based on the condition state of culverts, develop a long-term maintenance plan under the GASB-34 budget requirement.
- Determine condition state of the culverts using ultrasound.
- Derive a theoretical explanation of reduction of velocity and amplitude with ultrasound wave propagation.

CHAPTER 2
CONDITION ASSESSMENT OF CONCRETE CULVERTS

2.1 Concrete Culvert Life

The Highway Drainage Guidelines (AASHTO, 2007) identifies pH, soil resistivity, chlorides, sulfates and bedload as design concerns. NCHRP 2011 also identifies mechanical properties of soil, soil-water chemistry, streambed properties, and drainage area characteristics as culvert life reducers. Based on these concerns, pH of the soil and water, chlorides, sulfates, structural loading, bedding and abrasion are main reasons for culvert deterioration.

2.2 Material Constituents

Concrete is a complex mixture containing aggregates bonded by cement. The most commonly used cement is Portland cement (PCA, 1994). Aggregates such as gravels, crushed rock and sand are used in concrete for strength by filling voids and reducing shrinkage during hydration (ACI, 1996). Mineralogical nature and shape of aggregate will impact concrete characteristics. By adding water, cement will react with water forming a gel, and the gel will finally form a skeletal structure to bond aggregates. The mixture remains fluid or plastic until the development of the cement hydrates, which gradually solidifies to form a paste that surrounds the aggregates and binds them together giving form and strength to the mass (PCA, l994). The cement paste, comprised mainly of calcium silicate hydrate, has no clearly defined crystalline structure and its actual composition is indeterminate, yet to a very large extent its character determines the

durability of the concrete and the nature of deterioration (Mays, l992). The cement paste has inherent porosity due to a combination of gel voids, capillary voids and air voids. The capillary voids determine the concrete permeability. The initial porosity of concrete is governed by the water-cement ratio. In order to obtain workability and let the cement fully hydrate, the water-cement ratio should be between 0.4 and 0.7When concrete is in service, it is exposed to a wide variety of environments and, may deteriorate because of its physical and chemical properties (Perkins, l997). A pore structure with cracks will provide a pathway for aggressive liquids or gases to penetrate the concrete, causing further deterioration.

2.3 Voids in Concrete

Voids in cement-based materials influence the properties of concrete. While air voids within a certain range are beneficial for freezing-and-thawing resistance, large-size voids decrease strength and durability (Yim, et al., 2013). The porosity of the concrete is a key parameter that influences the condition state of the concrete. During hydration, most of the pores in the cement are eliminated; however, four kinds of pores remain. One of those kinds, ranging in size from a few fractions of nanometers to several nanometers, is called gel pores. They typically have a volume equal to 28% of the total porosity of the hydrated cement paste. These voids do not affect the durability of hydrated cement paste and its protection of the reinforcement because they are too small to allow significant transport of aggressive fluids such as salt water (Wonsiri, 2006). Capillary voids are another void type, which is not filled by particles that were created by hydration. These voids will have dimensions from 3-5 μm to 10-50 nm, depending on the water/cement ratio. The

third type of pores is entrained air pores. These are spherical and have diameters ranging from 10μm to less than 1mm. They are intentionally created in cement paste. Entrained air pores increase the resistance of concrete to freeze-thaw cycles. However, these voids are capable of adversely affecting the compressive strength (Wonsiri, 2006). During mixing, some air will be trapped in the cement and create entrapped air voids. They have dimensions of up to a few millimeters and will affect the durability of the concrete. Both chemical damage and physical damage will create cracks and increase the void fraction inside the cement. However, it is hard to detect void size and distribution inside the material. Thus, modern technologies are used to estimate the porosity and the concrete condition state.

2.4 Concrete Deterioration

Cement-based materials are critical worldwide building materials, with over 500 million tons of annual production in the USA (Meyer, 2004). Cement-based materials, as concrete, are also widely used in our infrastructures. Concrete has many advantages, but it can also easily be damaged or deteriorated. Because of that, it is necessary to have a maintenance plan to make these infrastructures work properly and extend their service life.

Evaluating the condition state will be the first step for proper maintenance of these structures. Such efficient evaluation will clearly point out the specific location that needs repairs. Generally, there are two forms of concrete degradation, namely, physical damage and chemical damage. Water is the main agent of deterioration, because when water flows through concrete it causes chemical damage due to reduction in pH when it is

trapped in the concrete, causing physical damage due to freezing/thawing. The water trapped in the concrete will turn to ice under low temperature. When water turns to ice, the volume of the water will increase. When water is frozen the volume of the ice will increase, creating stresses and breaking the concrete. Physical damage also includes abrasion, impact, erosion and cavitation. Erosion will occur due to wind, water and ice, because infrastructures are exposed to nature. Cavitation is caused by water flow. There is abrasion of concrete pavements, concrete slabs and others due to usage.

Chemical damage comprises carbonization, chloride and/or sulfate attack, leaching, bacterial corrosion and others. Review of chemical damage showed that loss of calcium ions is the most common type of deterioration of concrete. When carbon dioxide enters concrete through voids, it will react with calcium, decreasing the pH of the concrete. When the pH drops to below 10, the steel bar will corrode and cause physical damage of concrete. Cement is the bonding material in concrete. Typically, there are four major solid phases in hydrated cement. They are calcium silicate hydrate, calcium hydroxide, calcium sulfoaluminates and non-hydrated cement particles. Because cement is a porous material, water or air can enter the concrete through these pores. Salt water mainly due to flooding will also enter the concrete through voids or cracks, sulfate will react with the calcium hydroxide, and the water itself will dissolve ions such as calcium ions. All these processes will pull out calcium and form gypsum, which is a very soft material of the cement matrix. Then secondary ettringite is formed by the reaction between calcium aluminates and the sulfate. This will cause cracking, swelling, and other damage due to volume increase and high expansion stresses. Since the cement is gradually hardening, this damage mainly occurs in the cortex of the concrete. First,

ettringite was formed during casting while the cement is still in a plastic phase. In most concrete, the chlorides will attack the steel bars and leach calcium hydroxide. Three quarters of the particles in hydrated cement are formed by calcium ions. When concrete has a small number of isolated voids, the permeability of concrete is low. Low permeability concretes are beneficial in two aspects: (1) the impermeability of the concrete reduces the amount of free water that can enter the pores of the hardened concrete from external sources, which means low erosion and small pH change; and (2) the hydrated concrete contains a minimal amount of water that is freezable at normally-encountered temperature ranges or available as free water for ice formation (Pizhong et al., 2012). Chemical attacks will cause the cement to lose the calcium ions and enlarge its voids. When the voids grow and connect with each other, they cause an increase in the permeability of concrete and allow water or air to flow through the concrete. Therefore, the concrete condition state is directly related to its porosity because the degradation of concrete is caused by the intrusion of aggressive agents through interconnected pores.

2.5 Culvert Condition States

Once culverts are in place and operational, they are exposed to internal and external deterioration agents like acids, salts, debris, aging, alkalis, abrasion, erosion and moving traffic. The longer these agents are allowed to act on culverts, the more deteriorated they become. Condition assessment as a process has been summarized in the following steps:

- Measure the extent of damage/deterioration.
- Determine the effect of that damage/deterioration on the condition of facility.
- Set the scale of parameters that describe the condition of the facility as a whole.

- Compare the existing damage/deterioration with previous records of condition assessment.

The proposed condition states for culverts are defined below based on the Sewer Manual, 2001:

Condition State 1: (Excellent)

There is no evidence of active corrosion or deterioration of the culvert with any measurable sectional losses. This state refers to culvert condition where there is no visible deterioration. The time frame a culvert is in this state depends largely on the applied culvert coatings. Since there are no visible signs of culvert deterioration, no action is recommended after culvert cleaning and inspection.

Condition State 2: (Good)

There is minimal likelihood of collapse in the short term, but there is potential for further deterioration. The average sectional loss is less than or equal to 10% of culvert thickness. At such an early stage of its design life, culvert cleaning and painting can prolong service life of such culverts.

Condition State 3: (Fair)

There is minimal likelihood of collapse in the short term, but further deterioration is likely, including swelling with surface pitting. Section loss due to active corrosion is measurable, but does not affect the strength or serviceability of the structure. The average section loss is between 10 to 30% of culvert thickness. Deteriorated culverts can be repaired or rehabilitated provided that the deteriorated culvert could provide the necessary structural strength for the remaining life period. In the long-term repairing may not be a cost-effective option.

Condition State 4: (Poor)

Corrosion is advanced, with collapse likely in the foreseeable future. The culvert exhibits heavy section loss warranting analysis to ascertain the impact on the ultimate strength and/or serviceability of the structure. The average section loss is greater than 30% of section thickness. Under this condition state in-situ culvert rehabilitation techniques are considered. However, common repair techniques would not yield desirable results.

Condition State 5: (Very Poor)

Culvert is collapsed or collapse is imminent. At this point, the culvert cannot be repaired or rehabilitated. The only solution is replacing with a new culvert by either excavation or using trenchless technologies. Some of the trenchless technologies such as culvert slip-lining and culvert bursting can be used.

CHAPTER 3

CULVERT INSPECTION

In order to compute the optimum time and optimum allocation of funds to rehabilitate or replace culverts in a network, those culverts should first be inspected and culvert conditions should be determined (Meegoda et al., 2004). The assessment of culverts is a difficult exercise because they are usually substructures, submerged, or placed in remote locations. There are many inspection methods for culverts and sewers. The most reliable methods for assessing concrete strength are those methods that cause the most damage to concrete (Bungey and Millard l996). Tests that cause little or no surface damage are most suitable for determining comparative concrete quality (Malhotra and Carino l99l). Currently, destructive and non-destructive in-situ tests are used in estimating voids in concrete. Destructive tests require specimens to be removed from the structures to evaluate structural performance. This is not preferable as this test may damage the structure. Non-destructive tests (NDT) and partial destructive tests, which do no damage or slightly damage the structure, are widely used to evaluate concrete performance.

3.1 Non-Destructive Inspection Method for Concrete

Non-destructive testing (NDT) is a branch of engineering that is concerned with all methods of detecting and evaluating defects in materials without causing physical damage to the material or active intervention (Davies and Mamlouk, 1985). Nondestructive testing is used for in-service inspection and for condition monitoring (Van Cauwelaert et al., 1989). When compared with destructive tests, non-destructive

tests will not affect serviceability and safe operation of the structure. All NDT techniques have their applicability and limitations. The pipe materials and their operation will impact the choice of the NDT method selected. Thus, before the selection of an appropriate NDT method, a thorough knowledge of each NDT method, its applicability, and limitations along with a good understanding of the buried pipeline infrastructure is needed (Shivprakash, 2007).

Visual inspection is the most commonly used non-destructive test. A well trained and experienced technician can identify damage and provide information on specific inspection methods needed to identify the problem. Concrete is a composite material consisting of aggregates and a binder phase (Hansen et al., 2004). Reinforced concrete has re-bars. Concrete degradation may occur in the cement phase, the re-bars, the aggregate phase, or a combination of all phases. There are non-destructive tests to evaluate each type of degradation. Usually, half-cell electrical potential and carbonation depth measurement tests are used to detect the corrosion of re-bars in concrete. When using the half-cell electrical potential method, the potential of the re-bars relative to a reference half-cell will be measured. The concrete functions as an electrolyte and the risk of corrosion of the reinforcement in the immediate vicinity of the test location may be related empirically to the measured potential difference (IAEA 2002). If the potential difference is more negative than -0.5 V, the test concludes that corrosion exists. When re-bars are in good condition, the difference in potential should be less negative than -0.2 V. The carbonation depth test shows how deep carbon dioxide invades concrete. Usually a 1% phenolphthalein solution will be sprayed on a sample. The carbonated part will be uncolored and the normal part will be pink. Therefore, the depth of carbonation could be

detected. Some NDT methods, like the Schmidt rebound hammer and penetration resistance tests, evaluate the physical properties of the structure. These two tests are principally surface hardness tests of concrete which allow the strength of the surface layers to be known. Other NDT methods include the cover meter test, used to detect the diameter and depth of the bars under the surface, and the ground-penetrating radar, used to find the location of re-bars.

More than half of NDT methods, such as the Ultrasound method, Radiographic method, Computer Tomography and Infrared Thermography, are used to detect voids and cracks. The black body radiation law stipulates that all objects have infrared radiation when their temperature is above absolute zero. The human eye can only observe this radiation when the temperature is above 500°C, but a thermography camera can capture all frequencies. Heat will flow much faster through solid concrete than through voids. Imaging intact and damaged concrete under the sunlight, the surface heat will transfer into the concrete. Heat transfer is faster through the particles in intact concrete, but this will be slow in damaged concrete. For that reason, the surface temperature will be different. A thermography camera takes a picture of the structure; the localized differences in surface temperature will indicate voids in the concrete.

Radiographic testing and computer tomography are now combined to generate a 3-D map of the sample. This technology is based on the theory of x-ray attenuation in materials. There are two phenomena that cause attenuation: bulk density and the atomic number of the material. An x-ray's radiation intensity will decrease while passing through a material, but absorption or scattering will not occur or will minimally occur when radiation goes through voids. To obtain the 3D voids map, the original sample will

be scanned, vacuum saturated, and re-scanned. By subtracting the two density maps, the porosity distribution can be obtained (de Murphy et al., 2009). To obtain a higher resolution of scanning result, a high-power x-ray source, a larger number of detectors and a scanner with higher pixels will be used.

Ultrasound methods have been used since the mid-1940s for non-destructive testing of cement based materials (Han, 2004). Elastic waves that propagate in a porous material are directly related to its elastic parameters. Usually two parameters, ultrasound velocities and ultrasound attenuation, are measured to estimate mechanical properties of concrete. To get a clear picture of the concrete, high frequency ultrasound is needed. The wave length relates to the wave velocity and the frequency. When the wave length is larger than the voids scale, the wave will pass through the void with no change to the signal and vice versa. For a given material, the wave velocity is fixed. Also, higher frequency means smaller wave length for a given wave velocity. However, with high frequency there is higher attenuation and shorter penetration depth.

Table 3.1 Inspection Method Comparison

Method name	Advantage	Disadvantage
Visual Testing	• Cost and time effective • Provides more information of the specific test method related to the problem for further inspection.	• Test results vary depending on different people and different experiences.
Half-cell electrical potential method	• Time effective and simple process • Easy to find the compressive strength of concrete	• Surface smoothness, age of concrete, moisture content, temperature and the material in the immediate area will impact the result • Only gives the information of the local point/layer to which it is applied.
Schmidt rebound hammer test	• Time effective and simple process • Easy to find the compressive strength of concrete	• Surface smoothness, age of concrete, moisture content, temperature and the material in the immediate area will impact the result • Only gives the information of the local point/layer to which it is applied.
Carbonation depth test	• Cost and time effective • Easy to find the depth of carbonation in concrete	• Evaluates only the local point or area to which the solution is applied • Nothing about the cement phase
Radiographic method	• It can reveal discontinuities that are located on or below the surface • Measures the porosity in concrete	• The portable x-ray units' penetrating ability is less than 300 mm thick • It does not provide the depth of located damage.
Thermography	• Large monitoring capacity. • Fast response rate	• It is dependent on weather and temperature changes. • It does not detect a deep defect within the concrete
Ultrasound Method	• Detects presence of cracks, voids and other imperfections • Detects changes in the structure of the concrete which may occur with time • Values of elastic modulus of the concrete can be determined	• Moisture content will impact result • Influence of temperature of concrete is not taken into account • Shape and size of the concrete member will affect the result • Effect of reinforcing bars is not taken into account

3.2 Visual Method

All methods have their own advantages and disadvantages, and **Table 3.1** summarizes those. But for buried pipes the visual inspection method is the most common inspection method. Visual inspection is a NDT method used extensively to evaluate the condition or the quality of a component (Krstulovic et al., 1996). Visual inspection is a common name for several methods which detect the condition state of concrete based on the surface image or video. Most municipal pipeline systems are inspected visually by mobile Closed-Circuit Television (CCTV) systems or human inspectors (Gokhale et al., 1997). Usually large diameter culverts can be inspected by an experienced worker to track the deterioration. For small diameter pipes, an automatic robot carrying a stationary zoom camera will be sent into the pipe to take the images of the culvert. The image can be analyzed by a well-trained operator. But the CCTV method depends on image quality as well as the inspector's concentration and experience. Also, some types of defects will not be captured by the camera. Accordingly, the CCTV inspection method can provide useful results but it lacks reliability. Other newer methods include Laser based scanning technology, sewer scanner and evaluation technology. All these methods use a camera to take pictures of the culvert. A large amount of information is collected during the process. With the development of computer technology, industry is increasingly using machine vision systems to aid in manufacturing and quality-control processes (Newman and Jain, 1995). The image captured from the camera will be analyzed by the computer to extract defect information. Most computer vision techniques use the results and methods of mathematics, pattern recognition, artificial intelligence, psychophysiology, computer science, electronics and other scientific methods (Besl et al., 1985). Haralick and Shapiro,

2000, distinguished two levels, low and high, to simplify the vision understanding of the computer. Low-level is image processing and high-level is image understanding. The image processing includes gray scale transformation, image smoothing and color image processing. After that, the computer will segment the picture based on Edge-based method, Threshold-based method and Region-based method (Meegoda et al., 2006). Finally, the condition state assessment is based on image segmentation and proper mathematical modelling. The automatic vision method is efficient and commonly used. However, the real world is 3-dimensional and the picture is 2-dimensional. Surface deterioration can be captured by the image, but the culvert has thickness. As mentioned before, porosity is the key characteristic of concrete, but porosity can't be determined by surface images. Some deterioration looks like it may be very serious but is only a surface defect, whereas some cracks are very tiny on the surface but extend well inside of the culvert. A long-term management plan is mainly based on accurate condition assessment. So, to develop a long-term plan, some other inspection method should be considered.

3.3 Ultrasound Method

Ultrasound inspection is performed using a beam of very high frequency coherent sound energy wherein the frequency is much higher than that audible to humans (Birks et al., 1991). Ultrasound techniques that detect defects, measure the mechanical properties, or monitor the state of deterioration of concrete have been a topic of considerable interest to the civil infrastructure community (Malhotra et al., 2004, Bungey et al., 1996). Nondestructive test using ultrasound is a common method to evaluate the performance of concrete structures, where the velocity of the ultrasound is the most widely used

parameter for characterization. Jones (1949) proposed the use of ultrasound velocity measurements for nondestructive evaluation of Portland cement concrete. The ultrasound velocity method applies ultrasound to the test structure, and the wave propagates through the material and is received by the receiver. By analyzing the received signal, the condition of the material can be evaluated. The ultrasound pulse velocity is by far the most widely accepted method for assessing the quality of concrete in structures (Popovics et al., 1992). Later researchers found that in addition to the time domain analysis used in earlier studies, the frequency domain can provide significant information (Wei-Du, 1992, Popovics et al., 1992). There was significant research effort using time-of-flight methods to determine the depth of simulated cracks in concrete where the velocity of wave propagation in concrete is known and a characteristic wave pulse-crack interaction is realized (Lin et al., 1996, Sansalone et al., 1998, Wu et al., 1995). Elastic waves are directly related to the elastic properties of the porous material. Hence, ultrasound velocities can be used to estimate mechanical properties such as modulus of cement. When the ultrasound propagates in a homogeneous, linearly elastic material, the compression and shear wave velocity are related to the media's elastic moduli by the following expressions:

$$V_L = \sqrt{\frac{E(1-v)}{\rho(1+v)(1-2v)}} = \sqrt{\frac{K + \left(\frac{4}{3}\right) G}{\rho}} \tag{3.1}$$

$$V_T = \sqrt{\frac{E}{2\rho(1+v)}} = \sqrt{\frac{G}{\rho}} \tag{3.2}$$

Here V_L is the compression wave velocity, V_T is the shear wave velocity, E is the Young's modulus, v is the Poisson ratio and ρ is the density. These expressions clearly show the impact on ultrasound velocity of elastic properties of cement.

Since for porous material elastic moduli is a function of porosity (Guillon, et al., 2004 and Velez et al., 2001), ultrasound velocity in homogeneous material would depend on porosity. When an ultrasound wave propagates through a material, the wave velocity is related to its density and the elastic modulus (Jeong, 1994) and the elastic tensor depends on porosity.

Over the last past decades, extensive research has taken place in the development of efficient and reliable methods to identify defects (Mukherjee and Pal, 2005). For instance, ultrasound velocity is the most common NDT method used for material characterization. The velocity itself is not sufficient to obtain a clear picture of intensity of damage as it is insensitive to micro cracks. However, attenuation of the ultrasound signal can be effectively used for damage studies as attenuation of sound wave is sensitive to micro cracks. Thus, additional wave characteristics such as wave attenuation as a function of frequency should also be considered to complement the wave velocity information. In idealized materials, the signal amplitude is only reduced by the dispersion of waves. In natural materials, however, wave attenuation or further weakening of the signal is due to two basic causes: scattering and absorption. The combined effect of scattering and absorption produces wave attenuation. Scattering is the reflection of the wave in other directions than its original direction of propagation. Absorption is the process by which energy in the ultrasound beam is transferred to the propagating medium where it is transformed into a different form of energy, mostly heat. The wave carries

energy, and energy cannot be created or destroyed. In the scattering phase, the energy is still the sound energy just traveling in other directions and cannot be received in the direction of propagation. The amplitude decreases due to the energy loss during the wave propagation, but that energy does not disappear: It transfers to other forms of energy.

In this research, high-frequency ultrasound is used to characterize the degraded concrete. The sensitivity of ultrasound is higher when the wavelength becomes comparable to the size of the defect (Ould Naffa, 2002). Although a high frequency wave will cause high attenuation and short penetration distance, it is relevant to culverts. It is not like other concrete structures having a very thick dimension. Compared with a sound culvert, a degraded culvert wall only has several millimeters of thin layer of intact concrete with remainder of higher porosity and higher density of cracks. Thus, ultrasound wave velocity and attenuation can be used as a potential condition assessment technique for concrete.

CHAPTER 4

A VALIDATION OF THE MEASURED VARIATION OF ULTRASOUND WAVE VELOCITY WITH POROSITY OF DRY AND SATURATED CEMENT PASTE

Concrete is a cement-based building material which is critical worldwide, with over 500 million tons of annual production in the USA (Meyer, 2004). Unfortunately, various environmental factors affect cement-based materials, causing degradation, namely, aging, chemical and physical damage, freezing/thawing, fire, and corrosion of reinforcement (Almusallam, 2001 and Cabrera, 1996). The durability and integrity of concrete is affected by cement paste because concrete is made of a matrix of cement mortar and aggregate. Hydrated and hardened cement paste exhibits a multiscale fluid filled pore structure and an interconnected network of solid grains (Sayers, 1993). Hydrated cement paste properties such as strength, durability, shrinkage, and fracture behavior are affected by paste composition and structure (Mondal, et al., 2007). It is well known that aggressive agents such as salt water will move through interconnected pores leading to degradation of concrete. Resistance to penetrating agents is widely recognized as an indicator of the durability of cementitious material (Benavente, et al., 2004). Thus, cement paste porosity is a key structural property that needs to be quantified by performing in-situ tests.

This thesis provides a validation of the measured variation of ultrasound velocity with porosity of dry and saturated cement paste. Cement paste is a multiphase composite consisting of solid cement and microscopic voids filled either with air or water. The void content in cement paste is directly related to the reduction in both its strength and durability. Experimental tests show that ultrasound wave velocity is decreased with the

increase in porosity of cement paste, where the pore size would be similar in dimension to the wave length of the sound wave. For that reason, ultrasound can be used as a potential condition assessment technique and can also be used to characterize the micromechanical structure. However, the variation of ultrasound wave velocity depends on the fluid in the voids. In this research, using finite element analysis of multiphase composite, a theoretical explanation for the variation of ultrasound velocity with porosity of dry and saturated cement paste is provided. Several finite element simulations using software ANSYS and ABAQUS were run for both fully saturated and dry blocks of cement paste with different porosities. Then back-calculated elastic moduli values from ANSYS and ABAQUS simulations were used to compute the wave velocities of both fully saturated and dry cement paste with different porosities. The predicted ultrasound velocities with porosity for both dry and saturated cement paste were compared with laboratory measurements. If a good comparison is obtained, one can confirm that the ultrasound velocity is a function of elastic properties of cement, porosity and compressibility of the fluids in the voids.

Since for the porous material elastic moduli depend on porosity (Guillon, et al., 2004 and Velez et al., 2001), ultrasound velocity in homogeneous material would depend on porosity. When an ultrasound wave propagates through a material, the wave velocity is related to the density and the elastic modulus (Jeong, 1994) and the elastic modulus depends on porosity. Also, since the void content in cement paste is directly related to the reduction in both its strength and durability, ultrasound can be used as a potential condition assessment technique for concrete.

Since cement paste forms the matrix phase of mortar and concrete, in order to fully understand the behavior of mortar and concrete the first step would be to understand the performance of cement paste. Most researchers investigated performance of cement paste by assuming the cement paste as a two-phase homogeneous non-porous paste with pores. Maalej, et al., 2013, used different water/cement ratios to create different specimens with varying porosity values. Broadband ultrasound spectroscopy (Eggers and Kaatze, 2006) was used to induce ultrasound wave transmission into the materials using a single transducer. Ultrasound with 1MHz frequency was applied to the sample. To transfer sufficient energy to the sample, typically, adequate coupling should be applied. However, to avoid water penetration into the sample during the test, direct contact was chosen to instead of immersion coupling. The single transducer was used as both transmitter and receiver. The time to receive two signals $s1(t)$ which is the signal reflected from the top of the sample and $s2(t)$ which is the signal reflected from the bottom of the sample were read. Then, pulse velocity was obtained using the following equation:

$$V_L = \frac{2e}{\Delta t} \tag{4.1}$$

where e is the thickness of the sample and Δt is the time delay between signals $s1(t)$ and $s2(t)$. Experimental tests showed that the ultrasound wave velocity of saturated concrete of given porosity is higher than that of dry concrete. The results show that the contribution of moisture saturation on the ultrasound wave velocity is significant. Maalej, et al., 2013, showed that the ultrasound wave velocity decreased with the increase in porosity of cement paste (see **Figure 4.1**).

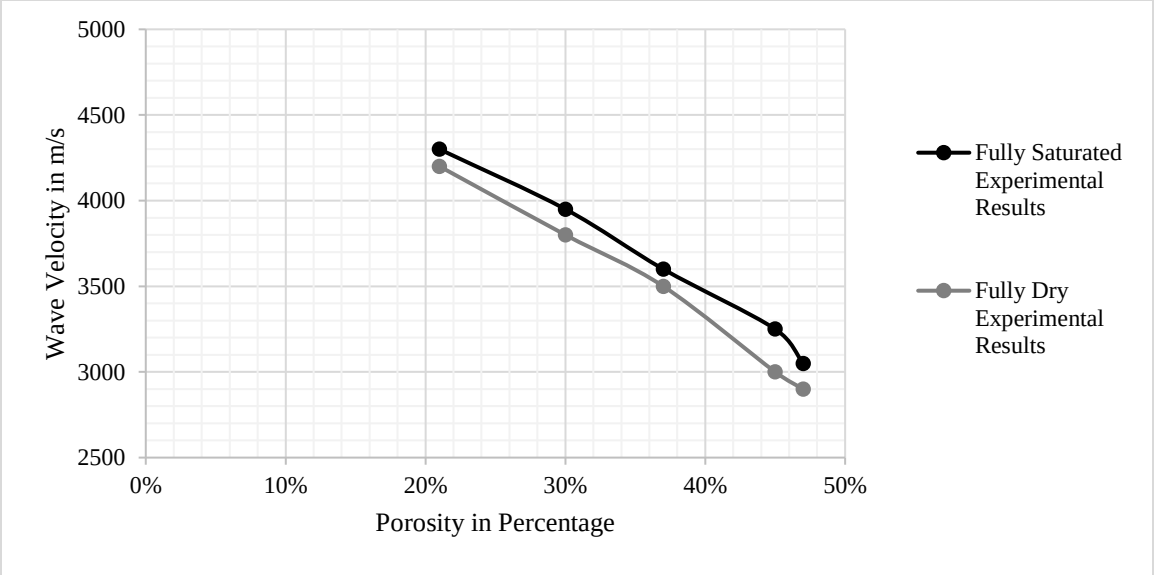

Figure 4.1 Experimental Data of Fully Saturated and Fully Dry Wave Velocity with Porosity (Maalej, et al., 2013).

However, there is no clear explanation on how the saturation degree will impact the ultrasound wave velocity. Maalej, et al., 2013, also compared the above experiment results to predictions from four theoretical micromechanical models. All micromechanical models could not accurately predict the experimented results especially when the voids are filled with air or water. Because of this, this research attempts to provide a theoretical basis for the measured variation of ultrasound velocity with porosity of dry and saturated cement paste using the Finite Element Method.

4.1 Finite Element Method Model Setup

Finite Element Method (FEM) is a numerical method for predicting how an object reacts to real-world forces and energy. It does not yield an exact solution, but rather an approximation to the exact solution. Since the late 1960s, the Finite Element Method has

been used for a wide range of engineering problems. By using the FEM, the continuous physical problem can be solved to calculate the discretized nodal values. FEM has been known to accurately calculate the elastic properties of objects (Cook, et al., 1989) and was successful in estimating the elastic moduli of composite materials (Bentz, 1997 and Pierard et al., 2007). In this research two commercially available software packages, ANSYS and ABAQUS were used, where the elastic modulus of cement paste with different porosities was back-calculated. Ultrasound testing in concrete is mainly used to evaluate the performance of the material under compressive loads (Hernández, 2002). As a result, in this research model simulations will be performed of material subjected to compressive loads.

4.1.1 Simulation of the Model Geometry

Like most of the micromechanics models, cement paste will be treated as two-phase composite including non-porous cement and voids. Consequently, a solid cement block is proposed and voids in the cement are idealized and concentrated together as inclusions inside solids. By adjusting the volume of the inclusions, different porosity values of cement can be simulated. Also by adjusting the material inside the inclusions, one can simulate dry and fully saturated situations. Before the geometry is scoped, the material properties should be input to the program.

4.1.2 Void Shape

In micromechanical models, inclusion shape is usually ignored such as in bounding methods of Hashin, 1960, Hashin and Shtrikman, 1963, and Walpole, 1966 or by using

specific shapes. It is convenient to have symmetrical inclusions such as ellipsoids, spheres, elliptical cylinders, circular cylinders, penny or needle shaped ellipsoids. Consequently, symmetrical inclusions are used in this research. The orientation will be at the center of the cement block related to the global coordinate system or symmetrically distributed inside the cement block.

4.1.3 Element Types and Boundary Condition

A 3D ANSYS SOLID element was used to simulate the non-porous cement paste. A 3-D and 8-node linear elements with three degrees of freedom for each node-translation in the X, Y and Z directions was used. The Hydrostatic fluid element (HSFLD242) was used to simulate the fluid inclusion such as a contained fluid inside a solid model and modeling fluid-solid interaction with incompressible or compressible fluids under uniform pressure. It can be used in geometrically linear as well as nonlinear static and transient dynamic analyses (Eric, 2011). When applying a vertical stress as a surface load on the top element face, it will be supported by the bottom face of the block, hence there is no vertical displacement and zero rotation of the bottom surface. The remaining four sides will be free boundaries.

4.2 FEM Simulation

Two different FEM software packages ANSYS and ABAQUS were used in this research, where ABAQUS was used to compare and validate ANSYS results.

4.2.1 FEM Simulations

First, the engineering properties of material should be supplied. In order to compare to the experimental results, the material engineering properties have to be the same as that reported in Maalej, et al., 2013. Their detailed experimental results were listed in Soltani, 2010. The values of bulk and shear moduli for the cement paste at zero porosity were obtained from ultrasound velocity measurements and ρ by using an inversion of Eqs. (3.1) and (3.2) and are listed in **Table 4.1**. The Density of the cement paste at zero porosity and those of pores (Maalej, et al., 2013) are listed in **Table 4.2**.

Table 4.1 Cement Paste Elastic Moduli at Zero Porosity

	Cement Paste at Zero Porosity		Pores	
	Bulk (MPa)	Shear (MPa)	Bulk (MPa)	Shear (MPa)
Dry	30,182	17,662	0	0
Saturated	33,919	17,884	2,200	0

Table 4.2 Densities of Dry and Saturated Phases

	Dry (kg/m^3)	Saturated (kg/m^3)
Cement Paste at Zero Porosity	2,579	2,579
Pores	1.204	1,000

The Young's modulus and Poisson's ratio of zero porosity cement paste is 44,337 MPa (9.26e8 Psf) and 0.28 respectively, which correspond to a wave velocity of 4688 m/sec (15381ft/sec) (Maalej, et al., 2013). The ultrasound wave velocity can also be calculated by elastic properties obtained from the FEM simulations. But to confirm the result, a pure solid block model was prepared with the geometry 0.3m*0.3m*0.3m (1FT*1FT*1FT). ANSYS was meshed with MultiZone method and Hexa Mapped mesh type as shown in **Figure 4.2** and the elastic modulus was back-calculated. Application of the vertical stress to back-calculate the elastic modulus to the top surface caused four side faces to expand.

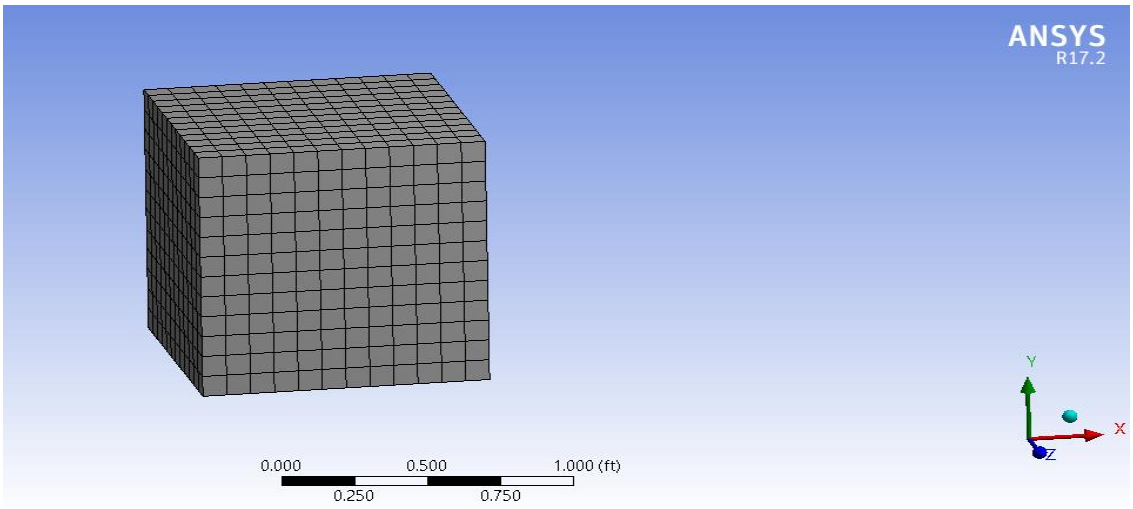

Figure 4.2 Pure block test model after mesh.

4.2.2 Back-calculation of the Elastic Modulus

After running the model, the elastic modulus should be back-calculated. According to the definition of the Young's modulus and Poisson's ratio, the displacement is the most important value obtained from simulation because Young's modulus E can be calculated

by dividing the tensile stress by the extensional strain in the elastic portion of the physical stress-strain curve.

$$E = \frac{F * L_0}{A_0 * \Delta L} \tag{4.2}$$

Where E is the Young's modulus, F is the force exerted on an object under compression; here 0.34 Mpa (7200Psf) was used. A0 is the actual cross-sectional area through which the force is applied, ΔL is the amount by which the length of the object changes, and L0 is the original length of the object. The F over A0 is equal to the applied stress Δσ and the L0 is equal to the original block height. Therefore, by obtaining the average displacement and using Equation (4.2), the Young's Modulus can be back-calculated. By using Equation (4.2), the Young's Modulus was obtained as 44,337Mpa (9.26e8 psf). Compare this value with the input: it is exactly the same. Please note that with an inclusion or a void, the back-calculated Young's Modulus would be lower than that of concrete without voids. **Figure 4.3 (a)** Shows by adding a hole to this model, the ΔL increases and causes the Young's Modulus to decrease to 39116 Mpa (8.18E8 psf). To test the accuracy of the simulation, a 20-node quadratic cubic element was used to compare with the 8-node linear cubic element. Displacements for both 8-node and 20-node element model were the same, confirming the adequacy of 8 node linear cubic element (see **Figure 4.3 (b) and (c)**.)

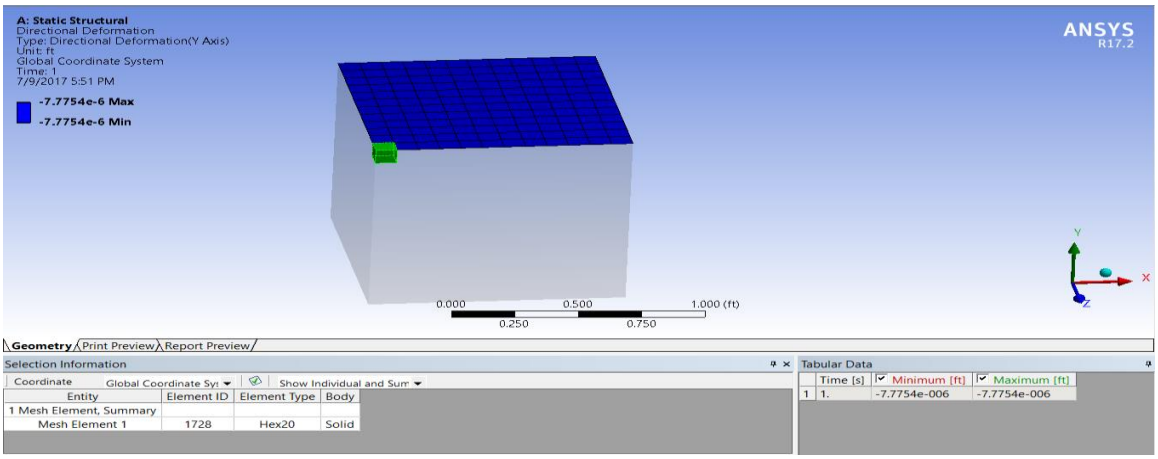

(a)

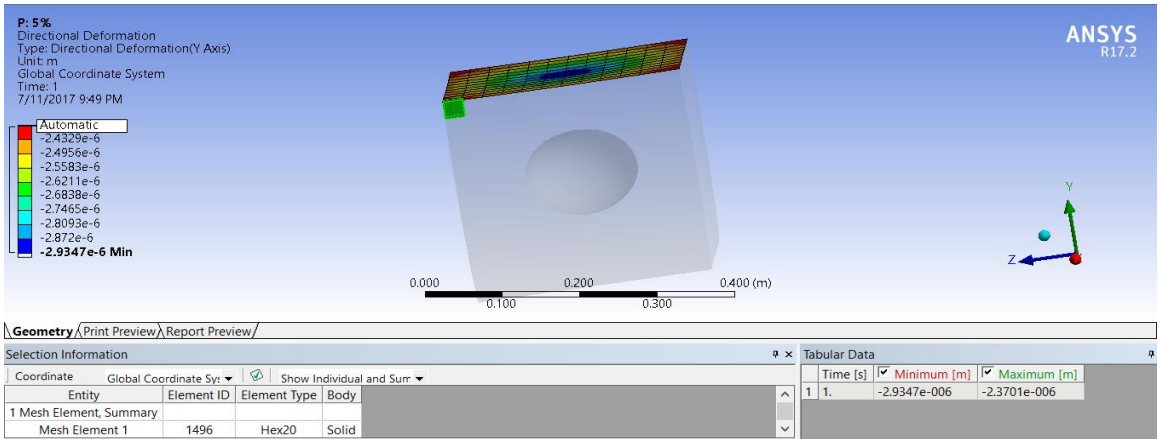

(b)

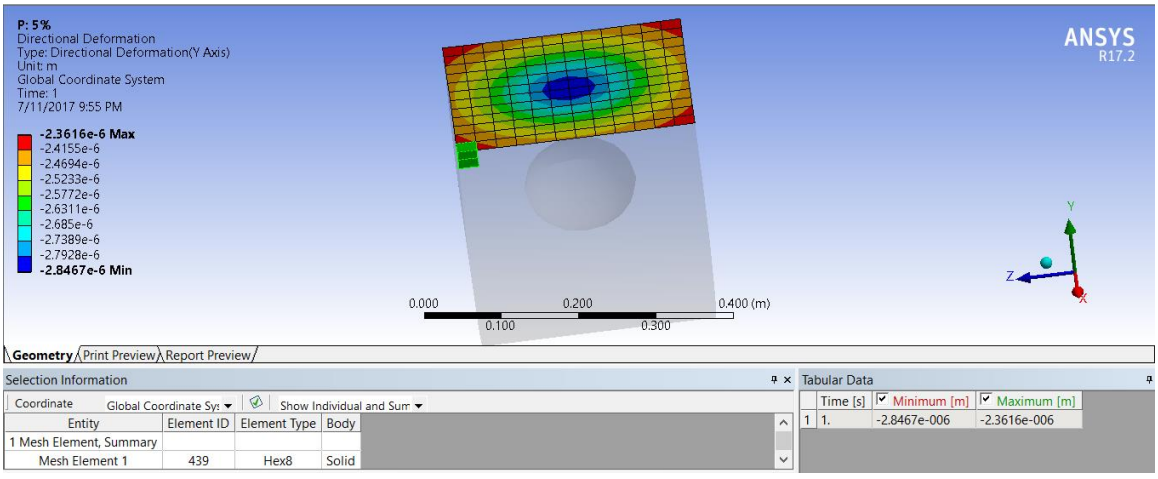

(c)

Figure 4.3 Length of the object changes.

4.2.3 Shape of Inclusions

As mentioned before, modeling geometry inclusions such as ellipsoids, spheres, elliptical cylinders, circular cylinders, penny or needle shaped ellipsoids is often used in micromechanical models. Ellipsoidal inclusions can be characterized by the aspect ratio, which is the vertical axis over horizontal axis.

Maalej (2011) showed five different aspect ratios:

$\alpha = 1$spherical inclusion;

$\alpha > 1$prolate spheroid (needle shaped inclusion);

$\alpha < 1$ oblate spheroid (penny shaped inclusion);

$\alpha = 0$ flat disk;

$\alpha = \infty$ cylinder.

The objective of this research is to compare the estimated wave velocity using simulation with the experimental data. In this research, circular cylinders and spheres were chosen as inclusions in the model. As the cement paste is being considered as a two-phase material, the inclusion is represented as a single equivalent inclusion or void at the center of the block. The size of the inclusion was adjusted to represent different void ratios. In other words, for different porosity values of cement paste void volumes were computed to calculate equivalent radius of circular cylinder and the sphere. Then with different size inclusions, the simulation was repeated with the same assigned materials mesh and boundary conditions. Using the average displacements from simulation and Equation (4.2) Young's modulus was calculated. For a certain porosity, different shapes like sphere and circular cylinders can be calculated. With the same porosity of 5%, the Young's Modulus of the model with the sphere shape inclusion was 39,116Mpa (8.18e8

psf), that for the model with the ellipsoid shape inclusion was 40,267Mpa (8.41e8 psf) and that for the model with circular cylinders was 38,399Mpa (8.02e8 Psf), with a maximum error of 5% with respect to spherical inclusion. Test results are shown in **Figure 4.4** and listed in **Table 4.3**. Based on simulation results, the shape of the inclusion has minimal impact on the back-calculated Young's modulus, so spherical voids were used in remaining simulations.

Table 4.3. Summarization of Back-calculated Young's Modulus and Associated Errors for Different Inclusion Shape

Inclusion shape	Porosity	Young's Modulus From ANSYS	Error
Sphere	5%	39166 MPa	
Circular Cylinder	5%	38399 MPa	2%
Ellipsoid with Axial Ratio of 1.3	5%	40267 MPa	3%

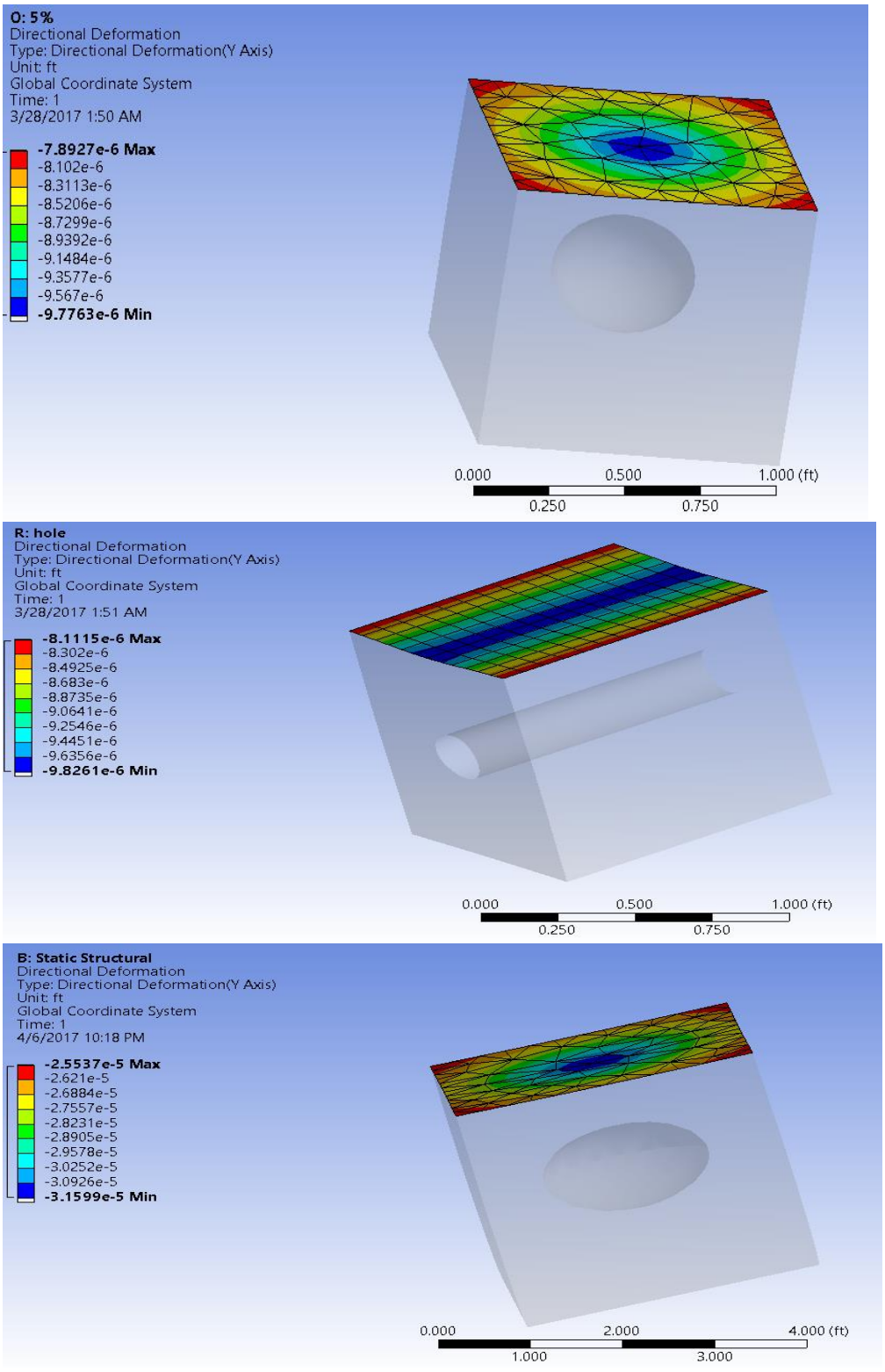

Figure 4.4 Different shape of inclusion.

4.2.4 Number of Inclusions and their distribution

In Section 4.2.3, one equivalent inclusion was used to represent the voids in the simulation; in reality even though cement was considered as a two-phase composite, voids in the concrete are randomly distributed. Thus, it is necessary to evaluate the impact of the above assumption. For a given porosity value of 10% several inclusions with varying distributions were simulated. For this purpose, 2, 4, 8, 9 and 10 equivalent spheres at different location were used, as shown in **Figure 4.5**.

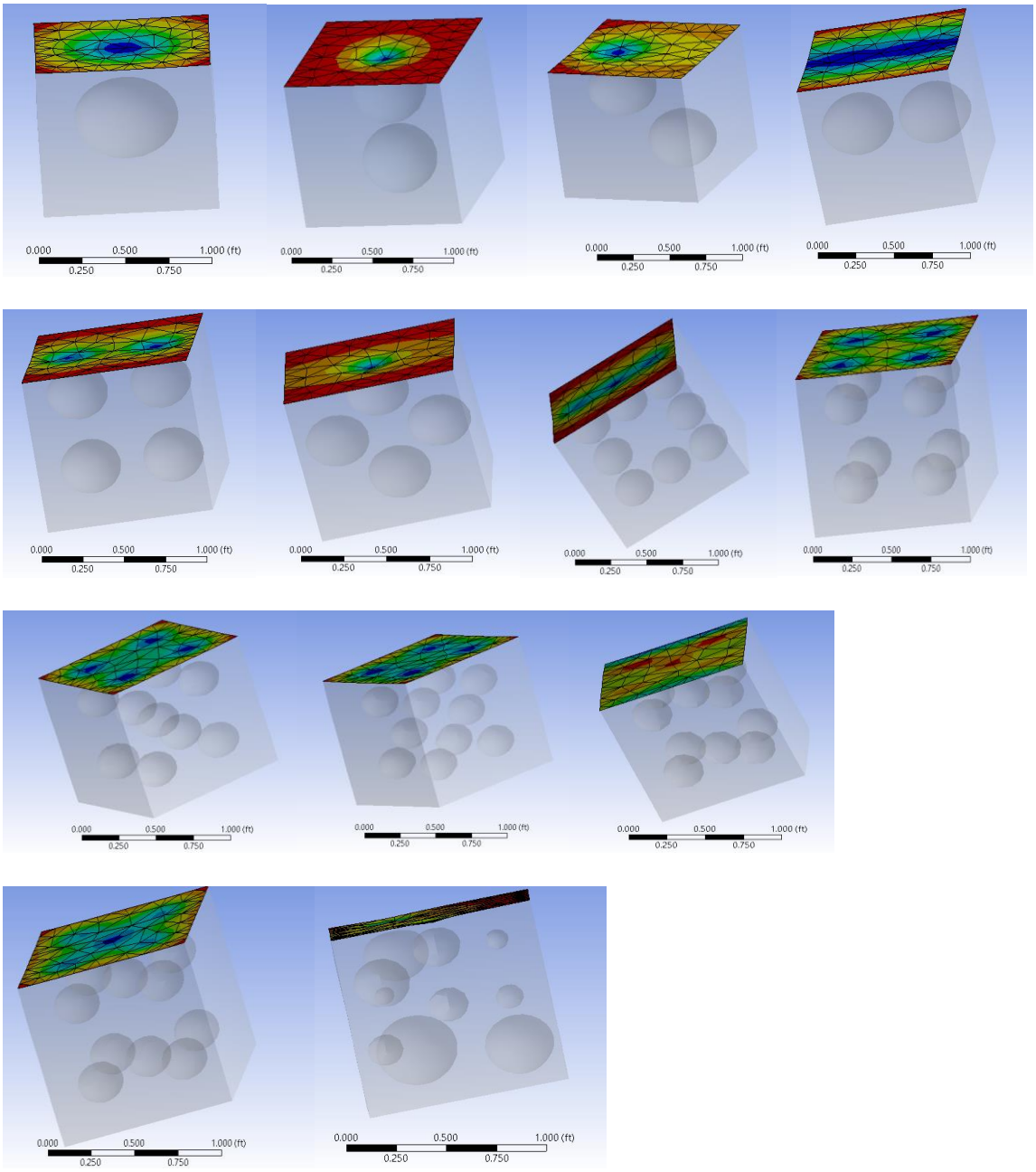

Figure 4. 5 Different numbers and distribution of spheres.

For example, two spheres can be placed vertically or horizontally. Similarly, 4, 8, 9 and 10 spheres were also placed at separate locations. **Table 4.4** compares impact of number of equivalent inclusions and their distribution for a given void ratio showing a maximum error of 5%.

Table 4.4 Summarize of Back-calculated Young's Modulus and Associated Errors for Different Numbers and Distributions of Spheres

Numbers and distribution	1 Single Sphere	2 Spheres Random	2 Spheres Vertical	2 Spheres Horizontal	4 Spheres Square	4 Spheres Star
Young's Modulus (Mpa)	37059	36819	38112	35718	37969	37115
Error		1%	3%	4%	2%	0%
Numbers and distribution	8 Spheres Vertical	8 Spheres Horizontal	9 Spheres	10 Spheres Horizontal	10 Spheres Vertical	10 Spheres Varied Sizes
Young's Modulus (Mpa)	38830	37825	37011	38017	37825	36820
Error	5%	2%	0%	3%	2%	1%

As shown in **Figure 4.5**, when results for 8, 9 and 10 inclusions with their distributions representing much closer similarity to real distribution of voids in cement paste were compared with those of one equivalent inclusion at the center, the error was found to be very small. In order to simplify computation, a single sphere at the center of the block was used for remaining simulations.

4.2.5 Variation of Porosity

As mentioned before, by adjusting the size of the sphere, the model can simulate different porosity values. Thence, five different porosity values were simulated. By using a given porosity value, the total volume of the void can be calculated and therefore the radius of sphere is calculated based on that volume. **Figure 4.6** shows the simulation results and the back-calculated computed Young's modulus values are shown in **Figure 4.7** with corresponding porosity values, which shows that the Young's modulus will decrease with the increase of porosity.

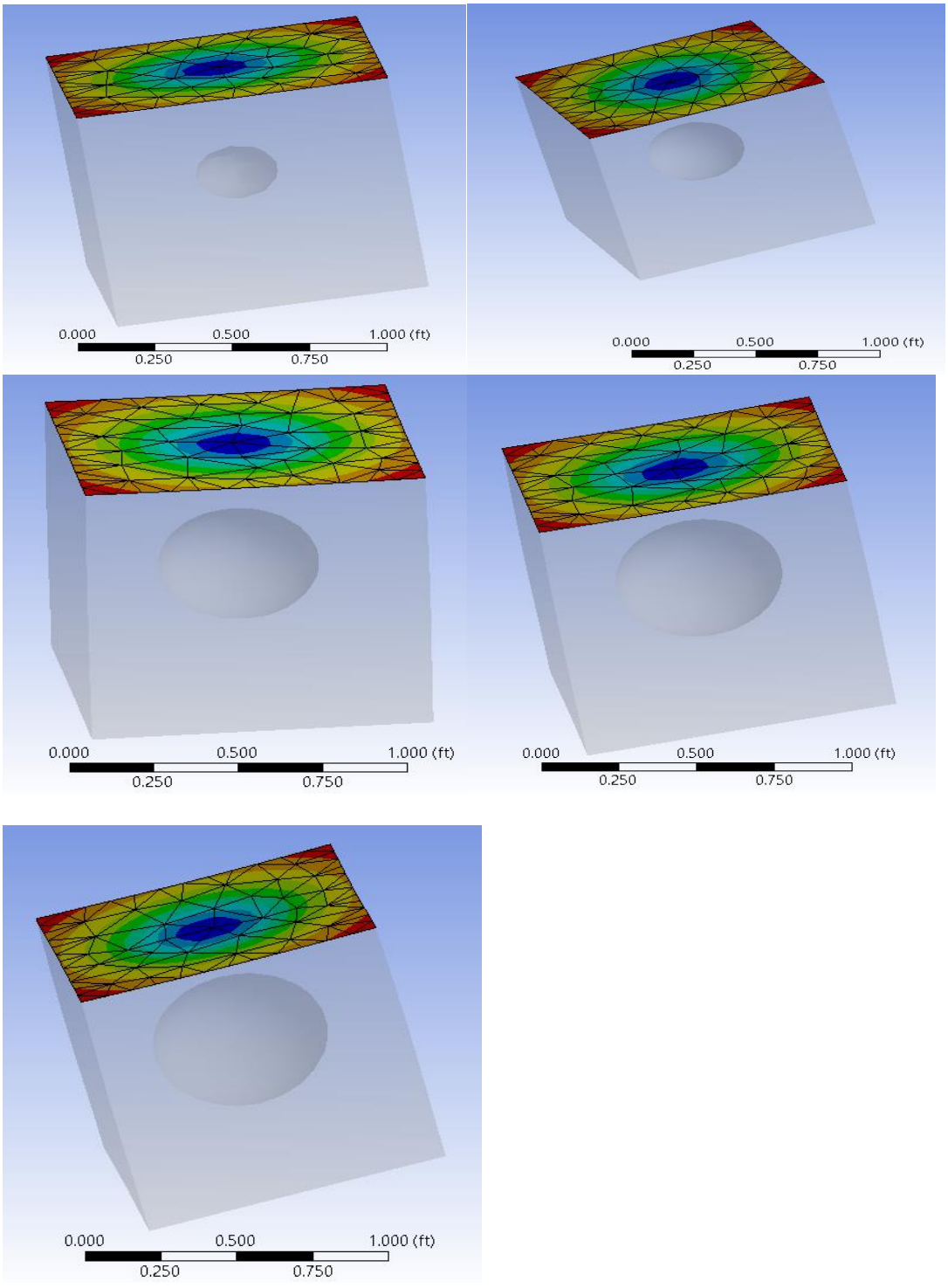

Figure 4.6 Different size spheres simulating different porosities.

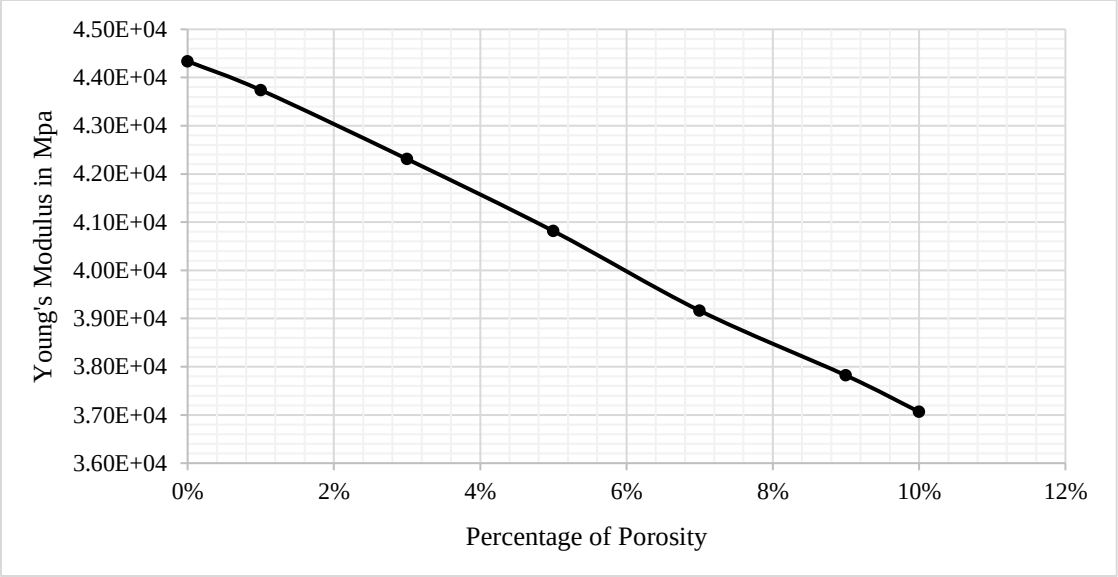

Figure 4.7 The variation of the Young's modulus with porosity.

4.2.6 Dry and Fully Saturated Inclusions

To test the changes in ultrasound velocity in dry or moisture saturated cement paste, different fluid elements were assigned to the sphere to simulate air and water filled voids. ANSYS can simulate the fully enclosed fluid by using HSFLD242, and ABAQUS can simulate the same using the concept of fluid cavity. Hence, both software provide the opportunity to test dry and fully saturated states by defining the inner surface of the inclusion with the correct type of element. For such simulations, first, the element type, e.g. air or fluid, should be selected. Then the element properties such as density, pressure or bulk modulus should be supplied, where the bulk modulus is the most important property of the element for both software. **Figure 4.8** shows the fluid element used in this simulation. When voids are filled with different fluids, the bulk modulus of the fluid would considerably impact the compressibility of the voids.

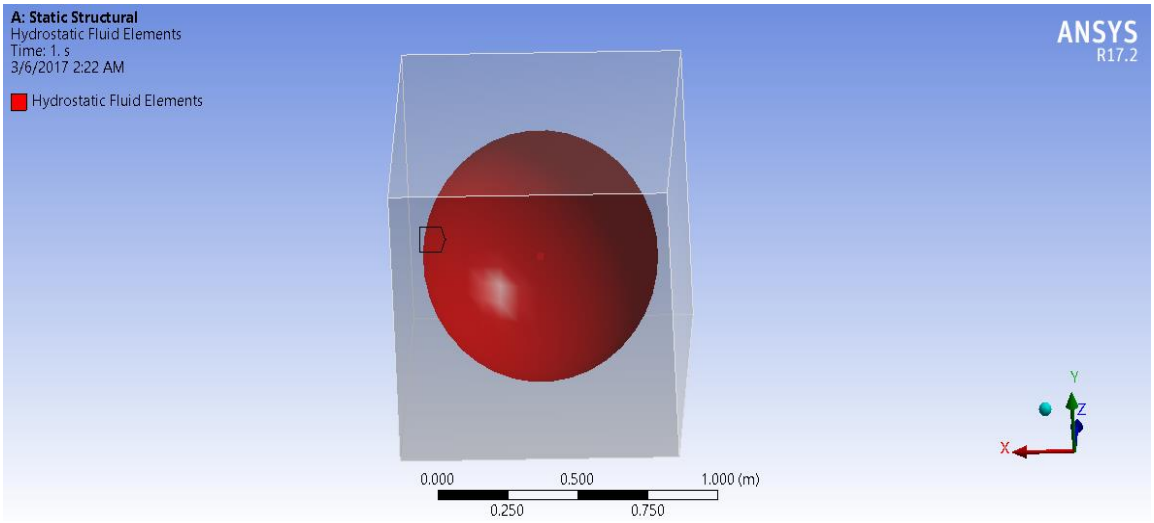

Figure 4.8 Hydrostatic fluid element.

4.2.7 Simulation Results

In this research, it was attempted to simulate the porosity values reported in Maalej, et al., 2013, specifically 21%, 30%, 40% and 45%. The void volume corresponding to above porosity values for one cubic foot volume was first computed. Then based on the above void volumes, radius of inclusion of the sphere at the center of the block was computed. After that, applying the zero-void elastic modulus of the cement paste was assigned to the block and the material of the inclusion defined as air. The same process was used to generate mesh and the previously defined boundary conditions were applied. By applying the vertical pressure on the top surface of the block, the enclosed fluid will expand and increase in fluid pressure inside the void. Consequently, the correct fluid pressure should be applied to the model. However, it is difficult to obtain a deformation versus pressure relationship for the inclusion. Please note that air is compressible and water is incompressible. As a result, the pressure inside the inclusion was assumed as still equal to 1 standard atmosphere and the applied pressure of 0.34Mpa (7200 psf) respectively to air

and water inclusion. First, the fluid element was assigned as air to simulate the dry condition. The initial pressure of the air in the sphere is one atmosphere and after the boundary conditions were applied, the pressure inside the inclusion was assumed as one atmosphere. Then, the average displacement in Y axis was used to compute the Young's modulus by using Equation (4.2). However, to back-calculate the wave velocity, Poisson's ratio should be determined. Accordingly, the average lateral displacement values were used to calculate the Poisson's ratio and the modified density based on the porosity. Finally, Equation (3.1) was used to obtain the longitude wave velocity. Then the radius was changed to simulate the different porosity values and the above procedure was repeated. To simulate the fully saturated situation, a fluid element was used instead of air and the above was repeated. But the pressure inside the inclusion is increased to applied pressure of 0.34Mpa (7200 psf). ANSYS vacuum simulation which was reported in **Figure 4.7** was extended and used to compare with the dry and saturated cement paste results. **Figure 4.9** shows the simulation results.

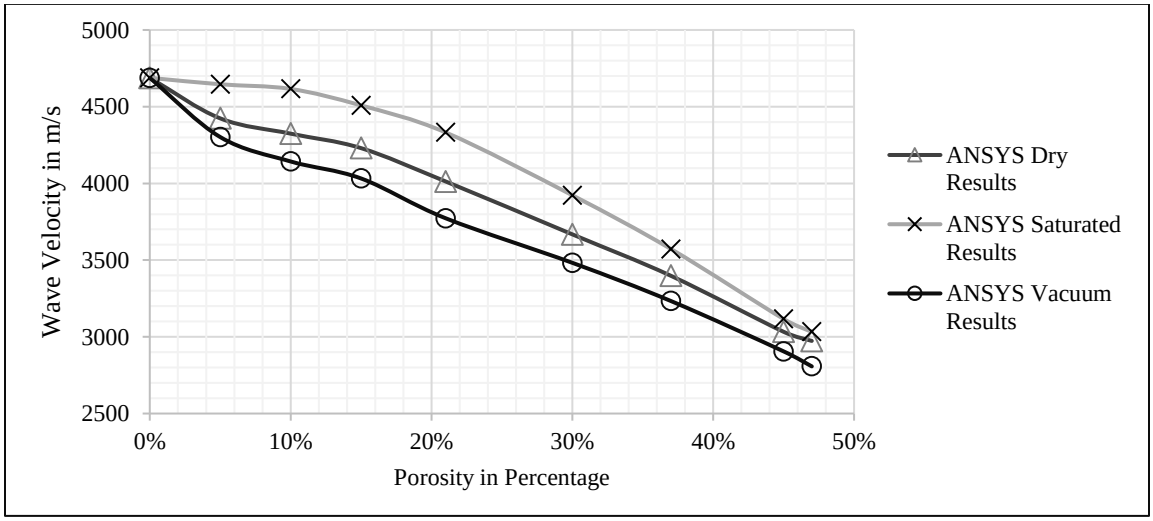

Figure 4.9 Variation of wave velocity with porosity based on ANSYS fully saturated, fully dry and vacuum results.

4.3 Discussion of Results

Figure 4.9 shows the impact of the compressibility of the material in the inclusion for a given porosity, with vacuum producing the lowest wave velocity followed by the dry void filled with air and finally the voids filled with incompressible water. Please note that for a porosity value of 21%, **Figure 4.9** shows wave velocities of 3775m/sec (12385ft/sec) for a vacuum inclusion with no compressibility of the inclusion, 4000m/sec (13123ft/sec) for an inclusion filled with partially compressible air, and 4325m/sec (14190ft/sec) for an incompressible inclusion filled with water. Compare those to a value of 4688m/sec (15380ft/sec) for no inclusion. The results are listed in **Tables 4.5 and 4.6**.

Table 4.5 Results for Simulating Different Porosity Under Fully Dry Situation

Fully Dry				
Porosity	Young's Modulus E in (Mpa)	Poisson's ratio	Density ρ in (kg/m^3)	Velocity in (m/s)
5%	41998	0.22	2450	4424
10%	38020	0.22	2321	4324
15%	34356	0.22	2192	4230
21%	28739	0.22	2038	4013
30%	21276	0.22	1806	3668
37%	16433	0.22	1625	3398
45%	11431	0.22	1419	3033
47%	10590	0.22	1367	2973

Table 4.6 Results for Simulating Different Porosity Under Fully Saturated Situation

Fully Saturated				
Porosity	Young's Modulus E in (Mpa)	Poisson's ratio	Density ρ in (kg/m^3)	Velocity in (m/s)
5%	42213	0.28	2500	4646
10%	40349	0.28	2421	4616
15%	37236	0.28	2342	4508
21%	32997	0.28	2247	4332
30%	25340	0.28	2105	3923
37%	19913	0.28	1995	3572
45%	14193	0.28	1868	3116
47%	13214	0.28	1837	3033

ANSYS model simulation results show that the ultrasound velocity will decrease when the cement paste porosity is increased no matter whether it is dry or saturated. As mentioned before, ultrasound testing in concrete is mainly used to evaluate the quality of the material based on its porosity. Typically, larger porosity produces weaker cement. With higher porosity of concrete, aggressive fluids can enter concrete and leaching of calcium can occur, forming weaker material such as gypsum. Also, voids filled with fluid have much lower elastic modulus. The ANSYS result also shows that, under the same applied vertical stress, there is higher deformation of the block with higher porosity, proving that the material becomes weaker when the porosity increases. From the simulation result, the ultrasound velocity will decrease with the increase in porosity, because higher porosity means lower elastic modulus. Thus, the ultrasound method is a potentially powerful tool for the condition assessment of concrete. With degradation, the porosity is increased, causing the material to become weaker. On that account, ultrasound velocity via elastic modulus and the porosity can be used to estimate the condition state

of structures. Maalej, et al., 2013, showed that the ultrasound wave velocity decreased with the increase in porosity of cement paste. However, there is no theoretical basis for the measured variation of ultrasound velocity with porosity of dry and saturated cement paste.

This study attempted to provide a theoretical explanation for the variation of ultrasound wave velocity with porosity for both dry and saturated cement paste using ANSYS simulations. In ANSYS simulations, the fluid is defined by the Hydrostatic fluid element, which needs the bulk modulus of fluid. The bulk elastic properties of a material determine its elastic deformation and hence the wave propagation. With different bulk moduli, the compressibility values of the air and water voids are different. As a consequence, the deformation of void filled with air or water will be quite different. Cement paste filled with a water void is much harder to compress due to the higher bulk modulus of water, when compared with that of a void filled with air. Ultrasound testing of concrete is mainly used to evaluate the quality of the material, via its compressibility. Ergo, voids filled with different fluids will have different moduli due to the different enclosed fluids. As a result, the wave velocity of saturated cement paste is faster than that of dry cement paste at the same porosity due to the lower compressibility of water in the voids. This causes the elastic modulus of saturated cement paste to be higher than that of dry cement paste for the same porosity. Back-calculated, the wave velocity of saturated cement paste is faster than that of dry cement paste, as shown in **Figures 4.10 and 4.11** show comparison of measured results from Maalej, et al., 2013, and simulation results from this research confirming a good comparison. **Figures 4.10 and 4.11** also provide a theoretical basis to validate the experimental results of Maalej, et al., 2013.

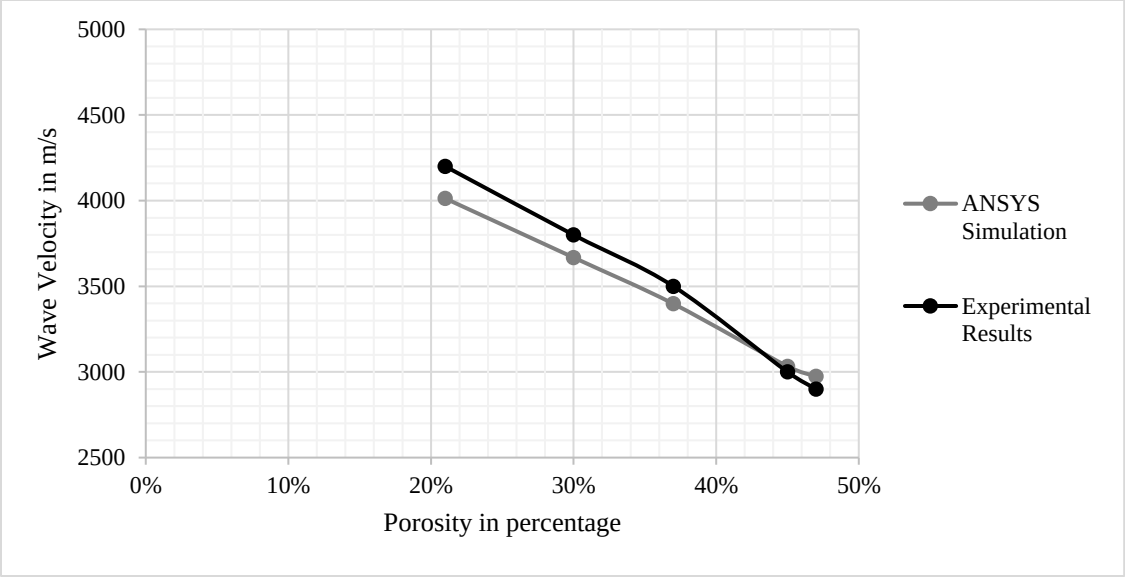

Figure 4.10 Comparison of back-calculated wave velocity of fully dry cement paste with those measured (Experimental results Maalej, et al., 2013).

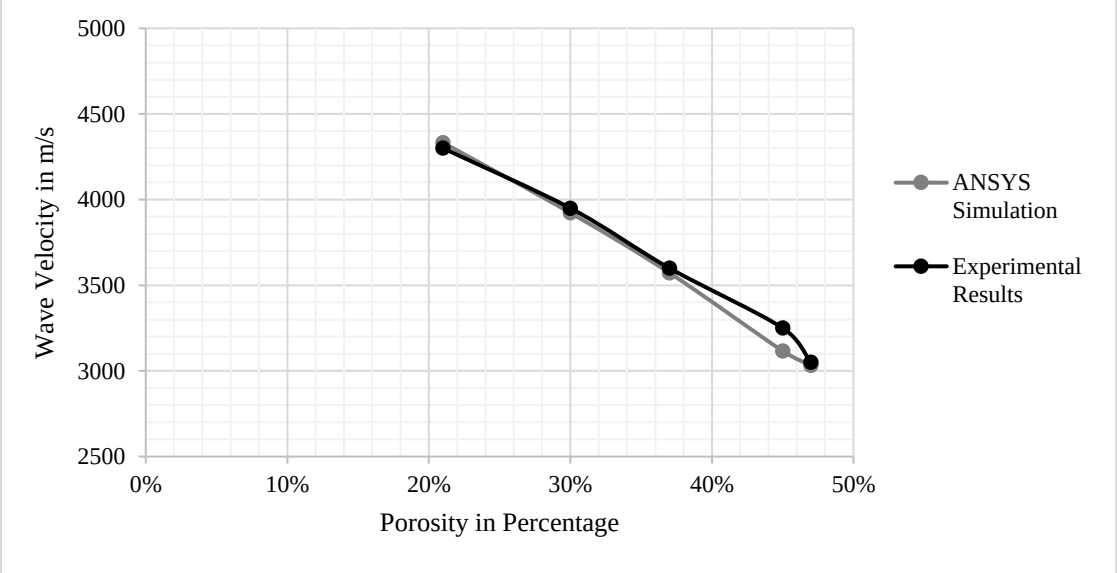

Figure 4.11 Comparison of back-calculated wave velocity of fully saturated cement paste with those measured (Experimental results Maalej, et al., 2013).

CHAPTER 5

ULTRASOUND METHOD

As mentioned before, the Ultrasound method has high potential for nondestructive evaluation of Portland cement concrete. Ultrasound phase velocity, which is the most common application of ultrasound testing, can indicate concrete quality and is used extensively in Civil Engineering. But ultrasound velocity is only sensitive to voids when their size is comparable to wavelength (Ould Naffa, 2002). Normally, low frequency ultrasound such as 50 kHz was applied for nondestructive testing of piles. However, this frequency can only detect large voids of size greater than 1". The voids in concrete pipes carrying fluids are μm to mm size. Because of that, no damage will be detected with low frequency ultrasound, because of large wavelength, where waves will have no impact on the small voids. When wave length matches void size, the sensitivity of ultrasound will be increased. The wave length is equal to the sound speed over frequency. Therefore, to accurately characterize small voids in concrete, high frequency ultrasound around 1 MHz is required.

5.1 Ultrasound Velocity

One of the most promising methods for concrete nondestructive testing is ultrasound velocity. The fundamental of this method is that material physical properties will contribute to the motion of any wave traveled. Since the 1940s, the pulse velocity of longitudinal stress wave was applied to measure the transmission velocity in concrete (Malhotra, et al., 2003). This test method is applicable to assess the uniformity and

relative quality of concrete, to indicate the presence of voids and cracks, and to evaluate the effectiveness of crack repairs (ASTM, 2002). It has a combination of an easy test procedure and accuracy, at a relatively low cost (Jones, 1960). This technique can detect areas of internal cracking, internal delamination, and relative strength parameters (Kaplan, 1958, Malhotra, 1991). The test is described in ASTM C597. Komlos, 1996, provides a critical comparison of several standards for the ultrasound velocity method from different countries.

In past decades, extensive research has been performed on the use of Ultrasound Pulse Velocity to determine concrete quality through nondestructive tests. It is possible to assess the quality and characteristics of concrete structures at a site by measuring the transit time of an ultrasound pulse velocity through the concrete (SolísCarcaño et al., 2008). The theory behind this method is that the density and the elastic modulus of the concrete will impact the ultrasound transmission velocity. To measure the velocity, a pair of transducers must be used to apply and receive the ultrasound signal. The signal can be used to determine the dynamic elastic modulus and Poisson's ratio of concrete. Many factors affect the results: the surface and the maturity of concrete, the travel distance of the wave, the presence of reinforcements, mixture proportion, aggregate type and size, age of concrete, moisture content, etc. However, factors significantly contributing to the ultrasound pulse velocity may have little influence on concrete strength (Lin et al., 2003). The ultrasound test methodology in concrete is based on the fact that the propagation time expresses the average density of the material, which might be correlated with the mechanical properties, such as the compressive strength and the elastic modulus (Popovics, 1998).

5.2 Ultrasound Attenuation

Ultrasound measurements include both velocity and attenuation of the ultrasound pulse to estimate mechanical properties of concrete. The existing literature shows that ultrasound velocity will decrease when the porosity of concrete increases. However, the velocity is not as sensitive as the wave amplitude for monitoring the microstructure of the concrete. The reduction of wave amplitude is called attenuation. In idealized materials, the signal amplitude is only reduced by the spreading of the wave. For natural materials, however, wave attenuation or further weakening of the signal is due to two basic causes: scattering and absorption. The combined effect of scattering and absorption produces wave attenuation. Scattering is the reflection of the wave in other directions than its original direction of propagation. Absorption is the process by which energy in the ultrasound beam is transferred to the propagating medium, where it is transformed into a different form of energy, mostly heat. The wave carries energy, and energy cannot be created nor destroyed. In the scattering phase, the energy is still sound energy traveling in other directions and is diverted from the direction of propagation. The amplitude decreases by means of the energy lost during the wave propagation, but that part of the energy cannot disappear and it is just transferred to other forms. Typically, ultrasound is a sound wave carrying energy. When ultrasound propagates in the concrete, it will exhibit a high degree of energy loss due to absorption and scattering.

5.2.1 Wave Propagation in Concrete

The response of a heterogeneous elastic body to a propagating wave is a function of the wavelength in comparison with the length scale of the heterogeneities (Anugonda, 2001).

When the wavelength is comparable to the scale of the microstructure of the concrete, scattering will occur. Due to the scattering, the wave energy will attenuate. The energy is not disappearing or missing; it just scatters in other directions which do not coincide with the incident wave. The wave amplitude will decrease due to this scattering loss. Scattering is an important attenuation effect in heterogeneous materials. When considering concrete as a two-phase composite, the interface of two varied materials will have different acoustic properties and the wave scattering will happen at this interface and cause the wave energy to attenuate. The diffusion process can describe the ultrasound energy transfer through highly scattered media. The energy flow will be governed by the diffusion equation which also includes dissipation. Dissipation from the viscoelastic cement matrix is another part of wave attenuation. Damage in concrete will affect both diffusion and dissipation. Diffusion and dissipation can quantify the material microstructure and the viscoelastic properties, respectively. However, traditional coherent ultrasound attenuation is really a combined effect of these two different attenuation mechanisms.

5.2.2 Ultrasound Diffusion Theory

Phase velocity and attenuation are two methods which can be used in the characterization of cement-based material using ultrasound. As discussed earlier, the velocity of ultrasound will decrease when the porosity of concrete increases. Attenuation is the reduction of amplitude of the ultrasound energy. Concrete is a heterogeneous material, and this will cause the ultrasound to scatter considerably. Past research has shown that the ultrasound energy density decrease can be explained by using one-dimensional

diffusion equation when the sound wave evolves in the scattering events. Punurai, 2006, stated that the diffusion process is probabilistic, which treats only the statistical aspects of the flow of energy. The total energy is conserved, and the equation that governs the energy flow is the diffusion equation with an additional term representing linear dissipation of heat. Hence, the diffusion of ultrasound also has the potential to measure the microstructure and the properties of material, and explain the reduction of amplitude of the ultrasound.

The diffusion equation was used to investigate the sound propagation in a slurry of glass beads in water (Page et al., 1995). Their research showed that the sound wave propagated in strong scattering material can be explained by the diffusion approximation. Weaver et al., 1998, stated that the diffusion approximation of ultrasound waves can be used in aluminum form when the wave length is comparable to the strut length of the aluminum form. Anugonda et al., 2001, applied the diffusion theory to characterize the concrete microstructure by performing a series of experiments on circular cylinders, and used the diffusion equation to model the energy dissipation. Their research suggested that the ultrasound attenuation is due to scattering from microstructure and dissipation from the cement matrix. Researchers at the Georgia Institute of Technology performed several investigations to inspect concrete using diffusion of ultrasound. Punurai, 2006, performed characterization of cement-based material and the microstructure of the material using ultrasound diffusion. That research measured the ultrasound attenuation in cement paste using ultrasound diffusion. Using the experiment data, the dissipation and diffusivities can be calculated. The experiment results also showed the diffusion equation governed the strong scattering and the transmission of scattered energy. Deroo et al., 2010,

established the correlation between the dissipation and diffusivity coefficients and the damage state of concrete. The above experiments showed that damage will cause the microstructure to change mostly in the form of porosity increases (damage creates more voids), and cause an increase in scattering, with a decrease in dissipation and diffusivity coefficients. By applying the scattering parameter to the diffusion equation, the microcrack damage of the concrete can be quantified.

5.3 High Energy Ultrasound

Ultrasound velocity provides the only readily available method of determining the extent of cracking within concrete; however, it is not reliable for use in detection of flaws within concrete when the concrete is wet (Bungey et al., 1996). Past research has shown that the ultrasound diffusion coefficient can characterize or evaluate the condition state of concrete with high reliability. However, past research did not consider the degree of saturation of the concrete. Concrete infrastructures are installed in natural environments, where many structures are designed to be in contact with water or carry water, such as waterfront structures, dams, water treatment ponds and pipelines. Culverts were designed to drain storm water. The water will penetrate the concrete to cause different degrees of saturation. Even the surface of the culvert may be dry but inside can be water saturated. During inspection, culverts may be partially under water, fully saturated, fully dry or have different degrees of saturation. By using the ultrasound method, the pulse velocity will be impacted by the degree of saturation of the concrete. Consequently, it is important to clarify the impact of the degree of saturation on the ultrasound attenuation and reduction in wave velocity.

None of the research listed above considered fluids in the voids. Since the degree of saturation will highly impact the test result, interpretation of material properties obtained from ultrasound tests would not yield satisfactory information for culverts carrying fluids. If the amplitude of ultrasound is not sufficiently high to deform the voids, the resulting wave velocity will not depend on the type of fluid inside the voids, since the wave will not be able to compress the voids. As shown in **Figure 5.1** (which is simply **Figure 4.9** with a horizontal dashed line representing wave velocity of 3500 m/s), for example if the measured wave velocity is 3500m/s, then for low amplitude one can expect a porosity value of 30%. However, if the amplitude is sufficiently high to compress the fluid, depending on the compressibility of fluid, one can expect a porosity value of 35% for dry cement and 38.5% for wet cement.

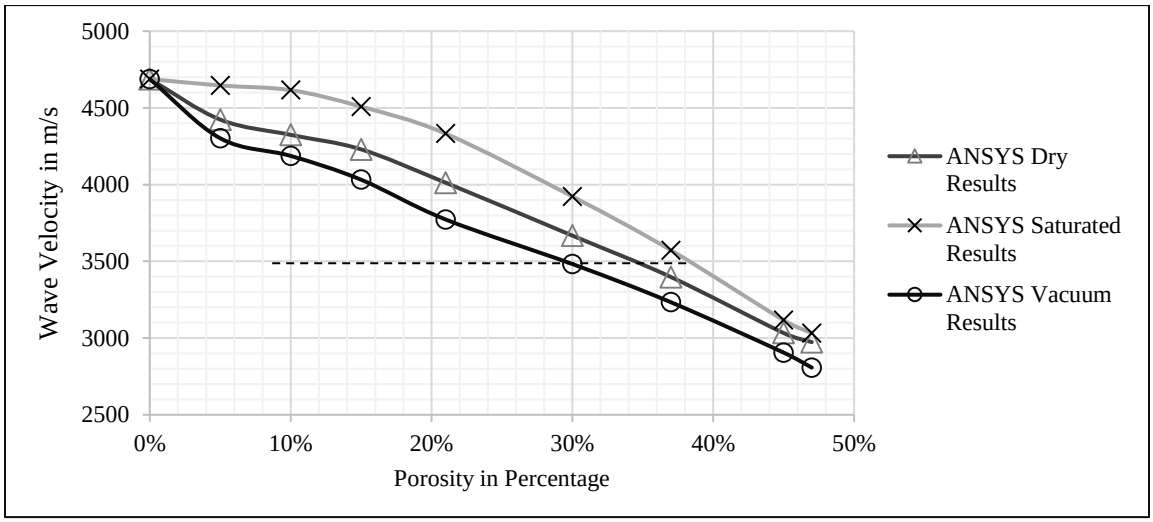

Figure 5.1 Impact of the compressibility of the fluid in the void.

To estimate the condition state of concrete under fully saturated conditions, the wave must go through this fluid. In consequence, the hypothesis of shock wave will be

tested to explain such energy transfer through voids, since the shock wave can carry energy through these voids. To generate the shock wave, high power ultrasound should be used. Generally, only high frequency and high-power level ultrasound can be used to accurately detect voids in fully saturated concrete. Please note that if there are no fluids in the voids, there is no wave transmission through the voids and if there is air, a limited amount of energy is transmitted, while if there is water, due to high compressibility of water, a significant amount of energy can be transmitted. As a result, for a given porosity, say 35%, one would obtain wave velocity of 3300m/s for vacuum, a lower wave velocity, wave velocity of 3500m/s for air and wave velocity of 3650m/s for water.

5.4 Hypothesis of Wave Propagation in the 1-D Pore Fluid- Shock Wave

In physics, a shock wave or shock can be defined as a wave that moves faster than the local sound speed. It is a type of propagating disturbance. Like an ordinary wave, a shock wave carries energy, and can propagate through a medium. However, it is characterized by an abrupt, nearly discontinuous change in pressure, temperature and density of the medium (Anderson, 2001). The sound wave velocity in concrete is much faster than that in air or water. Therefore, at the boundary of cement and a void a very high sound pressure will be generated. This could be explained in layman's terms as follows: For the wave velocity of a given frequency, the highest transmission velocity is in solids, which have a greater density, the lowest transmission velocity is in air, which has a lower density, and for water, transmission velocity is in between. Think of a piston with high wavelength pushing air with lower wavelength, causing a backlog of waves at the interface.

If the speed of the object is much lower than the speed of sound in gas, the density of the gas remains constant and the flow of gas can be described by conserving momentum and energy. The high sound pressure will push the wave particle in front of it. When an object moves faster than the speed of sound, and there is an abrupt decrease in the flow area, the flow is irreversible, entropy increases, and shock waves are generated. When a shock wave is created, there will be a jump condition between the fluid in front and the volume behind the shock. Shock waves travel faster than sound, and their speed increases as the amplitude of the piston is increased, but the intensity of a shock wave also decreases faster than that of regular sound waves (when the piston slows), because some of the energy of the shock wave is converted to heat in the medium in which it travels. This is called a decaying shock wave. By following the theory proposed by Glass, 1959, the decay can be explained by the overtaking of a shock wave by rarefaction waves. The shock wave and rarefaction wave calculation are described by Bukiet, 1988, for a detonation. The detonation creates a shock wave with the energy supplied from chemical reactions. By neglecting the burning, this theory can be easily extended to calculate the shock wave and the rarefaction waves generated by ultrasound wave propagation in porous concrete.

5.4.1 Elementary Theory

The conservation equation is used to describe the elementary one-dimensional gas dynamics as follows:

$$\begin{pmatrix} \rho \\ m \\ e \end{pmatrix}_t + \nabla * \begin{pmatrix} m \\ \frac{m^2}{\rho} + P \\ \left(\frac{m}{\rho}\right)(e+P) \end{pmatrix} = 0 \tag{5.1}$$

Here ρ is the density of gas, m is the momentum, P is the pressure and e is the energy per unit volume which is expressed as:

$$e = \rho\varepsilon + \frac{\rho u^2}{2} \tag{5.2}$$

Here u is the particle velocity and specific internal energy ε is:

$$\varepsilon = \frac{P}{\rho(\gamma - 1)} \tag{5.3}$$

With shock speed U, the conservation of mass can be written as:

$$\rho_1(u_1 - U) = \rho_0(u_0 - U) \tag{5.4}$$

Subscripts 0 and 1 represent the states ahead of and behind the shock. The conservation of momentum for the shock wave can be expressed as:

$$\rho_1(u_1 - U)^2 + P_1 = \rho_0(u_0 - U)^2 + P_0 \tag{5.5}$$

The conservation of energy for the shock wave can be written as:

$$(u_1 - U)(e_1 + P_1) = (u_0 - U)(e_0 + P_0) \tag{5.6}$$

By using the specific volume, $\tau = 1/\rho$, these equations can be reduced as:

$$\frac{\gamma_0\tau_0 P_0}{\gamma_0 - 1} - \frac{\gamma_1\tau_1 P_1}{\gamma_1 - 1} = \frac{(P_0 - P_1)(\tau_0 + \tau_1)}{2} \tag{5.7}$$

Equation (5.7) is known as the Hugoniot relation.

5.4.2 Riemann Problems for Shock Wave

A Riemann problem for shock wave can be set up by using the above equations. A simplified 1-D model is shown below for the mathematical analysis of the shock wave propagation.

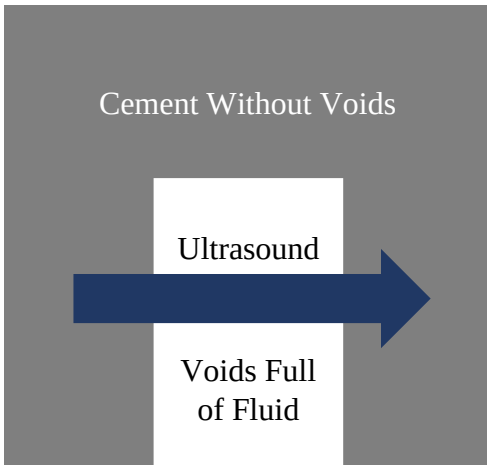

Figure 5.2 1-D model for the mathematical analysis of the shock wave propagation.

As mentioned earlier, when low energy ultrasound is applied the energy will not transmit through voids; part of the energy will scatter and part of the energy will propagate along the edges of voids. When high-power ultrasound is applied to concrete, the sound wave will deform the voids and high sound pressure will be generated at the edge of the voids. As a result, a shock wave will be generated and propagate through the voids. With the propagation of the shock wave, the downstream space is changed. Due to the space change, the density will change, and using the above equations one can obtain the shock velocity and pressure relationship. Typically, the Riemann problem is a common method used to solve the shock wave problem. To solve the Riemann problem, initial data can be set as follow:

$$S_L = (\rho_L, u_L, P_L) for\ Left\ wave\ (x < 0)$$

$$S_L = (\rho_R, u_R, P_R) for\ Right\ wave\ (x > 0)$$

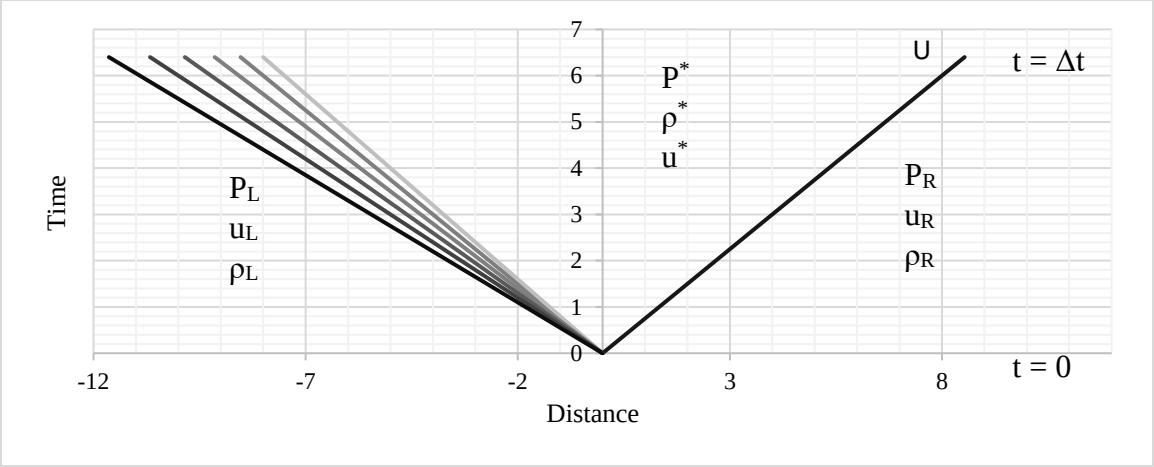

Figure 5.3 Right wave, left wave and a contact.

By using these initial data, the solution can be obtained using a right wave, a left wave and a contact as shown in **Figure 5.3**. The right and left waves can be a shock or rarefaction. Since the model being used is a 1-D model, it only applies to ultrasound on one side. The high pressure is on the left, in the concrete, and is propagating toward the void; the only solution will consist of a right shock. If the piston stops or the ultrasound is discontinued, a rarefaction will follow the shock. The equations for rarefactions can be found using the following Riemann invariants for left and right rarefaction respectively:

$$\frac{u_L}{2} + \frac{c_L}{\gamma_L - 1} = \frac{u_*}{2} + \frac{c_*}{\gamma_* - 1} \tag{5.8}$$

$$\frac{u_R}{2} + \frac{c_R}{\gamma_R - 1} = \frac{u_*}{2} + \frac{c_*}{\gamma_* - 1} \tag{5.9}$$

Using the adiabatic gas law, the following is obtained:

$$P_L {\rho_L}^{-\gamma_L} = P_* {\rho_*}^{-\gamma_*} \tag{5.10}$$

$$P_R {\rho_R}^{-\gamma_R} = P_* {\rho_*}^{-\gamma_*} \tag{5.11}$$

Here * denotes the state on the inside of the wave, or mid-state. Due to the left and right states connecting to states with same velocity and pressure, Bukiet, 1988, expressed this in terms of velocity as a function of pressure. Newton's iteration scheme was used to find the mid-state's velocity and pressure, given any initial right and left states.

Then the shock wave speed and mid-state density can be computed by using Equations (5.4) and (5.7). And the Equations (5.8) to (5.11) can be used to calculate the rarefactions. Using the above procedures, one can obtain convergence using Newton's method. Bukiet, 1988, presented equations for the iterative method used in computing the mid-state velocity and pressure and presents as follows:

Right shock:

$$u = u_R + \frac{A_R(\alpha_R - 1)}{(D_R\alpha_R + E_R)^{1/2}}, \frac{du}{dP} = \frac{\alpha_R D_R + 3\gamma_R - 1}{\sqrt{2\rho_R P_R}(D_R\alpha_R + E_R)^{3/2}} \tag{5.12}$$

Right rarefaction:

$$u = u_R + \frac{2C_R({\alpha_R}^{B_R} - 1)}{E_R}, \frac{du}{dP} = \frac{1}{H_R {\alpha_R}^{J_R}} \tag{5.13}$$

With:

$$\alpha_S = \frac{P}{P_S};\ A_S = \sqrt{\frac{2P_S}{\rho_S}};\ B_S = \frac{\gamma_S - 1}{2\gamma_S};\ C_S = \sqrt{\frac{\gamma_S P_S}{\rho_S}};\ D_S = \gamma_S + 1;\ E_S = \gamma_S - 1;$$

Here S is the side, R and L denote the state of air at right or left side of mid-state. By using above equations, the shock velocity can be calculated.

5.4.3 Shock wave velocity

With high power ultrasound and this one-dimensional model, high sound pressure at the edge of the voids will push fluid in front to generate a shock wave from a moving piston. Therefore, the right shock wave equation can be used. As discussed before, the shock wave will only be generated when the particle velocities are faster than their respective sound speeds. The sound speed in air is 350m/s and that in water is 1500m/s. To demonstrate calculations, 1600m/s particle velocity is used to generate the shock wave. The air in front of the shock is undisturbed, so it will behave like normal air.

By using Equation (5.12), the u_L is the left side particle velocity which equals to 1600m/s. Subscripts L, R here present the air state in front and behind the shock. Hence, the u_R is equal 0m/s, as the air in front of the shock is undisturbed. Same for pressure and density: P0 is the normal air pressure equal to the 101,325pa, the density is equal to the 1.225kg/m^3 and γ for normal air equals to 1.4. By substituting these values into Equation (5.12), unknown P_1 can be calculated. This case was developed such that a shock is moving to the right and there is no left wave.

$$1600 = 0 + \frac{\sqrt{\frac{2 * 101325}{1.225}}\left(\frac{P1}{101325} - 1\right)}{[(1.4+1)\frac{P1}{101325} + (1.4-1)^{1/2}} \tag{5.14}$$

By solving Equation (5.14), two P1 values are obtained, but the shock wave is a strong compression wave with a jump condition of density, pressure and velocity across the shock. Thus, for a right shock using $P_1 > P_R$ a P_1 value of 3,979,240.57 pa was obtained. As noted before, Equation (5.4) can be used to calculate the shock speed. To solve Equation (5.4), the density behind the shock should be obtained from Hugoniot equation. By applying the pressure after the shock, the density behind the shock equals 6.4kg/m^3.

After the shock wave generated by the 1600m/s particle velocity at the solid void interface and using the Equation (5.4), U, the shock speed can be obtained as equal to 1978.53m/s which is faster than the local speed of sound and has the pressure and density discontinuity in front and behind the shock.

5.4.4 Rarefaction Zone

In the previous section, it was stated that shock waves are generated by high-power sound waves. The shock is generated by solid particles acting like a piston due to high power ultrasound. The sound wave is a longitudinal wave and particles will move in the direction of the wave propagation around its original position like an oscillating piston. Once the piston slows down or is brought to rest, a rarefaction wave is generated at the face of the piston, and, as the velocity of the shock is subsonic relative to the gas behind it, a rarefaction wave eventually overtakes the shock wave causing the shock to weaken. Moreover, since there is finite energy, the ultimate speed of the shock will be that of a regular sound wave of the fluid (Burnside et al., 1964).

As the piston is stopped, the rarefaction wave is generated; since the rarefaction wave is moving at gas velocity plus the sound speed u+c (Friedrichs et al., 1948), it will be faster than the shock wave. As a result, the rarefaction will merge with the shock and weaken the shock. Rarefaction waves are a smooth fan zone with continuously changing pressure, density and velocity. It connects the state of air behind the shock (ρ_b, P_b, and u_b) and the state in front of the stopped piston (ρ_p, P_p and u_p). Here subscripts b and p denote the state behind the shock and the state in front of the piston. Equations (5.8) through (5.11) can be used to calculate the rarefaction. Due to its smooth change, once the front

and tail rarefaction speeds are known, the middle state can be easily calculated. The front of the rarefaction is just behind the shock, and the pressure, density and particle velocity are given by the shock speed. As a result, the particle velocity of the front rarefaction is u_b=1600m/s and the sound speed (c_b) of the front rarefaction follow the following equation:

$$c = \sqrt{\frac{\gamma P}{\rho}} \tag{5.15}$$

Using this data from the shock speed calculations, the front rarefaction velocity is equal to $u_b+c_b=1600+\sqrt{\frac{1.4*3979240}{6.4}}$ = 2532.76m/s, which is faster than the shock speed.

When the piston is stopped, the rarefaction will be generated, for this reason, the velocity of the tail of the rarefaction is equal to the piston velocity as u_p= 0m/s. Since the rarefaction is propagated to the right, input the u_p value to the right rarefaction Equation (5.13).

$$0 = 1600 + \frac{2\sqrt{\frac{1.4 * 3979240}{6.4}}\left(\left(\frac{Pp}{3979240}\right)^{\left(\frac{1.4-1}{2*1.4}\right)} - 1\right)}{1.4 - 1} \tag{5.16}$$

$$3{,}979{,}240 * (6.4)^{-1.4} = 210{,}116 * (\rho_p)^{-1.4} \tag{5.17}$$

Then, the pressure of the tail rarefaction (P_p) is found to be equal to 210,116pa. The front and tail rarefaction's state can be related by Equation (5.11). Hence, substituting the pressure and density of the front rarefaction as calculated before, ρ_p can be calculated and found to be equal to 0.78kg/m^3.

By repeating Equation (5.15), the sound speed at the tail rarefaction is c_p=612m/s. Since the particle velocity of tail rarefaction is equal to 0, the tail rarefaction velocity is

equal to 612m/s. Now the front and tail of the rarefaction are known, and these will help to compute the state for the whole rarefaction area.

Assume:

$$k1 = \frac{dx}{dt} = u + c = u_* + c_* \tag{5.18}$$

$$k2 = \frac{u_R}{2} - \frac{C_R}{\gamma_R - 1} = \frac{u_*}{2} - \frac{C_*}{\gamma_* - 1} \tag{5.19}$$

$$k3 = P_R {\rho_R}^{-\gamma_R} = P_* {\rho_*}^{-\gamma_*} \tag{5.20}$$

Due to the smooth change in velocity in the rarefaction zone, the k1 has its own velocity range between the tail rarefaction velocity of 612m/s and the front rarefaction velocity 2352m/s. The subscript R denotes the state on the right side of the rarefaction and is equal to the front rarefaction's pressure velocity and density. Consequently, k2 and k3 can be calculated and equal to -1531.92 and 295711.5. Since k1, k2 and k3 has such relationship, let k1 minus two k2 to get:

$$k1 - 2 * k2 = 6\sqrt{1.4 * \frac{P_*}{\rho_*}} \tag{5.21}$$

From Equation (5.20),

$$P_* = k3 * \rho_*^{1.4} \tag{5.22}$$

Substitute P_* in Equation (5.21) by using Equation (5.22) to obtain:

$$\rho_* = [\frac{(\frac{k1 - 2k2}{6})^2}{1.4k3}]^{2.5} \tag{5.23}$$

Here k2 and k3 are constant, ergo knowing the front rarefaction's state and by using different values of k1, the density of every point in the rarefaction can be found. Then,

using the density and Equation (5.11), the pressure for every point in the rarefaction can be calculated as shown below:

$$P_* = \frac{P_R * {\rho_*}^{1.4}}{\rho_R^{1.4}} \tag{5.24}$$

After computing the pressure and density the sound speed can be calculated by using Equation (5.15). Finally, the particle velocity of the rarefaction can be determined by using Equation (5.25), and by adding particle velocity u_* and sound velocity c_* together, every point in the rarefaction zone can be calculated.

$$u_* = 2 * [(\frac{u_R}{2} - \frac{C_R}{\gamma_R - 1}) + \frac{c_*}{\gamma_* - 1}] \tag{5.25}$$

Figures 5.4, 5.5 and 5.6 show the pressure, density and velocity distributions behind the shock wave. Please note that the right side is the front rarefaction wave approaches the shock wave, its pressure and density values are equal to the state behind the shock wave, but its speed is higher than the shock wave speed.

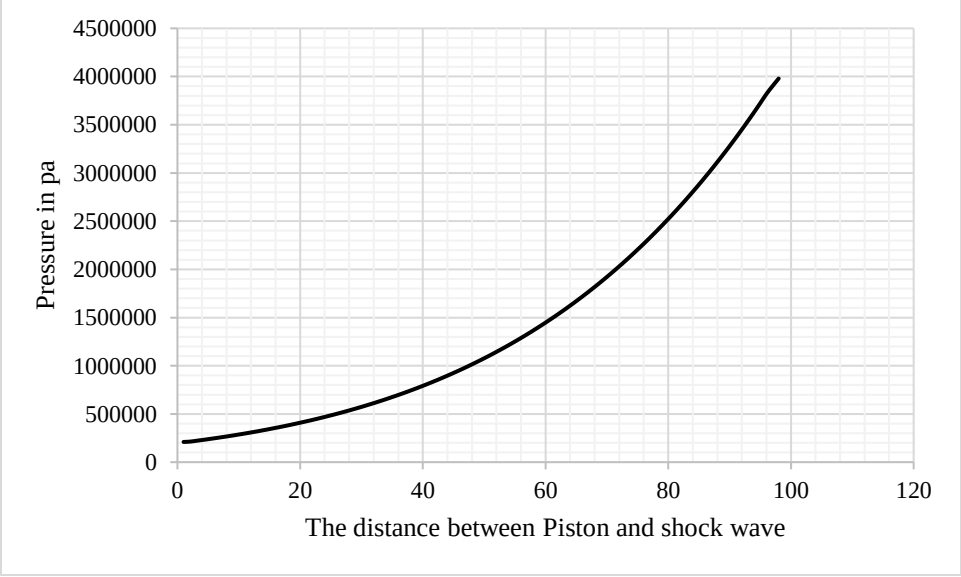

Figure 5.4 Rarefaction zone pressure distribution.

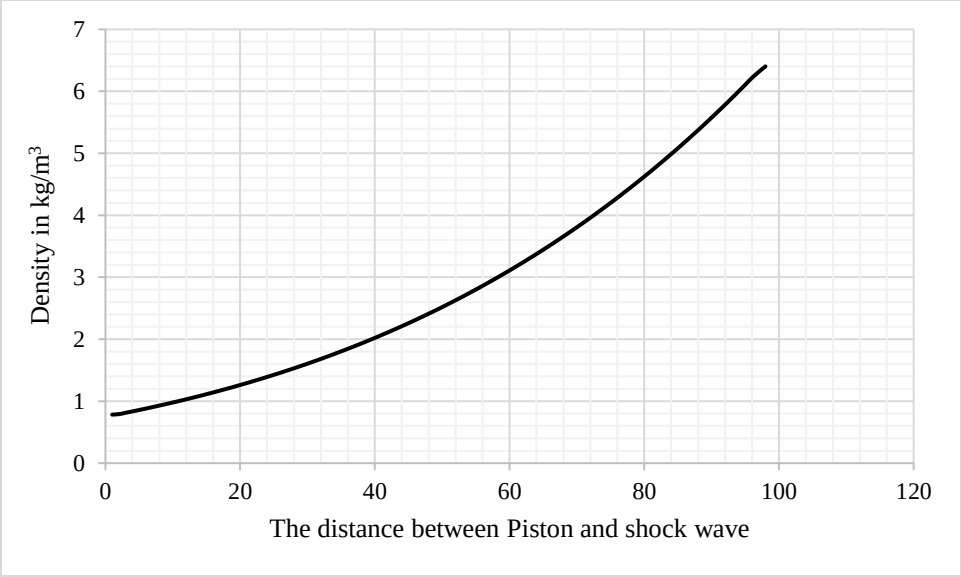

Figure 5.5 Rarefaction zone density distribution.

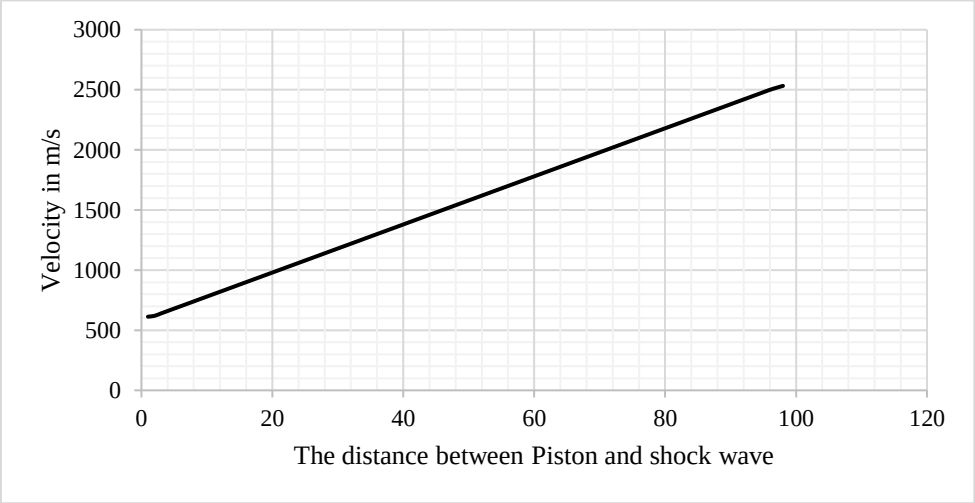

Figure 5.6 Rarefaction zone velocity distribution.

5.4.5 Decay of the Shock Wave

The above calculations show that the rarefaction is faster than the shock wave. When it meets the shock, the shock is weakened, causing the shock speed to decrease. Literature research showed that the decay of a shock wave is a very complicated problem, where the interaction between rarefaction and the shock is difficult to model, describe or simulate.

But this reaction should follow the conservation of energy, which means it still should follow Equations (5.5) through (5.13). To numerically calculate the process, the following assumptions were used: First, the rarefaction zone is a smooth zone and it should contain an infinite number of points, but in this research, the zone was discretized into a finite number of points. Each point has its pressure, velocity and density and each of these points is defined separately. Ergo, each encounter of rarefaction waves with the shock wave can be accounted, otherwise the rarefaction waves will continually hit the shock wave and the state will dynamically change. Second, the decrease in shock wave velocity is continuous but is modeled as discrete. Based on the above assumptions, with each rarefaction wave encounter with the shock wave, the shock speed is changed. Third, the pressure and density may be changed due to the encounters of the shock wave and each rarefaction wave. Here the particle velocity is assumed to be constant. Actually, the new shock speed is calculated based on the particle velocity just behind the reaction and the undisturbed air in front of the shock.

By using discrete rarefaction waves, the point next to the first rarefaction wave was selected. The particle velocity is equal to 1,586m/s. This point is just behind the shock, when the rarefaction wave encounters the shock wave; the state at this point is just behind the reaction zone. The air in front of the shock is still undisturbed. Then a similar shock speed calculation is performed using Equation (5.12); the u_L is the left side particle velocity which is equal to 1,586m/s. Subscripts L, R here present the air state in front and behind the shock. Ergo, the u_R is equal to 0m/s, because the air in front of the shock is undisturbed. Same for the pressure and density, P0 is the normal air pressure equal to 101,325pa, the density is equal to 1.225kg/m^3 and γ for normal air equals 1.4.

Substituting these values into Equation (5.12), a function with only one unknown, P_L as shown below,

$$1586 = 0 + \frac{\sqrt{\frac{2 * 101325}{1.225}}\left(\frac{P1}{101325} - 1\right)}{[(1.4 + 1)\frac{P1}{101325} + (1.4 - 1)^{1/2}} \tag{5.26}$$

By solving Equation (5.26), two P1 values will be obtained, but the shock wave is a strong compression wave with a jump condition relating density, pressure and velocity across the shock. Therefore, the condition for a right shock wave using $P_L > P_R$ to obtain the P_L is equal to 39,176,247pa. As noted before, Equation (5.4) can be used to calculate the shock speed. To solve Equation (5.4), the density behind the shock should be obtained using the Hugoniot equation. After applying the pressure behind the shock, the density behind the shock equals 6.39kg/m^3. Then, the shock speed can be found by using Equation (5.4), and the result equals 1963m/s. Here, since the state behind the shock has changed, the rarefaction zone needs to be refreshed and a point selected in the refreshed rarefaction zone. By repeating this process, the shock speed is being reduced as shown in **Figure 5.7**.

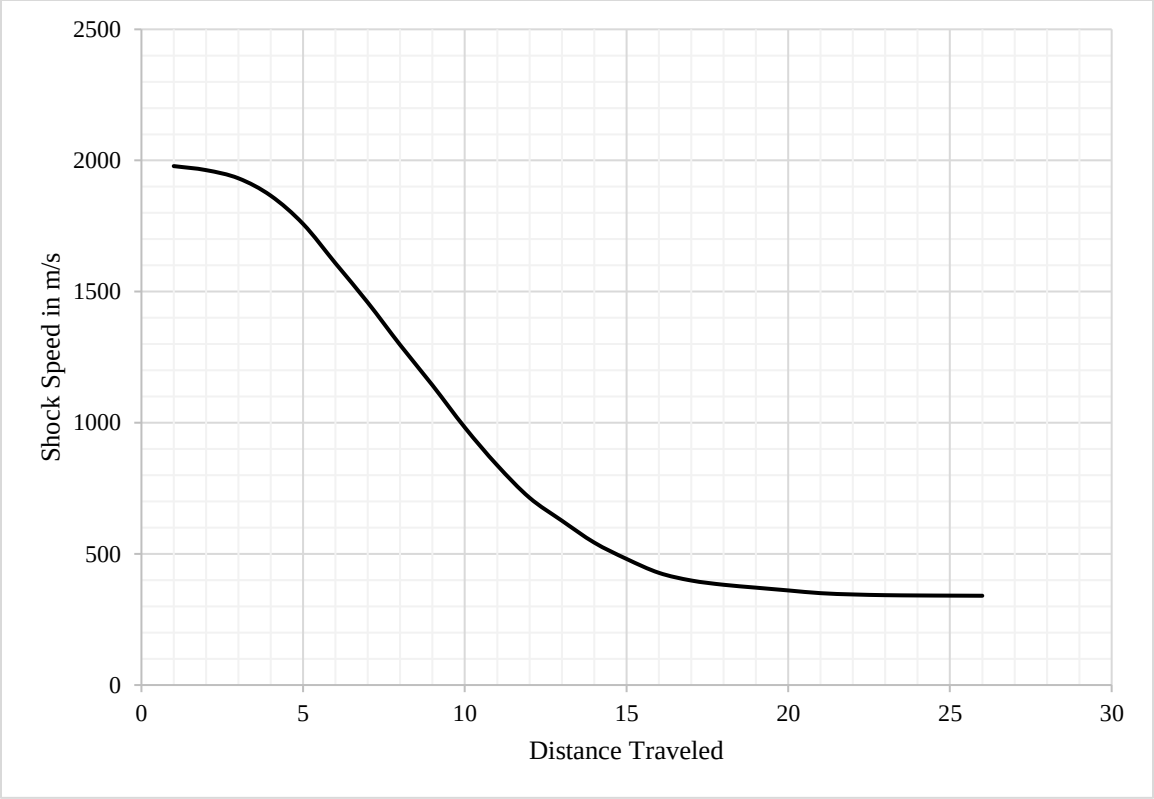

Figure 5.7 Shock speed decrease with distance traveled.

From **Figure 5.7**, at the beginning the decrease in shock speed is very slow, because the rarefaction just begins to overtake the shock. But with the speed decrease, many more rarefaction waves overtake the shock wave and a rapid decrease in shock speed occurs. Finally, the shock wave becomes very weak just like the normal sound wave and its speed never decreases below the sound speed in air which is 340 m/s. Also, this speed decrease can explain the ultrasound velocity decrease with the increase in cement porosity because in our model, the larger porosity means a larger distance for the shock to travel inside the void. The shock wave speed is significantly reduced due to the larger number of encounters with rarefaction waves. Noted, due to the third assumption the results in **Figure 5.7** are likely to be more valid quantitatively for smaller distances

traveled than for larger distances due to complicated wave interactions that have been neglected in the analysis, but the results should be qualitatively appropriate.

5.4.6 Dissipation of Shock Wave Energy

As mentioned, when ultrasound propagates through concrete, there will be reduction of velocity and reduction in amplitude. The reduction in amplitude is due to the dissipation of ultrasound energy. Since energy is conserved, it is just transferred from one form to another; in this case, it becomes heat. Thus, it is necessary to investigate the dissipation of shock wave energy. Recall Equation (5.2), where *e* is the energy per unit volume, $e = \rho\varepsilon + \frac{\rho u^2}{2}$ and specific internal energy $\varepsilon = \frac{P}{\rho(\gamma-1)}$. Combine these two equations together to obtain $e = \frac{P}{(\gamma-1)} + \frac{\rho u^2}{2}$. This is the total energy and by integration of *e* with distance, the total energy of between the piston and the shock front.

$$\int_{t0}^{t} \frac{P}{(\gamma-1)} + \frac{\rho u^2}{2}\, dt \tag{5.27}$$

To perform the total energy calculations, several key points in time should be selected. The first one is when the shock wave is just generated but no rarefaction waves are generated. The second is when rarefaction waves are generated and propagated a finite distance. The third will be when the first rarefaction wave is about to encounter the shock wave and the final one will be after the first rarefaction wave has already encountered the shock wave. As the shock wave is supersonic, extremely small time steps are used in this calculation. To simplify the calculation, the time step will be used as unit time. Please note that for a consistent definition, the internal energy density per unit volume should have the same units as pressure (Needham, 2010). The term in this

research is energy density per unit volume too, used as a measure of the internal energy per unit distance of the gas.

The first energy calculation will be made when the shock wave is generated, and after it has propagated one unit of time. By using the equation in 5.27 to obtain $\int_0^1 \frac{3979240}{(1.4-1)} + \frac{6.4*1600^2}{2}\, dt$, the shockwave energy density will be equal to $\frac{3979240}{(1.4-1)} + \frac{6.4*1600^2}{2} = 18{,}140{,}100$. During this time, the distance that the wave propagates is equal to shock speed times the time which equals to 1978.52*1=1978.52.

With energy density times the distance it traveled, the total energy can be calculated as 3.6E10. After 1-unit time, the piston stops and rarefaction waves will be generated. Assuming the rarefaction travels 1-unit time, in the meantime the shock has traveled 2-time units. This situation should be separated into 3 zones. Zone 1 will be the shock to the front rarefaction. Zone 2 will be the rarefaction zone. And Zone 3 is between the tail rarefaction and the boundary (piston).

The particle velocity in Zones 1 and 3 are constant, so the total energy still equals to the energy density times the travel distance. Zone 2 is the rarefaction zone; as mentioned before, the rarefaction zone is a smooth and continuously changing zone. To integrate this zone Simpson's Method is used (see appendix A).

The rarefaction is faster than the shock wave, and during that unit time its leading edge will be closer to the shock wave. The distance between the rarefaction and shock is equal to 1978*2-2532*1=1424.28. The shock speed is still constant hence the total energy in Zone 1 is equal to 1424.28*18140100=2.58E10. Zone 3 is similar to Zone 1 and its energy is equal to $\int_0^1 \frac{210115}{(1.4-1)} + \frac{6.4*0^2}{2}\, dt * 612 * 1 = 3.21E8$. Here 612 is speed of

the tail of the rarefaction wave and the distance it travels is equal to 612*1. Zone 2 from the Simpson's method yields 1.04E10; as a result, total energy is 3.65E10.

When the rarefaction continues to propagate and almost hits the shock, the time step will be after 3 units of time after the shock wave was generated. At this time, the gap between the shock and front of the rarefaction is down to 870, which means Zone 1 continues to shrink and the rarefaction is about to encounter the shock wave. The total energy equals to 1.58E10. Zone 3 is expending due to propagation; consequently, the total energy is = 525290*612*2 or 6.43E8. By combining energy from Zone 2 using the Simpson's method, the total energy equals to 3.65E10.

The last point will be just after the rarefaction wave encountered the shock wave. Shock speed is decreased but due to the rarefaction continually hitting the shock wave, Zone 1 has disappeared. Zone 3 is still slowly expanding and the total energy is equal to 1.1E9. In consequence, the majority of energy is from Zone 2. The front of the rarefaction wave has encountered the shock wave and the shock wave speed has decreased. Also, there is a change in the state of the air behind the shock wave. After refreshing the rarefaction zone, data is obtained from the new rarefaction zone and, using the Simpson's method, the calculation is performed. By adding energy from Zone 3, the total energy is equal to 3.68E10. From the energy calculations from these four points, the total energy is conserved as expected, because all equations are derived from the conservation of energy equation. But it also shows that the energy will slowly spread as the wave propagates. The energy density is decreased with a larger traveled distance. Thus, this could explain the reason that with the increase in porosity, the amplitude of the wave will be reduced. In the solid cement phase, with no shock wave, the energy transfer

is via the sound wave. However, when it propagates and arrives at the edge of the voids, shock waves are generated. With larger voids, the waves need to travel a larger distance, and during this propagation the energy spreads over a larger volume and the energy density is decreased, causing decreased amplitude.

CHAPTER 6
LONG-TERM MANAGEMENT

6.1 Culvert Management

Once a culvert is inspected, its condition state can be assigned. Video inspection can be automated to determine the condition state (Meegoda et al., 2006). Once the condition state of a culvert is known, then the optimum time and also optimum allocation of funds to rehabilitate or replace the culvert can be computed. At this point a culvert management system can be developed (Mills 2002, Meegoda et al., 2009, 2011 and 2012). The starting point of a culvert management system is the development of culvert deterioration curve. The typical deterioration and condition state curve which describes the deterioration of culverts is usually a function of age, or time in service. Age is a composite surrogate for environment-related data and axle-load related data. Culvert age is fairly well correlated with environmental variables such as freeze index, salting, etc. Meegoda et al., 2008, developed a deterioration curve for culverts based on the Weibull model. The deterioration curve proposed by Meegoda et al., 2008, is based on two assumptions. The first assumption is that a culvert has failed when its serviceability has decreased to 5% and its age has reached 150% of its expected service life. Second, the characteristic life parameter θ is equal to (td) γ/ln (2), where td is the original designed life of the culvert. As a result, shape parameter γ can be back-calculated as 3.6. The designed service life is typically 100 years for concrete culverts, while it is typically 75 years for metal culverts (Bhagwan, 2009). Therefore, the deterioration curve proposed by Meegoda et al., 2008, can be converted to that shown in **Figure 6.1**. A culvert in condition state 1 would have a 100-80 percent condition classification and that in condition state 2 would have a 79-60

percent condition classification. Please note that it is not sufficient to quantify future deterioration based on **Figure 6.1**: Regular inspections should be performed and the condition state of the culvert should be reassessed.

Once the condition states of culverts in the network are known after inspection, the following financial information is required for culvert management decisions, where the following is known for the ith culvert in the system, where n is the number of culverts in the network (i=1,2,…, n):

- Condition state of each culvert based on prior inspection
- Age or date of installation of each culvert with year last inspected and cleaned (Ti). Please note that date of installation may be difficult to obtain if the old records are not available. However, proposed analysis can be performed based on condition state.
- Year to be considered (t, where t=0 for the current year, and t=1 for the next year)
- Expected life (td or μi) and variance (μi) for each culvert based on the condition state.
- Cost of installation for each culvert; it is also assumed to be the same as cost of replacement (Ai,t)
- Current value of the culvert after do nothing/rehabilitation/replacement (Bi,t)
- Cost of inspection of each culvert (Ei,t)
- Cost of repair or rehabilitation of each culvert and not replacement (Fi,t)

Please note that the agency cost would be either Ai,t (cost of replacement) or Fi,t (cost of repair or rehabilitation). One may also include inspection cost, but inspection is usually considered to be a routine operation. In order to perform a cost estimate (to obtain Ai,t [cost of replacement], Fi,t [cost of repair or rehabilitation] or Ei,t [cost of inspection]), market value will provide the best available measure of unit costs. Here the estimation of unit cost of new installation or rehabilitation is based on unit cost data listed in RSMeans, a national yearly heavy construction cost estimating book, and Bid Express,

an online information service for bidding provided by BidX.com (Meegoda et al., 2012). These unit cost values were incorporated into the culvert management system in order to estimate capital costs, asset worth, maintenance, repair and new construction costs.

Assessing the user cost or financial risk associated with failure is the most challenging issue in effective management of culverts. Though it can be argued that the cost or risk associated with failure is independent of culvert length, it may depend on culvert size, geographic location, whether it is laid along roadway or across roadway, and the proximity to critical structures such as subways, hospitals and hazardous waste sites. The user cost is usually associated with culvert failures, such as flooding, roadway collapses resulting in traffic delays and expensive repairs. Flooding, associated detours and collateral damage are difficult to quantify. Since such damage claims can be paid by insurance, they are not included in this analysis.

The objective of culvert management is to a) determine the optimum allocation of the current maintenance budget by identifying culverts that are to be inspected, and those that are to be repaired or rehabilitated, b) to estimate the minimum annual budget needed over a given planning horizon, and c) to comply with GASB-34 requirements. This analysis should also be capable of making project level decisions to repair, rehabilitate, replace, or do nothing for a given culvert. The following section lays out the ground rules for project and network level decisions.

It is expected that regional and/or field offices maintain culvert records requiring inspection and rehabilitation/replacement. As stated earlier, yearly maintenance and rehabilitation work to be carried out in the current year is based on the condition state of the culvert during the previous year. The decision to inspect, repair, rehabilitate, replace

or do nothing depends on the current condition state determined from culvert inspections (Matthews et al., 2012). If the current condition state of a culvert is unknown due to budgetary constraints, the selection is somewhat different. Meegoda et al., 2005, provides examples of the following situations to obtain project level decisions.

- Do nothing
- Repair a culvert
- Rehabilitate a culvert
- Replace a culvert

It was observed from the culvert inspection data that most culverts in condition state 1 require no action. Those in condition state 2 may require minor repair, while those in condition state 3 would require either repair or rehabilitation. Condition state 4 would definitely require major rehabilitation and condition state 5 is slated for replacement. For each choice, one should calculate the difference between the cost of the choice or action and improvement in the value of culvert based on its condition state, and select the option with the highest difference. If a culvert is repaired, rehabilitated or replaced, its value should be based on the improved performance value of the culvert and not based on the book value as accounted by most asset managers. This is a unique feature of the proposed method. Similarly, the current value of a culvert is assigned based on its improved performance value, rather than that given in a book, as is the practice of most asset managers (Meegoda 2012). Based on the above analysis, one can see that do nothing is not a choice for a culvert of condition state 3, 4, and 5. Some culverts with condition state 1 and 2 may be left without any treatment, due to lack of funds. If this occurs, the overall value of the network decreases, which is the case for most US civil infrastructures. Also, culverts needing rehabilitation are replaced. There are currently many inexpensive and effective rehabilitation methods that would bring a culvert back to almost new or

condition state 1, and hence should be considered instead of replacement. Decisions to repair, rehabilitate, replace or simply do nothing for a given culvert depend on its condition state. **Table 6.1** was developed based on ACPA 2013 and **Table 6.2** was developed based on Rajani and Makar, 2000.

Table 6.1 Decision Tree for Concrete Culverts

Condition state	Description	Implications			Recommended technique	Final state
		Joint	Slabbing	Cracking		
1	No visible deterioration	No structural defects	No structural defects	No structural defects	No	1
2	Transverse or longitudinal crack; culvert is not slabbing; The joint has small defects	The joint gap is less than manufacture's recommendation; no significant vertical offset at the joint; cracks at joint less than 0.1; there aren't cracks or spalls that compromise joint performance	Culvert is not slabbing; there is delamination or incipient spalling, but no reinforcing steel exposed; culvert is stabilized	Longitudinal crack <=0.01"	Note in inspection for cracking and no action need for joint	2
3	Transverse or longitudinal crack; the culvert is slabbing; The joint has some small problems	The joint gap is bigger than manufacturer's recommendation; cracks at joint less than 0.1; there aren't cracks or spalls that compromise joint performance	Culvert is stabilized; there is delamination or incipient make the reinforced exposure but we can protect steel through the structural repair.	Transverse crack	Filling a crack with a flexible sealant; structural repair for the slabbing with Portland cement grout; Seal joint by Internal grouting	2
				Longitudinal crack <=0.1" ; spalling that exposes reinforcing	Filling a crack and/or slabbing groove with Portland cement grout; Seal joint by Internal grouting	2
				Longitudinal crack <=0.1" ; no spalling that exposes reinforcing	Note in inspection for cracking; structural repair for the slabbing with Portland cement grout; Seal joint by Internal grouting	2
4	Longitudinal crack; the culvert is slabbing and the joint has some problems	The joint gap is bigger than manufacture's recommendation and no significant vertical offset at the joint, but the cracks at joint are greater than 0.1"	There is delamination or incipient make the reinforced exposure but we can protect steel through the structural repair. culvert is stabilized	Vertical offset across crack	Sealing the cracks with structural epoxy type materials placed in the crack plane or Full Barrel repairs such as: Cured in place liners, Epoxy resin Liner, or slip line systems. Seal joint by Internal grouting further investigation to determine if future slabbing of the pipe wall is of concern.	1
				0.1"<crack<0.2"	Sealing the cracks with structural epoxy type materials placed in the crack plane or Full Barrel repairs such as: Cured in place liners, Epoxy resin Liner, or slip line systems; seal joint by Internal grouting.	1
5	Serious longitudinal crack, slabbing and joint problems	The joint gap is bigger than manufacture's recommendation but there is significant vertical offset at the joint and cracks or spalls that compromise joint performance	There are spalls that expose reinforcing steel and the culvert is not stabilized	Culvert is not stabilized or crack>0.2"	Replace culvert section with tight joints	1

Table 6.2 Decision Tree for Metal Culverts

Condition state	Description	Implications	Criteria	Recommended technique	Final state
1	Like new	No visible deterioration	No visible deterioration corrosion or deterioration	No action required	1
2	Initiation of corrosion	Both the interior and/exterior surface of the culvert began to corrosion.	Coatings, linings still intact. Tiny and shallow corrosion pitting. Tiny cracks appear. Remaining surface area more than 90% of original.	Schedule for Catholic Protection and Re-inspection within the next 5-10 years. Note in inspection.	2
3	Crack or corrosion pits before leak	The corrosion deepens including cracks corrosion pits and graphitization	Coatings and/or linings have some damage. The corrosion pitting enlarges and deepen. Cracks visible, but did not form Circumferential cracking or Longitudinal cracking. Remaining surface area thickness 70% ~89% of original.	Re-inspection in next 5 years. Schedule for structural repair such as cement or rehabilitation within the next 5-10 years.	2
4	Leak begin (Partial failure)	Further deepening corrosion pits and cracks. The culvert wall start breaks. Internal or external stresses larger than the strength of the culvert wall. The leak or burst will be initiated depending on the size of the break.	Large area of internal or external corrosion. Almost no lining or coatings. Large tracts of corrosion pitting and mass of blow-out holes. Longitudinal cracking larger diameters <12 in the culvert start Leaking. Bell splits appear. Remaining surface area 50%~ 69% of original.	Schedule for rehabilitation such as: Cured in place liners, Epoxy resin Liner, or slip line systems within the next 3-5 years.	1
5	Break or failure	Water appearing on the ground surface and/or the hydraulic balance change in the culvert system.	Severe internal or external corrosion. Collapse evident. Large cracks/ holes. Longitudinal cracking larger diameters >12 in. Circumferential cracking smaller diameters <12 in. Remaining surface area less than 50% of original.	Replacement required.	1

Both list the rehabilitation options for concrete and metal culverts based on the five condition states. Please note that **Tables 6.1 and 6.2** were developed for a more stringent drinking water infrastructure but can be used for culverts. The proposed rehabilitation technique in **Tables 6.1 and 6.2** would upgrade the condition state, therefore, enhancing the service life. For instance, a culvert in condition state 3 is upgraded by adding a liner to become condition state 2. Also, it is very expensive to replace culverts, and with the cost of one replacement, several other culverts can be

rehabilitated to almost perfect condition. Consequently, such decisions should be based on network level analysis. In this research, a small network (consisting of 15 pipes) was used for illustration.

The following is an example of such cost calculations. Consider the 18" diameter 61' long concrete culvert located at mile-post 12 on NJ route 130 with a condition classification of 40%. Based on RSMeans and Bid Express the replacement cost of that culvert is $10,920; hence the current value is $4,376 (40% of $10,920). Based on **Figure 6.1**, if do nothing is the choice of action, the following year the culvert classification will drop to 38.9% because of deterioration, cracks, etc., and this will continue yearly.

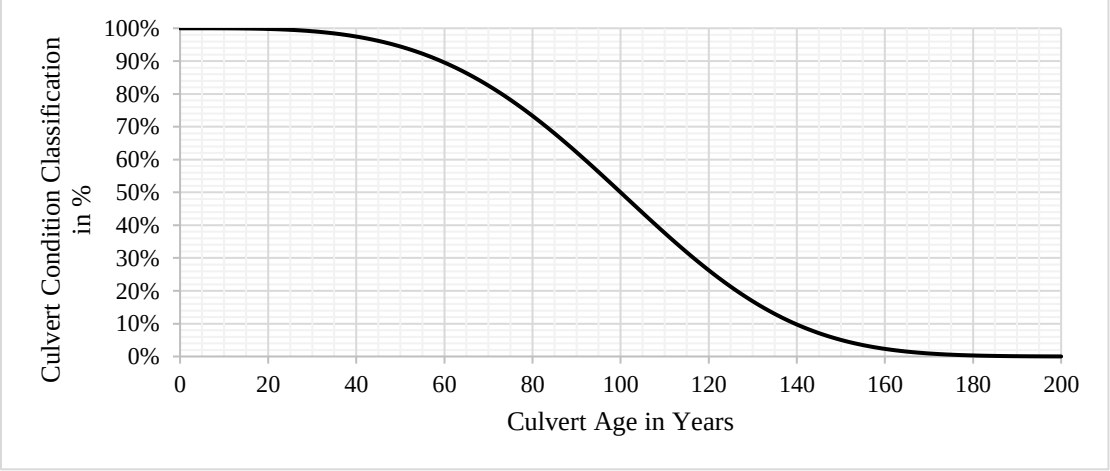

Figure 6.1 Deterioration curve for concrete.

Therefore, after 20 years the condition classification will become 18.5%. Its value after 20 years would be $2,023 (18.5% of $10,920). The culvert deterioration will continue with each passing year until culvert failure. However, if there are funds to fix this culvert during the current year, the culvert performance will be substantially improved with a longer service life. The choice of repair as per **Table 6.1** is Cured in

Slip lining at a cost of $4,769, reaching a final condition classification of 90%. If the Slip lining method was applied to fix the culvert, the current value would be $9,844 (90% of $10,920). Please note that current value based on book value would be $9,145 ($4,769+$4,376) but based on the condition rating, its value is $9,844. The culvert value based on the condition rating is higher than the book value. For this reason, the Cured in Slip lining is justified as the corrective action for this culvert. Once the culvert is rehabilitated, the following year do nothing would be the choice of action. After rehabilitation, the culvert will continue to deteriorate until failure. This deterioration can be modeled if the original deterioration curve is shifted as shown in Figure 6.2.

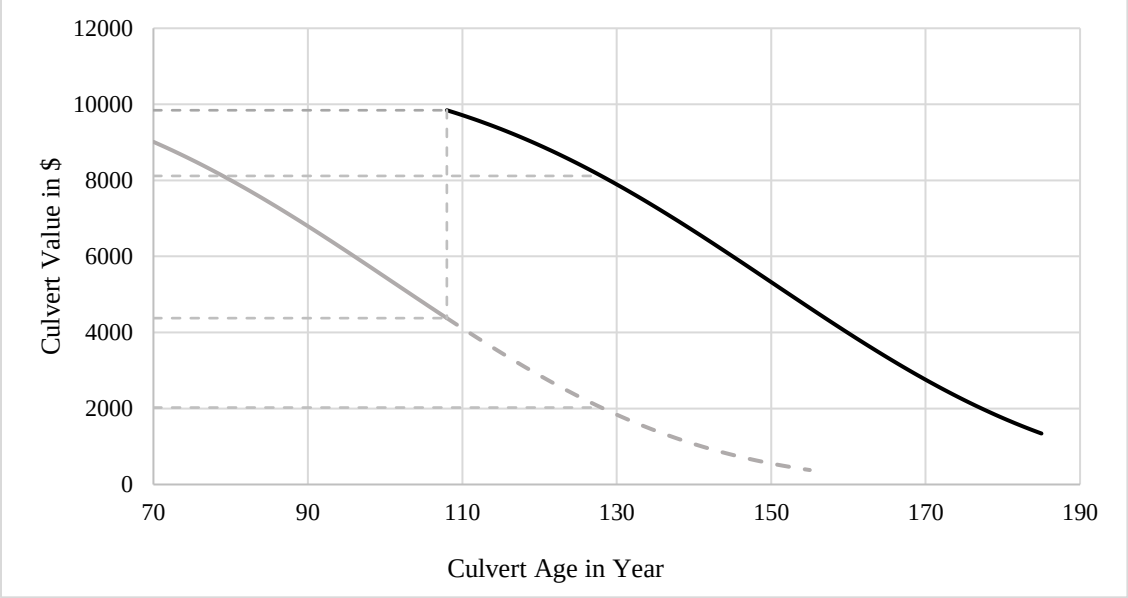

Figure 6.2 Deterioration curve for example concrete culvert.

Based on **Figure 6.2**, after 20 years and with rehabilitation, the condition classification will drop to 74%. Accordingly, after 20 years, the value of the rehabilitated culvert will be $8,117 (74% of $10,920).

6.2 Computation of Long-term Annual Maintenance Cost

In order to illustrate different methods to obtain the minimum budget, 15 culverts listed in **Table 6.3** were used as the sample culvert network. This is a condensed version of 40 culverts listed in Meegoda, 2013 where PVC and brick culverts were eliminated due to lack of detailed data. **Table 6.3** consists of 11 concrete culverts and four cast iron culverts. The total replacement and current values of the culvert network are $444,742 and $196,879, respectively, with an overall network condition classification of 43% (196,879/444,742). **Table 6.3** also lists the appropriate repair and rehabilitation costs based on **Tables 6.1 and 6.2**. Please note that culverts with a condition classification higher than 80% require no action, those between 60% and 79% require repair, those between 20% to 59% require rehabilitation, and those below 19% require replacement. In this analysis **Figure 6.1** is used to obtain the yearly deteriorations of the fifteen culverts listed in **Table 6.3**. For example, culvert #7 in **Table 6.3** is 94 years old, and according to the curve, the condition classification is 57%. The next year its condition classification would be 56%, with a condition classification value of 45% after ten years. The following three methods are used to compute the minimum long-term maintenance cost of the culvert network:

- Long-term Maintenance Cost based on Modified Worst First Method
- Long-term Maintenance Cost based on Optimization
- Long-term Maintenance Cost based on Maximum Deterioration Rate

Table 6.3 Details of the Selected Culvert Network

NO.	Route	Mile post	Condition Classification in %	Culvert Age in years	Material	Diameter (inches)	Length (feet)	Replacement Value in $	Current Value in $	Cost of Repair in $	Cost of Rehabilitation in $	Cost of Replacement in $
1	RT35N	5	73%	60	Metal	12.00	118.00	13,354	9,790	1,361		
2	RT130S	11	66%	65	Metal	18.00	23.00	2,603	1,720	265		
3	RT 23N/S	0	14%	100	Metal	15.00	115.00	13,015	1,847			13,015
4	RT 17S	19	6%	110	Metal	18.00	103.00	11,657	744			11,657
5	RT130	12	72%	81	Concrete	18.00	100.00	17,901	12,939	1,153		
6	RT130S	12	65%	88	Concrete	24.00	69.00	10,371	6,696	796		
7	RT15S	13	57%	94	Concrete	15.00	57.00	14,249	8,182	2,574		
8	RT15	11	49%	101	Concrete	18.00	245.00	43,857	21,381	13,188		
9	RT130	12	40%	108	Concrete	18.00	61.00	10,920	4,376		4,769	
10	RT1	9	49%	101	Concrete	30.00	155.00	30,577	14,907		18,820	
11	RT1N	11	33%	114	Concrete	15.00	217.00	54,248	17,861		16,965	
12	RT66	12	25%	121	Concrete	18.00	350.00	62,654	15,814		27,363	
13	RT33 W/E	15	25%	121	Concrete	18.00	200.00	35,802	9,036		15,636	
14	RT 49E&W	0	100%	1	Concrete	21.00	412.00	61,928	61,928			
15	RT 206	38	9%	141	Concrete	36.00	305.00	61,607	5,657			61,607
							Total	444,742	192,879			

6.3 Long-term Maintenance Cost based on Modified Worst First Method

Infrastructure managers are generally responsible for assessing culverts based on inspection, but recommendations for rehabilitation/replacement are made by regional and field offices. Those recommendations are to be examined and prioritized at the main office while adhering to budgetary allocations. Such decisions would result in the best utilization of funds allocated for the planning horizon and in a net improvement in total network asset value. In this modified worst first method, a fixed yearly budget is allocated and project level corrective actions are suggested for each culvert for each year. Then the budget allocation is changed and the analysis is repeated. One could imagine this procedure as current practice of fixed budget allocation projected into the future. The financial analysis of a culvert networks starts with the creation of culvert groups within a project. In the case of this project, each culvert comprises a group of one. Users have the option to select some of the groups to be included in the optimal solution no matter how much they cost. After a project has been defined, the financial analysis will allow users to review the project input data. The project level culvert optimization consists of selecting the best restoration option (do nothing, repair, rehabilitate or replace) based on condition classification. The last three columns of **Table 6.3** provide appropriate cost of corrective action for each culvert; if no value is given, that means the selection is do nothing. Usually the project level do nothing option is selected for culverts in excellent condition. Please note that for the long-term budget calculations the total replacement value of culverts at condition state 5 should be lower than 20% of the whole network replacement value to obtain reasonable results. For example, culverts # 3, 4, and 15 in the selected culvert network are in condition state 5 with a total replacement value of $86,279, or 19%

(86,279/444,742) of the whole network replacement value. Therefore, the selected culvert network should provide valid results.

Once **Table 6.3** is developed, the budgetary action can be computed for each year for given annual budgets of $14,000, $12,000, $10,000, $9,000, $8,000, $7,000, $6,000 and $5,000. Please note that the above annual maintenance budgets are approximately 1% to 3% of the network values. **Tables 6.4 and 6.5** show the calculation for a given annual budget of $6,000 for the first two years.

Table 6.4 Sample Computations for the First Year with the Modified Worst First Method for $6,000 Budget

Year 1											
No.	Condition Classification in %	Condition Classification after 1yr in %	Replacement Value in $	Current Value in $	Culvert Value after 1 year without Fix in $	Recommended Technology	Cost of Fix in $	New Condition	Culvert Value after 1 year with Fix in $	Fix or Not	Culvert Age in years
1	73.31%	71.93%	13,354	9,790	9,606	clean	1,361	2.00	9,790	-	60
2	66.09%	64.57%	2,603	1,720	1,681	clean	265	2.00	1,720	-	65
3	14.19%	13.22%	13,015	1,847	1,720	replacement	13,015	1.00	13,015	-	100
4	6.38%	5.83%	11,657	744	679	replacement	11,657	1.00	11,657	-	110
5	72.28%	71.23%	17,901	12,939	12,751	clean	1,153	2.00	12,939	-	81
6	64.57%	63.40%	10,371	6,696	6,576	clean	796	2.00	6,696	-	88
7	57.42%	56.20%	14,249	8,182	8,008	cement coating	2,574	2.00	11,357	-	94
8	48.75%	47.50%	43,857	21,381	20,834	cement coating	13,188	2.00	34,954	-	101
9	40.07%	38.86%	10,920	4,376	4,243	slip lining	4,769	1.00	9,865	-	108
10	48.75%	47.50%	30,577	14,907	14,525	slip lining	18,820	1.00	27,623	-	101
11	32.93%	31.78%	54,248	17,861	17,239	slip lining	16,965	1.00	49,007	-	114
12	25.24%	24.22%	62,654	15,814	15,172	slip lining	27,363	1.00	56,601	-	121
13	25.24%	24.22%	35,802	9,036	8,670	slip lining	15,636	1.00	32,344	-	121
14	100.00%	100.00%	61,928	61,928	61,928	do nothing	0	1.00	61,928	-	1
15	9.18%	8.63%	61,607	5,657	5,319	replacement	61,607	1.00	61,607	-	141
		Total	444,742	192,879							

Table 6.5 Sample Computations for the Second Year with the Modified Worst First Method for $6,000 Budget

Year 2											
No.	Condition Classification in %	Condition Classification after 1yr in %	Replacement Value in $	Current Value in $	Culvert Value after 1 year without Fix in $	Recommended Technology	Cost of Fix in $	New Condition	Culvert Value after 1 year with Fix in $	Fix or Not	Culvert Age in years
1	71.93%	70.52%	13,354	9,606	9,417	clean	1,361	2	9,606	-	61
2	64.57%	63.01%	2,603	1,681	1,640	clean	265	2	1,681	-	66
3	13.22%	12.28%	13,015	1,720	1,599	replacement	13,015	1	13,015	-	101
4	5.83%	5.31%	11,657	679	619	replacement	11,657	1	11,657	-	111
5	71.23%	70.16%	17,901	12,751	12,559	clean	1,153	2	12,751	-	82
6	63.40%	62.23%	10,371	6,576	6,454	clean	796	2	6,576	-	89
7	56.20%	54.97%	14,249	8,008	7,833	cement coating	2,574	2	11,357	-	95
8	47.50%	46.26%	43,857	20,834	20,287	cement coating	13,188	2	34,954	-	102
9	38.86%	37.65%	10,920	4,243	4,111	slip lining	4,769	1	9,865	-	109
10	47.50%	46.26%	30,577	14,525	14,144	slip lining	18,820	1	27,623	-	102
11	31.78%	30.65%	54,248	17,239	16,624	slip lining	16,965	1	49,007	-	115
12	24.22%	23.21%	62,654	15,172	14,544	slip lining	27,363	1	56,601	-	122
13	24.22%	23.21%	35,802	8,670	8,311	slip lining	15,636	1	32,344	-	122
14	100.00%	100.00%	61,928	61,928	61,928	do nothing	0	1	61,928	-	2
15	8.63%	8.11%	61,607	5,319	4,996	replacement	61,607	1	61,607	-	142
		Total	444,742	188,950							

In **Tables 6.4 and 6.5** ‘cv’ means current value of culvert and ‘fix’ means value of the culvert after one year with the suggested corrective action. The symbol ‘nfix,’ is for the culvert value after one year without ‘fix’, where ‘nfix’ is computed using the appropriate deterioration shown in **Figure 6.1**. It should be noted that culvert failure is assumed when the condition classification of a culvert drops below 5%. Ergo, there should be sufficient funds in the budget to take appropriate action for every culvert before its condition classification drops below 5%. This calculation involves first predicting the next year’s condition classification based on the initial condition classification and the depreciation curve (**Figure 6.1**), then checking for any culvert with condition classification below or near 5%, and second, checking cost to take appropriate action for

each culvert and selecting culverts that can be corrected with the allocated funds. If there is a balance, that amount is carried forward and added to the budget of the following year. Please note that the total selected fix cost values should be smaller than the allocated budget ($\sum_{i=1}^{15} Cost(fix) \leq budget$) and the updated network value after fix should be larger than the current value ($\sum_{i=1}^{15}\big(fix(i) + nfix(i)\big) > Current\ value$).

The following steps illustrate computations shown in **Tables 6.4 and 6.5**:

1. Calculate current year condition classification for each culvert
2. Based on current condition classification, calculate that for the next year using **Figure 6.1**
3. Check whether future condition classification of any culvert is below 5%
4. Compare the total cost of correcting those culverts and the allocated budget
5. Use funds to first correct culverts with condition classification close to 5% and if there are sufficient funds use that to correct other culverts with optimum selection to have higher overall network value.
6. Repeat step1 to step 5 for next year.

This computation should proceed for the design life of each culvert in the network and should be stopped only for the following two reasons:

1. If there are insufficient funds to correct a culvert that would have condition classification below 5%. This means there are no funds to fix that culvert before failure.
2. If condition classification of every culvert is above or near 70%. Computation should be stopped as there would be excess maintenance funds in future years. This means all culverts in the network are fixed and now the culvert network is at a good condition state.

Tables 6.4 and 6.5 show the calculation of a given annual budget of $6,000. Please note that culvert #4 is near 5% or at 6% of its service life and needs $11,657 to fix. But the allocated budget is only $6,000 and that is not sufficient to correct culvert #4 during the first year. Also, all other culverts are still at acceptable condition level, thus the suggested action would be do nothing during the current year to save funds to correct

the culvert #4 following year. During year 2 there is $6,000 from the previous year plus the new budget of $6,000 or $12,000. This amount is sufficient to correct culvert #4. At this stage, the calculated new network value is $196,103, which is higher than the current network value of $188,950. Consequently, the above investment is justified. With a $12,000 investment at year two and after correcting culvert #4 there is a balance of $343 ($12,000-$11,656). This $343 is carried forward to year 3. Now note that culvert #15 is near the condition classification 5%, so funds are now needed to correct culvert #15. Please note that the action point for repair, rehabilitation, and replacement of a culvert is not fixed. Culverts which are eligible for rehabilitation can wait for a few years without much damage to the system. However, if the culvert condition state is near or below 5% it will fail. Then it will cost much more to replace due to collateral damage. For that reason, the worst pipe is fixed first. **Table 6.6** summarizes the above calculations for 30 years using the modified worst first method and lists network value every two years for annual budgets of $14,000, $12,000, $10,000, $9,000, $8,000, $7,000, $6,000 and $5,000.

Table 6.6 Thirty Year Summary of Modified Worst First Method for Several Budgets

Every Year New Network Value Based on Different Budget																
Budget	Year 1	Year 2	Year 4	Year 6	Year 8	Year 10	Year 12	Year 14	Year 16	Year 18	Year 20	Year 22	Year 24	Year 26	Year 28	Year 30
$ 5,000	$192,879	$188,950	$192,321	$184,893	$177,661	$170,640	$163,844	No Result	No Result	No Result	No Result	No Result	No Result	No Result	No Result	No Result
$ 6,000	$192,879	$188,950	$192,321	$184,893	$177,661	$170,639	$163,842	No Result	No Result	No Result	No Result	No Result	No Result	No Result	No Result	No Result
$ 7,000	$192,879	$188,950	$192,321	$184,893	$177,661	$170,639	$163,842	No Result	No Result	No Result	No Result	No Result	No Result	No Result	No Result	No Result
$ 8,000	$192,879	$188,950	$192,321	$184,893	$177,661	$170,639	$235,183	$242,412	$257,974	$281,548	$316,724	$311,607	$306,419	$ 301,164	$354,845	$ 372,180
$ 9,000	$192,879	$188,950	$192,321	$184,893	$177,661	$229,129	$242,409	$279,764	$302,008	$318,714	$332,846	$328,189	$323,438	$ 377,067	$387,888	$ 388,853
$ 10,000	$192,879	$188,950	$192,321	$184,893	$177,661	$241,830	$247,247	$306,370	$300,977	$344,437	$381,318	$392,138	$391,373	Good condition	Good condition	Good condition
$ 12,000	$192,879	$199,927	$192,321	$184,893	$235,679	$252,936	$310,250	$324,624	$337,313	$390,466	$393,360	Good condition	Good condition	Good condition	Good condition	Good condition
$ 14,000	$192,879	$199,927	$192,321	$184,893	$258,704	$270,318	$337,483	$370,052	$394,782	$395,249	Good condition	Good condition	Good condition	Good condition	Good condition	Good condition

Please note that network value is reported every two years to save space in **Table 6.6**. With an annual budget of $5,000, $6,000 and $7,000, computation was stopped after 12 years as the budget was insufficient to correct culvert #15 and it reached a condition classification below 5%. When the network values with above annual budgets are compared, one can observe that the lower budgets such as $5,000, $6,000 and $7,000 are not sufficient as there is insufficient budget to fix some culverts before failure. The above information is plotted in **Figure 6.3**.

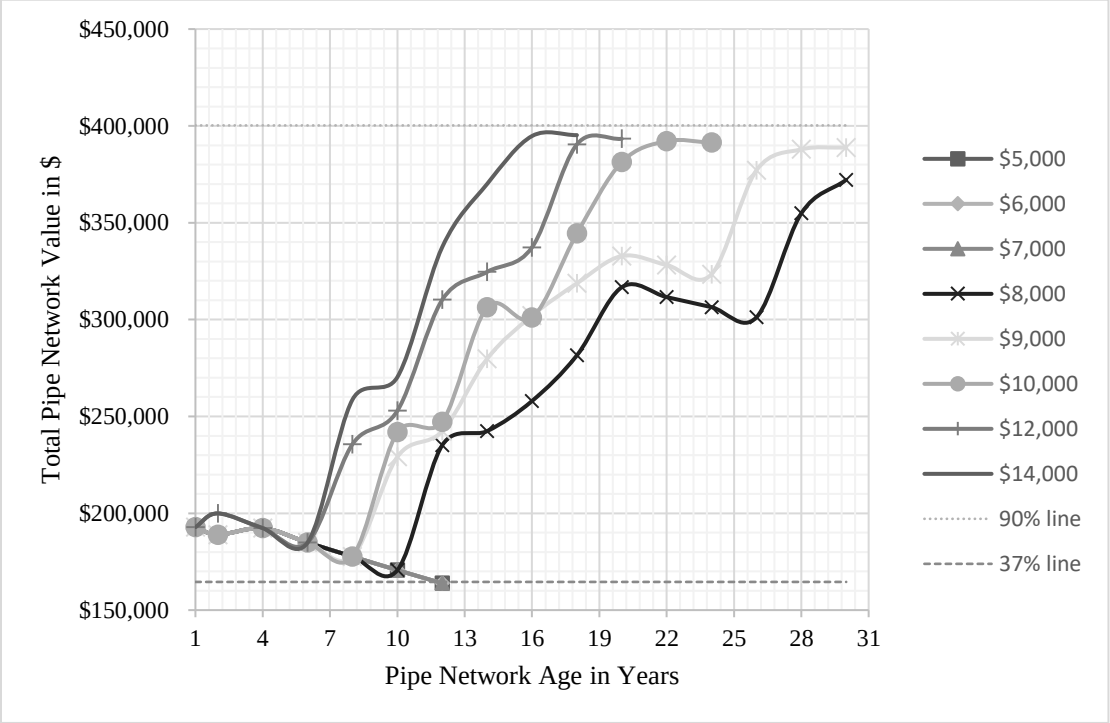

Figure 6.3 Thirty-year summary of modified worst first method for several budgets.

Figure 6.3 shows that for annual budgets of $5,000, $6,000 and $7,000, the average network condition state reaches a value of 37%. Now consider annual budgets of $10,000, $12,000 and $14,000: they are over-disbursed as after 24 years the average network condition state reaches a value of 89% and all culverts are replaced so every

culvert is like new. For annual budgets of $8,000 and $9,000 it can be observed that the whole network is at a good condition over the 30-year span and each culvert in the network is fixed. Thus, based on **Table 6.6** and **Figure 6.3** one can conclude that an annual budget of $8,000 is sufficient to maintain the selected network. However, if $8,000 is selected as an annual budget, one can find that at year 30 all culverts are corrected or replaced, but some culverts reach lower condition classifications. Therefore, $9,000 is the optimum budget as required by the Phase II of Governmental Accounting Standards Board, Statement No. 34 (GASB 34). The optimum budget is the value which an agency is required to invest in order to improve the overall condition state of its infrastructure systems.

6.4 Long-term Maintenance Cost Based on Optimization

In this research, the computer program LINGO was used for the budget optimization. LINGO is a comprehensive tool designed to build and solve linear, nonlinear, quadratic, quadratically constrained, second order cone, stochastic, and integer optimization models in a fast, easy and efficient manner.

To use LINGO, the following values are first defined: ci is the cost to correct culvert i; fi is value of culvert i after one year and with corrective action; nfi is value of culvert i after one year without corrective action; deci(i,1) is to correct the culvert i; deci(i,2) is not to correct the culvert i; bt is the allocated budget; rpvi is the replacement value of culvert i; yri is the age of the culvert i; ti is the year for which to compute condition classification of culvert i; csi is the current condition classification of culvert i; csi' is the next year condition classification of culvert i; cvi is the current value of culvert

i; ocsi is the original condition state of culvert i; and mat is culvert material, where mat=1 means metal culvert and mat=2 means concrete culvert.

The objective is to maximize value of the culvert network after one year by fixing at least one or more culverts and to make sure the new value after one year is larger than the current value and the total cost is smaller than the allocated budget.

$$Max\ nv = \sum_{i=1}^{15} (f_i * deci(i,1) + nf_i * deci(i,2)) \tag{6.1}$$

$$\sum_{i=1}^{15} c_i * deci(i,1) \leq bt \tag{6.2}$$

$$\sum_{i=1}^{15} (f_i * deci(i,1) + nf_i * deci(i,2)) > \sum_{i=1}^{15} cv_i \tag{6.3}$$

The current condition classification of culvert i is computed, based on **Figure 6.1**.

$$cs_i = e^{[-(t_i/t_d)^{\gamma}\, ln(2)]} \tag{6.4}$$

Here, the shape parameter γ can be back-calculated as 3.6. Once the csi and csi' value is computed, nfi and cvi values are computed as shown below.

$$cvi = cs_i * rpv_i = e^{[-(t_i/t_d)^{\gamma}\, ln(2)]} * rpv_i \tag{6.5}$$

$$nfi = cs_i' * rpv_i = e^{\{-[(t_i+1)/t_d]^{\gamma}\, ln(2)\}} * rpv_i \tag{6.6}$$

Because the nfi means do nothing and the culvert is allowed to depreciate, its value should be based on the condition classification of the following year. Thence, nfi uses the condition classification of the following year. There is also a constraint that if the condition classification of a culvert below 5% is failure, that culvert must be fixed first.

$$\text{csi}<0.0531 \text{ then deci (i,1) } =1 \tag{6.7}$$

The program calculates minimum budget, thus new object function is:

$$Min \sum_{i=1}^{15} c_i * deci(i,1) \quad (6.8)$$

Since culvert cleaning will not change its condition state and since four culverts (culvert #s 1, 2, 5 and 6) are at good condition state, no culvert cleaning is included but rehabilitation is added for these four culverts. When these four culverts drop to a poor condition state, they will be rehabilitated.

Equation (6.9) shown below is a constraint where the change in condition state is compared instead of the total value next year with or without fix. Therefore, if the culvert is in good condition then there is no need to fix and let it deteriorate. When its condition state drops to the next condition state (say from 3 to 4), drops to condition state 5 or condition state below 10%, it has to be fixed or replaced. Hence, LINGO was run three times with ocs - cs=15%, 20%, and 25%.

$$ocs_i - cs_i > 0.15 \; or \; 0.2 \; or \; 0.25 \; then \; deci(i,1) = 1 \quad (6.9)$$

For ocs-cs=15%, there is one culvert (13) that drops into condition state 10%, therefore, this culvert needs to be replaced. Based on the result from LINGO, the total years needed to let the network approach a good overall condition state is 21 years and the total investment is $221,331. Accordingly, the average yearly investment is $10,540 ($221,331/21) with the average condition state of the network at 87% after 21 years.

For ocs-cs=20%, there are two culverts (12, 13) that drop into condition state 10% and need replacing. Over 28 years is needed for the network to approach a good condition state with a total investment of $257,860. Ergo, the average yearly investment is $9,209 ($257,860/28) with the average condition state of the network at 88% after 28 years.

For ocs-cs=25%, there are three culverts (11, 12, and 13) that drop into condition state 10% and should be replaced. Over 31 years are needed for the network to approach a good condition state with a total investment of $295,142. Thence, the average yearly investment is $9,521 ($295,142/31) with the average condition state of the network at 91% after 31 years.

Table 6.7 summarizes the results of budget optimization using LINGO, where LINGO is run from year 1, data is contributed to obtain the minimum budget, and the computation is repeated for years 2, 3, 4, etc., until all culverts in the network are in good condition state. To fix all culverts in the culvert network listed in **Table 6.3**, LINGO requires over 20 years, and the minimum budget of every year is different.

Table 6.7 Comparison of Results from LINGO and Modified Worst First Methods

Budget per Year	Year21	Year22	Year23	Year24	Year25	Year26	Year27	Year28	Year29	Year30	Year31
$ 9,000	74%	74%	73%	73%	72%	85%	86%	87%	88%	87%	88%
$ 9,209								88%			
$ 9,521											91%
$ 10,000	86%	88%	88%	88%							
$ 10,540	87%										

Table 6.7 also compares the output from LINGO with the modified worst first method. The darker rows list results from the modified worst first method and the lighter rows list results from LINGO. One can observe that results from the two methods are almost the same. The LINGO method has some limitation as the program cannot use the same budget for every year. However, with a very large network it is expected that the

minimum budget of every year will vary within a narrow range and that it will have a budget value similar to that from the modified worst first method.

6.5 Long-term Maintenance Cost Based on Maximum Deterioration Rate

This method is only applicable to a network of new culverts. If it is assumed that all fifteen culverts in **Table 6.3** were installed this year, then the system value of the culvert network would be $444,742. Since all fifteen culverts have different deterioration curves as presented by **Figure 6.1**, the rate of deterioration can be computed separately from the slope of each curve. **Figure 6.4** shows the rate of deterioration with time for concrete culverts.

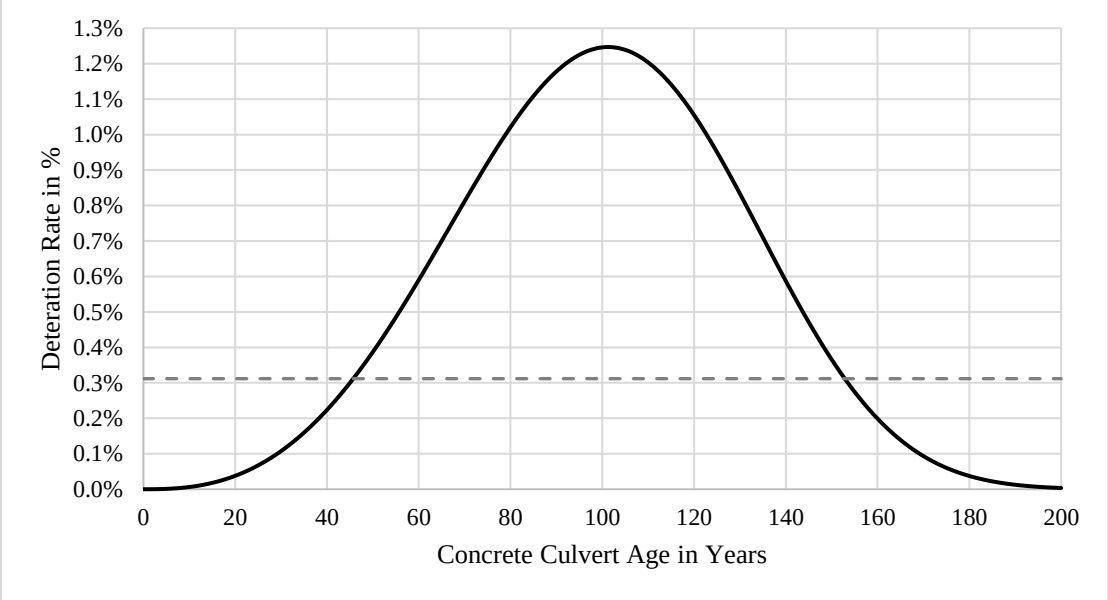

Figure 6.4 Rate of deterioration for concrete culverts.

From **Figure 6.4**, the maximum rate of deterioration is approximately 1.24% at year 101, and the replacement value for all concrete culverts in the network is $342,186 (see **Table 6.1**). As a result, it can be assumed that if one contributes 1.24% of the network value into the system or $4,243 (1.24% of $342,186) all concrete culverts can be maintained. Ergo, the total annual investment value to maintain all fifteen culverts is $4,918 ($675+$4243).

This annual investment value of $4,918 can be compared with the annual investment value of $5,000 from the modified worst first method. Based on the results from the modified worst first method shown in **Table 6.6**, if $5,000 per year is used as the annual budget, it can be shown that at year 10 one culvert of the culvert network (culvert #15) will drop below 5%, and this means at year 10 there are insufficient funds to correct culvert #15. This is due to the age of selected culverts in the network with overall condition classification of 37%. Consequently, this method can only be used to compute the absolute minimum maintenance budget for any infrastructure network. Please note that value obtained from the maximum deterioration method is the lower bound, which is only applicable for a new network. But for the old network it just provides a lower bound hence this value can be used as the starting point for worst first method.

CHAPTER 7
CONCLUSION AND FUTURE WORK

7.1 Conclusions

In this research, three methodologies were developed for optimum time and optimum allocation of funds to rehabilitate or replace culverts based on their condition state. These three methods were used to compute the long-term yearly maintenance budget.

1. Maximum deterioration can only be used to estimate the lower bound value.
2. The modified worst first method is computationally intensive but provides the optimum budget.
3. The LINGO method would provide the total budget to fix all culverts at different condition states to make sure they do not drop to a lower condition state or failure.

For the specific culvert network studied, it can be concluded that the optimization method provides an upper bound value, maximum deterioration rate method provides the lower bound value and the modified worst first method provides the GASB 34 Phase II budget. Before making a long-term maintenance plan, culvert condition state should be determined, preferably using the Ultrasound method to conduct non-destructive tests. This research demonstrates the feasibility of using ultrasound measurement to determine the condition state of culverts.

Experimental tests showed that ultrasound wave velocity is decreased with the increase in porosity of cement paste. Back-calculated wave velocity values using FEM simulation using ANSYS and ABAQUS validated the measured variation wave velocity with porosity of dry and saturated cement paste. FEM simulation showed that under fully saturated conditions the wave velocity is faster than that under dry conditions. By comparing the simulated and back-calculated wave velocities with those measured for

different porosities, this study attempted to provide a theoretical basis variation of ultrasound wave velocity with porosity for both dry and saturated cement paste.

Review of existing theories could not account for higher ultrasound wave velocity of cement paste with fluid saturated voids. However, FEM simulation results can predict larger ultrasound wave velocity of fluid. Ergo, an idealized 1-D model was used to simulate shock wave velocity propagation. Numerical calculation of shock wave propagation shows that the higher voids will cause encounters with rarefaction waves causing shock wave decrease in speed. Also, the energy will spread to a longer distance and the total energy density will decrease causing a reduction of wave amplitude.

7.2 Future Research

It is believed that a long-term management plan for a culvert network can satisfy the requirement of GASB-34 and obtain the minimum budget that maximizes the overall condition state of culvert networks. However, the above analysis did not include rate of inflation. To obtain an accurate analysis, the rate of inflation and the value of money should be included. Another important task is to streamline the different repair, rehabilitation, and replacement cost values between literature resources and real-life applications. In future study, these will be further investigated to eliminate the above limitation.

Based on the preliminary calculation shown, the shock wave can be used to explain the reduction in ultrasound velocity and amplitude. The preliminary result presented many limitations was subject to several assumptions. The calculations presented here are

fundamental verification of the initial work performed in France. There are still limitations: for example, how ultrasound will work when it is a relined culvert.

APPENDIX
SIMPSON'S METHOD AND COMPUTER CODE

Simpson's method is a powerful method for numerical integration. It is a Newton- Cotes formula for approximating the value of a definite integral by using quadratic polynomials. It is always used to get approximate value for difficult integral for a parabolic arc. The Simpson's rule formula is

$$\int_a^b f(x)dx \approx \frac{\Delta x}{3}(y_0 + 4y_1 + 2y_2 + 4y_3 + 2y_4 \cdots + 4y_{n-1} + y_n) \quad \text{(A.1)}$$

Here $\Delta x = (b-a)/n$ for n+1 points. To be noticed [a, b] should be divided into an even number of subintervals of equal length. By knowing each y value on this parabolic, it is easy to use Simpson's rule to get the approximate area under the parabolic between a and b. Since the rarefaction is a smooth change zone, the state for every point in this zone is different as shown in **Figure A.1**, thus it is difficult to calculate the total energy along the rarefaction zone.

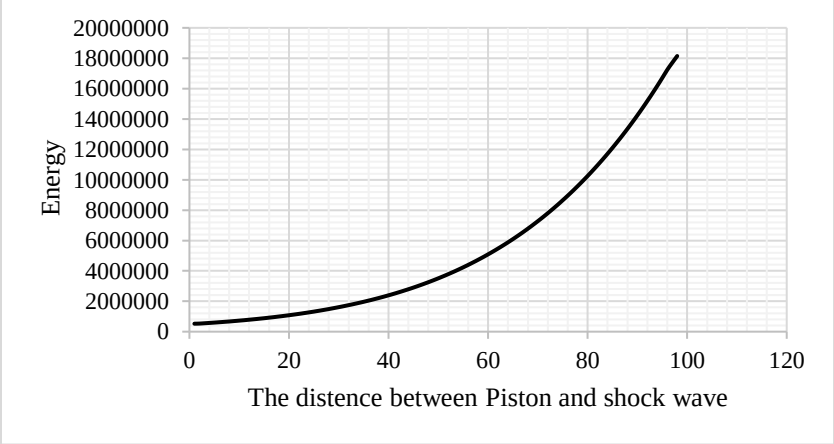

Figure A.1 The energy distribution of the rarefaction zone.

To calculate the total energy of the rarefaction zone by Simpson's rule, the location of the front and tail rarefaction should be known. If we use 5-point Simpson's rule. For example, the location of front and tail rarefaction are known as a, b. Then h=(a-b)/4. So, five analysis points are x_0, x_0+h, x_0+2h, x_0+3h and x_0+4h and x_0=b. Since the energy for each point can be calculated by $e = \frac{P}{(\gamma-1)} + \frac{\rho u^2}{2}$. And get energy equal E_{x0}, E_{x0+h}, E_{x0+2h}, E_{x0+3h} and E_{x0+4h} then the total energy can be get by the following equation:

Energy= $\frac{h}{3}(E_{x0}, +4E_{x0+h} + 2E_{x0+2h} + 4E_{x0+3h} + E_{x0+4h})$.

Following is the C-code for solving the Simpson's method automatically by computer. This code also has the hardware to calculate the total energy of the whole sock and rarefaction zone.

C code for Simpson's method provided by Dr. Bruce G. Bukiet

```
/* trapezoidal rule and Simpson's rule for integration */

#include <math.h>
#include <stdio.h>

main()
{
double left,right; /* left and right ends of interval */
double x0,h; /* need a multiple of 4 for intervals */
/* int halvings=5; */
int halvings=10;
int count = 1;
double fof();
double f1of();
double get_ustar();
double values();
double trap,simp,five;
double fx,fxph,fxp2h,fxp3h,fxp4h;
double pi = 3.141592653589793;
double error;
```

```
double gamma;
double pa, rhoa, ua;
double pb, rhob, ub;
double p_piston, u_piston, rho_piston;
double shock_speed = 5421.359954;
double u_plus_cF, u_plus_cB;
double x_cur;
double time = 2.0; /* CHANGE THE TIME */
double dt = 0.0; /* CHANGE THIS LINE */
double new_shock_location = 0.0; /* CHANGE THIS LINE */

double int1, int2, int3, int4;
double gamma_cur, rho_cur, u_cur, p_cur, c_cur;
gamma = 1.4;
pa = 101325.;  ua = 0.0; rhoa = 1.225;
pb = 29986571.75;  ub = 4500.0; rhob = 7.2080037;
p_piston = 1143296.069;  u_piston = 0.0; rho_piston = 0.6988906;

u_plus_cF = ub + sqrt(gamma * pb / rhob);
u_plus_cB = u_piston + sqrt(gamma * p_piston / rho_piston);
printf("upluscF = %f t_catch = %f\n",u_plus_cF,u_plus_cF/(u_plus_cF-shock_speed));

/* let time = 1 */
int1 = shock_speed * f1of(gamma, rhob, ub,pb) + (51000 -
shock_speed)*f1of(gamma,rhoa,ua,pa);
printf("Original Integral for Energy = %lf \n",int1);

/* time is now 2 seconds */
/* first zone - between piston and back of rarefaction */
int1 = (time - 1.) *u_plus_cB * f1of(gamma, rho_piston, u_piston, p_piston);
int3 = (time*shock_speed - u_plus_cF*(time - 1.)) * f1of(gamma, rhob, ub, pb);
int4 = (51000. - time * shock_speed) * f1of(gamma, rhoa, ua, pa);
printf("int1 %f int3 %f int4 %f \n", int1, int3, int4);
left = u_plus_cB * (time - 1.); right = u_plus_cF * (time - 1.);
h = (right - left)/4.;

printf("h          trapezoid     Simpson's    5-point\n");

while (count <= halvings){
        x0 = left;
        simp = 0.0;
        /* since time = 1, x is dx/dt */
        while (x0 < (right-h)) /* to eliminate posible round-off problems*/
        {
                x_cur = x0;
                get_ustar(gamma, rhob, ub, pb,x_cur,&u_cur,&c_cur,&p_cur,&rho_cur);
```

```
                fx = f1of(gamma, rho_cur, u_cur, p_cur);

                x_cur = x0+h;
                get_ustar(gamma, rhob, ub, pb,x_cur,&u_cur,&c_cur,&p_cur,&rho_cur);
                fxph = f1of(gamma, rho_cur, u_cur, p_cur);

                x_cur = x0+2.*h;
                get_ustar(gamma, rhob, ub, pb,x_cur,&u_cur,&c_cur,&p_cur,&rho_cur);
                fxp2h = f1of(gamma, rho_cur, u_cur, p_cur);

                x_cur = x0+3.*h;
                get_ustar(gamma, rhob, ub, pb,x_cur,&u_cur,&c_cur,&p_cur,&rho_cur);
                fxp3h = f1of(gamma, rho_cur, u_cur, p_cur);

                x_cur = x0+4.*h;
                get_ustar(gamma, rhob, ub, pb,x_cur,&u_cur,&c_cur,&p_cur,&rho_cur);
                fxp4h = f1of(gamma, rho_cur, u_cur, p_cur);

                simp += ((h/3.) * (fx + 4.* fxph + 2.* fxp2h + 4. * fxp3h
                        + fxp4h));
                x0 = x0 + (4.*h);
        }
        printf("%f %f\n",h,simp+int1+int3+int4);
        h = h/2.;
        count++;
}

/* time is now time you want seconds */
/* first zone - between piston and back of rarefaction */
int1 = (time + dt - 1.) *u_plus_cB * f1of(gamma, rho_piston, u_piston, p_piston);
/* there is no zone 3 */
int4 = (11000. - new_shock_location) * f1of(gamma, rhoa, ua, pa);
int3 = 0.0;
printf("int1 %f int3 %f int4 %f \n", int1, int3, int4);
left = u_plus_cB * (time+ dt - 1.); right = new_shock_location;
h = (right - left)/4.;

printf("h          trapezoid     Simpson    5-point\n");
while (count <= halvings){
        x0 = left;
        simp = 0.0;
        /* since time = 1, x is dx/dt */
        while (x0 < (right-h)) /* to eliminate posible round-off problems*/
        {
                x_cur = x0;
                get_ustar(gamma, rhob, ub, pb,x_cur,&u_cur,&c_cur,&p_cur,&rho_cur);
```

```
                fx = f1of(gamma, rho_cur, u_cur, p_cur);

                x_cur = x0+h;
                get_ustar(gamma, rhob, ub, pb,x_cur,&u_cur,&c_cur,&p_cur,&rho_cur);
                fxph = f1of(gamma, rho_cur, u_cur, p_cur);

                x_cur = x0+2.*h;
                get_ustar(gamma, rhob, ub, pb,x_cur,&u_cur,&c_cur,&p_cur,&rho_cur);
                fxp2h = f1of(gamma, rho_cur, u_cur, p_cur);

                x_cur = x0+3.*h;
                get_ustar(gamma, rhob, ub, pb,x_cur,&u_cur,&c_cur,&p_cur,&rho_cur);
                fxp3h = f1of(gamma, rho_cur, u_cur, p_cur);

                x_cur = x0+4.*h;
                get_ustar(gamma, rhob, ub, pb,x_cur,&u_cur,&c_cur,&p_cur,&rho_cur);
                fxp4h = f1of(gamma, rho_cur, u_cur, p_cur);

                simp += ((h/3.) * (fx + 4.* fxph + 2.* fxp2h + 4. * fxp3h
                        + fxp4h));
                x0 = x0 + (4.*h);
        }
        printf("%f %f\n",h,simp+int1+int3+int4);
        h = h/2.;
        count++;
}
}

double fof(x)
double x;
{
double temp;
double pi = 3.141592653589793;

        /* return ( 1. / (x*x + 1.)); */
        temp = exp(x)-0.5*(exp(2) - 1.);
        return (temp);
}

double f1of(gamma, rho, u, p)
double gamma, rho, u, p;
{
double temp;

temp =  p / (gamma - 1.) + rho * u * u / 2.;
printf("f1of value = %f\n",temp);
```

```
return(temp);
}

double get_ustar(gamma, rho_R, u_R, p_R, u_plus_c,u_cur,c_cur,p_cur,rho_cur)
double gamma, rho_R, u_R, p_R, u_plus_c;
double *u_cur, *p_cur, *rho_cur, *c_cur;
{
                *u_cur = (2./(gamma + 1)) * (u_plus_c + 0.5 * (gamma - 1.) * u_R -
sqrt(gamma * p_R/rho_R));
                *c_cur = u_plus_c - *u_cur;
                *p_cur = p_R * pow(((*u_cur - u_R) * (gamma - 1.))/(2. * sqrt(gamma *
p_R / rho_R))+1,(2. * gamma / (gamma - 1)));
                *rho_cur = rho_R * pow((*p_cur/p_R), 1./gamma);
return((2./(gamma + 1)) * (u_plus_c + 0.5 * (gamma - 1.) * u_R - sqrt(gamma *
p_R/rho_R)));
}
```

REFERENCES

Almusallam, A. A., (2001). "Effect of Degree of Corrosion on the Properties of Reinforcing Steel Bars," Construction and Building Materials, Vol. 15, Pp. 361-368.

American Association of State Highway and Transportation Officials, (2007). "Highway Drainage Guidelines: Fourth Edition: Chapter 14 – Culvert Inspection, Material Selection, and Rehabilitation Guideline" American Association of State Highway and Transportation Officials (AASHTO), Washington, D.C.

American Concrete Culvert Association, (2013). "Post Installation Evaluation and Repair of Installed Reinforced Concrete Culvert," <Http://www.Concrete-Pipe.Org/Pdf/Post_Install_Inspect_081011.Pdf> (Aug. 2013).

American Concrete Institute (ACI), (1996). "Specifications for Structural Concrete for Buildings." American Concrete Institute.

American Concrete Pipe Association, (2008). "Concrete Pipe Historical Overview of The Rpc Industry Materials & Manufacturing Process or Reinforced Concrete Pipe," <Http://Www.Concretepipe.Org/Wp-Content/Uploads/2015/04/Techmod1-Historical-Overview.Pdf > (Dec. 2015).

American Society for Testing of Materials (ASTM), (2002). "Standard Test Method for Pulse Velocity through Concrete," ASTM C597-02; ASTM: West Conshohocken, PA, USA.

Benavente, D., García Delcura, M. A., Fort, R., And Ordóñez, S., (2004). "Durability Estimation of Porous Building Stones from Pore Structure and Strength," Engineering Geology, Vol. 74, Pp. 113-127.

Bentz, D. P., (1997). "Three-Dimensional Computer Simulation of Portland Cement Hydration and Microstructure Development," Journal of the American Ceramic Society, Vol. 80, Pp 3–21.

Besl, P. J., Delp, E. J., and Jain, R., (1985). "Automatic Visual Solder Joint Inspection." IEEE J. Robot. Automation, 1, 42–56.

Bhagwan, J.N., (2009). "Compendium of Best Practices in Water Infrastructure Asset Management." Contributions from South Africa, Global Water Research Coalition, 211.

Birks, A. and Green, R., (1991). "Nondestructive Testing Handbook," 2nd ed., Vol. 7. American Society for Nondestructive Testing, Columbus, Ohio, USA.

Bukiet B., (1988). “Application of Front Tracking to Two-Dimensional Curved Detonation Fronts.” SIAM J. SCI STAT. COMPUT, Vol. 9, 1, 80-99.

Bungey J.H., Millard S.G., (1996). “Testing of Concrete in Structures,” Third Edition, Blackie Academic & Professional Bishopbriggs, UK.

Burnside R. R. and Mackie A. G., (1965). “A Problem in shock wave decay.” Journal of the Australian Mathematical Society, Vol, 5, Issue 2, Pp.258-272.

Cabrera, J. G., (1996). “Deterioration of Concrete Due to Reinforcement Steel Corrosion,” Cement & Concrete Composites, Vol. 18, Pp.47-59.

Cook, R. D., Malkus, D. S., Plesha, P. E., (1989). “Concepts and Applications of Finite Element Analysis,” John Wiley & Sons.

Courant R. and Friedrichs K. O., (1948). “Supersonic Flow and Shock Wave.” Inter-science Publishers.

Davies, T. G. and Mamlouk, M. S. (1985). “Theoretical Response of Multilayer Pavement System to Dynamic Non-Destructive Testing.” Transp. Res. Rec., Transp. Res. Board, Washington, D.C., 1022, 1–7.

Department of Transportation. (2012). “Moving Ahead for Progress in the 21st Century (MAP-21)’. < https://www.fhwa.dot.gov/map21/> (June. 1 2015).

Eggers, F., and Kaatze, U., (1996). “Broad-Band Ultrasound Measurement Techniques for Liquids,” Measurement Science & Technology, Vol. 7, Pp. 1–19.

Eric M., (2011). “Hsfld241/242: Modeling Enclosed Liquids,” <Http://Www.Padtinc.Com/Blog/The-Focus/Hsfld241242-Modeling-Enclosed-Liquids> (Feb. 10, 2017).

Gokhale, S. R., Abraham, D. M., and Iseley, T., (1997). “Intelligent Sewer Condition Evaluation Technologies - An analysis of three promising options.” North American NO-DIG 1997 Conference, North American Society for Trenchless Technology, 253–265.

Goueygou M., Lafhaj Z. And Soltani F., (2009). “Assessment of Porosity of Mortar Using Ultrasound Rayleigh Waves,” NDT & E International, Vol. 42, Pp. 353–360.

Guillon, E., Benboudjema F., and Moranville, M., (2004). "Modelling the Mechanical Evolution of a Chemically Degraded Cement Paste at the Microstructure Scale," Proceedings of Framcos 5th International Conference on Fracture Mechanics of Concrete and Concrete Structures.

Han, N., (2004). "Role of Nde In Quality Control During Construction of Concrete Infrastructures on The Basis of Service Life Design." Construction and Building Materials 18, 163-172.

Hansen, T. C., Radjy, F. And Sellevold, E. J., (1973). "Cement Paste and Concrete," Annual Review of Materials Science Vol. 3: 233-268.

Hashin, Z. (1960). "The Elastic Moduli of Heterogeneous Materials," Journal of Applied Mechanics. Vol. 29, Pp.143-150.

Hashin, Z. And Shtrikman, S., (1963). "A Variational Approach to the Theory of The Elastic Behaviour Of Multiphase Materials," Journal of The Mechanics and Physics of Solids. Vol. 11, Pp.127-140.

Hernández, M. G., Anaya, J. J., Izquierdo, M. A. G., and Ullate, L. G., (2002). "Application of Micromechanics to the Characterization of Mortar by Ultrasound," Ultrasounds, Vol.40, Pp. 217–221.

International Atomic Energy Agency, (2002). "Guidebook on Non-Destructive Testing of Concrete Structures," Iaea, Issn 1018-5518.

Jeong, H., Hsu, K., Robert, E. S., and Liaw, P. K., (1994). "Characterization of Anisotropie Elastic Constants of Silicon-Carbide Participate Reinforced Aluminum Metal Matrix Composites: Part II. Theory," Metallurgical and Materials Transactions A, Vol. 25, Pp.811–819.

John, D. A., (2001) [1984]. Fundamentals of Aerodynamics (3rd Ed.), McGraw-Hill Science/Engineering/Math, ISBN 0-07-237335-0.

Jones, R., and Gatfield, E. N., (1960). "Testing Concrete by Ultrasound Pulse Velocity Technique," D. S. I. R. ROAD Technical Paper No. 34, pp. 3-8.

Kaplan, M.F., (1958). "Compressive Strength and Ultrasound Pulse Velocity Relationships for Concrete in Columns." ACI J., 29(54-37), p. 675.

Olmos K., Popovich S., Nurnbergerova T., Babal B. and Popovics J. S., (1996). "Ultrasound Pulse Velocity Test of Concrete Properties as Specified in Various Standard," Cement and Concrete Composites, Vol. 18, No. 5, Pp. 357-364.

Krstulovic, O. N., Woods, R. D., and Al Shayea, N., (1996). “Nondestructive Testing of Concrete Structures Using the Rayleigh Wave Dispersion Method.” ACI Mat. J., 93, 75–86.

Lencis, U., Udris, A., and Korjakins, A., (2013). “Moisture Effect on the Ultrasound Pulse Velocity in Concrete Cured Under Normal Conditions and At Elevated Temperature,” Construction Science.

Lin, Y. and Su, W., (1996). “Use of stress waves for determining the depth of surface-breaking cracks in concrete structures.” ACI Materials Journal, 93, 494– 505.

Lin Y., Lai C. And Yen T., (2003). “Prediction of Ultrasound Pulse Velocity (UPV) In Concrete,” ACI Materials Journal, Vol. 100, No. 1, Pp. 21-28.

Lopez, M., Lissenden, C., Chao, X., And Li, S., (2009). “Technology Evaluation on Characterization of the Air Void System in Concrete,” Fhwa-Pa-2009-013-Psu 020, Commonwealth of Pennsylvania Department of Transportation.

Maalej, S., (2011). “Micromechanical Model: Correlation Between Hydraulic and Acoustic Parameters of Cement-Based Materials,” Ph.D. Dissertation, <Https://Tel.Archives-Ouvertes.Fr/Tel-00590429> (Oct. 20, 2015).

Maalej, S., Lafhaj, Z., Bouassida, M., (2013). “Micromechanical Modelling of Dry and Saturated Cement Paste: Porosity Assessment Using Ultrasound Waves.” Mechanics Research Communications 51(2013) 8-14.

Malhotra. V. M., and Carino N. J., (1991). “Handbook on Nondestructive Testing of Concrete,” CRC Press, Boca Raton, FL, 343p.

Malhotra, V. M. and Carino, N. J., E., (2004). Handbook of Nondestructive Testing of Concrete, 2nd Ed. CRC Press, ASTM International, PA

Malhotra, V.M and Nicholas, J.C., (2003). “Handbook on Nondestructive Testing of Concrete Second Edition;” CRC Press: Boca Raton, FL, USA.

Matthews, J., Selvakumar, A., Sterling, R., and Condit, W., (2012).” Analysis of Wastewater and Water System Renewal Decision-Making Tools and Approaches.” J. Pipeline Syst. Eng. Pract., 3(4), 99–105.

Mays G. C., (1992), “Durability of Concrete Structures,” E.&F.N. Spon, London, pp.3-9

Mcnamee, P., Dornan, D., Bajadek, D., and Chait, E., (1999). “Understanding Gasb-34’s Infrastructure Reporting Requirement,” A Paper Written for State and Local Officials Who Will Be Involved in Efforts to Respond to, And Comply With, The Infrastructure Reporting Requirements of GASB 34. Price Waterhouse Coopers, Llp.

Meegoda, J. N., (2013). “Long-Term Maintenance of Culverts,” Transportation Research Board (CD-ROM), TRB, Washington D.C., Paper # TRB 13-2818.

Meegoda, J. N. and Abdel-Malek, L., (2011). “A Stochastic Framework for Sustainable Infrastructure-Application to Pipes and Culverts,” Transportation Research Board (CD-ROM), TRB, Washington D.C., Paper # TRB 11-2848.

Meegoda, J. N., Juliano, T. M., Ayoola, M. G. and Dhar, S. K., (2004). “Inspection, Cleaning, Condition Assessment and Prediction of Remaining Service Life of Culverts.” Proceedings of the 83rd. Transportation Research Board Meeting (Cd-Rom), Trb, Washington, D.C. Paper #04-4426.

Meegoda, J., Juliano, T. and Banerjee, A., (2006). “A Framework for Automatic Condition Assessment of Culverts,” Journal of Transportation Research Board, #1948, 26-36.

Meegoda, J. N., Juliano, T. M., Potts, L., Tang, C., Liu, S., Bell, C. And Marhaba, T., (2012). "Implementation of a Drainage Information, Analysis and Management System" Transportation Research Board (CD-ROM), TRB, Washington D.C., Paper # TRB 12-1605.

Meegoda, J. N., Juliano, T. M., Ratnaweera, P. And Abdel-Malek, L., (2005). "A Framework for Inspection, Maintenance and Replacement of Corrugated Steel Culvert Pipes," Journal of Transportation Research Board, # 1911, 22-30.

Meegoda, J., Juliano, T. and Tang, C., (2009). “A Culvert Information Management System,” Transportation Research Board (CD-ROM), TRB, Washington D.C., Paper # Trb 09-2024.

Meegoda, J., Juliano, T. and Wadhawan, S., (2008). “Estimation of the Remaining Service Life of Culverts,” Transportation Research Board (CD-ROM), TRB, Washington D.C., Paper # TRB 08-1523.

Meyer, C., (2004). “Concrete Materials and Sustainable Development in the USA,” Structural Engineering International, Vol. 14, Pp. 203-207.

Micevski, Tom, Kuczera, G. And Coombes, P., (2002). “Markov Model for Storm Water Culvert Deterioration,” Journal of Infrastructure Systems, Vol.8, No.2, 49-56.

Mills, D., (2002). "Asset Management and Reporting Systems," GASB 34 Workshop, Efc/Awwa, Chapel Hill, NC.

Minnesota Department of Transportation, (2012). “A Research Plan and Report on Factors Affecting Culvert Pipe Service Life in Minnesota,” Minnesota DOT. Mn/Rc 2012-27.

Mohammad, N., Sam, S., Deepak, B., Baris, S., Rahul, P., And Diego, C., (2008). "An Asset Management Approach for Drainage Infrastructure and Culverts," Midwest Regional University Transportation Center, <Http://www.Uta.Edu/Ce/Cuire/Msu-Uta-Uc%20culvert%20asset%20management%20final%20report%20june%2030-2008%20r1.Pdf > (Aug. 2015)

Mondal, P., Shah, S. P., and Marks, L. (2007). "A Reliable Technique to Determine the Local Mechanical Properties at The Nanoscale for Cementitious Materials," Cement and Concrete Research, Vol. 37, Pp.1440-1444.

Mukherjee, D. P. and Pal, S., (2005). "Advances in Pattern Recognition." Pattern Recognition Letters, 26(4), 395–398.

National Cooperative Highway Research Program, (2011). "Alternate Pipe Material Selection Protocol." National Cooperative Highway Research Program, Nchrp Project 20-07(264), Washington, D.C.

Needham C. E., (2010). "Blast Waves, Shock Wave and High Pressure Phenomena." Springer-Verlag Berlin Heidelberg.

Newman, T. S. and Jain, A. K., (1995). "Survey of Automated Visual Inspection." Computer Vision Image Understanding, 61(2), 231–262.

Ould Naffa S., Goueygou M, Piwakowski B, Buyle-Bodin F., (2002). "Detection of chemical damage in concrete using ultrasound." Ultrasound, 40, 247-251.

Perkins P. H., (1997). "Repair, Protection and Waterproofing of Concrete Structures." E & FN Spon, London.

Pierard, O., González, C., Segurado, J., Lorca, J. L., and Doghri, I., (2007). "Micromechanics of Elasto-Plastic Materials Reinforced with Ellipsoidal Inclusions," International Journal of Solids and Structures, Vol.44, Pp. 6945–6962.

Pizhong Q., David I. M., Fangliang C., (2012). "Concrete Performance Using Low-Degradation Aggregates," Washington State Transportation Center, Wr-Rd790.1.

Popovics, S., (1998). "Strength and Related Properties of Concrete - A Quantitative Approach." Nova York: John Wiley and Sons.

Popovics, S. and Popovics, J. S., (1992). "A critique of the pulse velocity method for testing concrete." Proc. of Nondestructive Testing of Concrete Elements of Structures, 94–103.

Portland cement Association (PCA), (1994). "Design and Control of Concrete Mixtures." Portland cement Association.

Rajani, B and Makar, J., (2000). "A Methodology to Estimate Remaining Service Life of Grey Cast Iron Water Mains," National Research Council of Canada.

Sayers, C. M. And Dahlin, A., (1993). "Propagation of Ultrasound Through Hydrating Cement Pastes at Early Times," Advanced Cement Based Materials, Vol. 1, Pp.12-21.

Shivprakash I., (2007). "Multi-Sensor Based Condition Assessment System for Buried Concrete Pipe." Ph.D. Dissertation, Pennsylvania State University.

Solís-Carcaño R. and Moreno E., (2008). "Evaluation of Concrete Made with Crushed Limestone Aggregate Based on Ultrasound Pulse Velocity." Constr. Build. Mater., 22(6): 1225-1231.

Soltani, F. (2010). "Caractérisation de la pâte de ciment par des méthodes ultrasonores," Ph.D. Dissertation. Ecl, Lille, France.

Turgut P., (2004). "Research into the Correlation between Concrete Strength and UPV Values." NDT. Net, 12: 12.

Van Cauwelaert, F. J., Alexander, D. R., White, T. D., and Barker, W. R., (1989). "Multilayer Elastic Program for Back-calculating Layer Moduli in Pavement Evaluation." Non-destructive Testing of Pavements and Back-calculation of Moduli, ASTM STP 1026, ASTM, 171–188.

Velez, K, Maximilien, S., Damidot, D., Fantozzi, G. And Sorrentino, F., (2001). "Determination by Nano-Indentation of Elastic Modulus and Hardness of Pure Constituents of Portland Cement Clinker," Cement and Concrete Research, Vol. 31, Pp. 555-561.

Walpole, L. J., (1966). "On Bounds for the Overall Elastic Moduli of Inhomogeneous Systems-I," Journal of the Mechanics and Physics of Solids. Vol. 14, Pp. 151-162.

Water Research Centre, (2001). "Sewerage Rehabilitation Manual (IV Edition)," Vol. I Rehabilitation Planning, Water Research Centre, Marlow, Uk, Wrc.

Wei-Du L., (1992). "Frequency Spectrum Analysis of Ultrasound Testing Signal in Concrete." Proc. of Nondestructive Testing of Concrete Elements of Structures.

Wonsiri, P., (2006). "Cement-Based Materials' Characterization Using Ultrasound Attenuation," Ph. D Dissertation, Georgia Tech Theses and Dissertations 19045. Http://Hdl.Handle.Net/1853/10493

Wu, T. T., Fang, J. J., and Liu, P.-L., (1995). “Detection of the depth of a surface breaking crack using transient elastic waves.” Journal Acoust. Soc. America, 97, 1678–1686.

Yim, H., Kim, J., Lee, B., Kw, H., (2013). “Air Voids Size Distribution Determined by Ultrasound Attenuation,” Construction and Building Materials Vol.47 Pp. 502-510